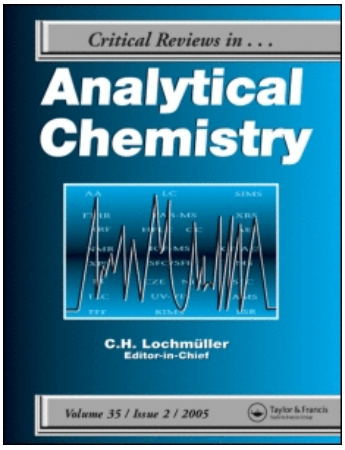

Critical Reviews in Analytical Chemistry
Publication details, including instructions for authors and subscription information:
http://www.informaworld.com/smpp/title~content=t713400837

Atomic Ionization Spectrometry: Prospects and Results

Yu. Ya. Kuzyakov[a]; N. B. Zorov[a]
[a] Department of Chemistry, Moscow State University, Moscow, U.S.S.R.

To cite this Article Kuzyakov, Yu. Ya. and Zorov, N. B.(1988) 'Atomic Ionization Spectrometry: Prospects and Results', Critical Reviews in Analytical Chemistry, 20: 4, 221 — 290
To link to this Article: DOI: 10.1080/10408348808050067
URL: http://dx.doi.org/10.1080/10408348808050067

ATOMIC IONIZATION SPECTROMETRY: PROSPECTS AND RESULTS

Authors: **Yu. Ya. Kuzyakov**
N. B. Zorov
Department of Chemistry
Moscow State University
Moscow, U.S.S.R.

Referee: John C. Travis
Center for Analytical Chemistry
National Institute of
Standards and Technology
(NBS)
Gaithersburg, Maryland

I. INTRODUCTION

There are different methods of ionization of atoms (e.g., interaction with electrons, interaction with hard gamma-radiation, etc.). This article discusses a method for the determination of element traces, whose application is associated with the ionization of atoms in the gaseous state during their interaction with laser radiation. In view of its great spectral radiance, a laser's interaction with a medium (consisting of atoms and molecules capable of absorbing photons of laser radiation) leads, or may lead, to such changes in the electric characteristics of the medium that advanced electronics provide the possibility of the particles' detection.

The uniquely high monochromaticity of laser radiation makes it possible to perform efficient selective excitation and ionization of atoms and molecules. The selective laser ionization technique has been successfully used for spectroscopic investigations of atoms and molecules in discharges[1-3] and flames.[4] Analytical chemists are interested in it because it presents one of the most advanced analytical opportunities, i.e., the detection of single atoms.[5] Due to its high sensitivity, this method has attracted increasing attention.[6-9]

The names of various methods used in analytical spectroscopy, as a rule, reflect the subjects of investigations and the processes forming the basis for determination of these subjects, e.g., the atomic absorption or the atomic fluorescence analytical method. In the analytical methods based on selective laser ionization, atoms are usually the subjects. The processes that can detect these atoms are associated with ion production. Therefore, in the present paper we refer to this analytical method as the atomic ionization method.[7] Papers dedicated to analytical application of this method could use other terms such as laser-enhanced ionization (LEI), optogalvanic spectroscopy, or resonance ionization spectroscopy (RIS).

Practical applications of this method in analytical chemistry are associated with techniques of the production of analyte atoms. Two kinds of atomizers have been used in most studies of this method for determination of small amounts of elements in substances. The first is a flame into which the analyte is injected, and the second is a crucible filled with the substance to be analyzed, which is heated up to high temperatures at which the vapors of the substance flow out through a small hole into a vacuum chamber. Therefore, for the most part, this paper discusses the use of atomizers of these kinds. The use of other kinds of atomizers (laser ablation, cathode sputtering, etc.) is briefly discussed in a separate section of the paper.

II. PHYSICAL PRINCIPLES OF ATOMIC IONIZATION SPECTROMETRY

The principle behind the method is that the occurrence of electric charges resulting from

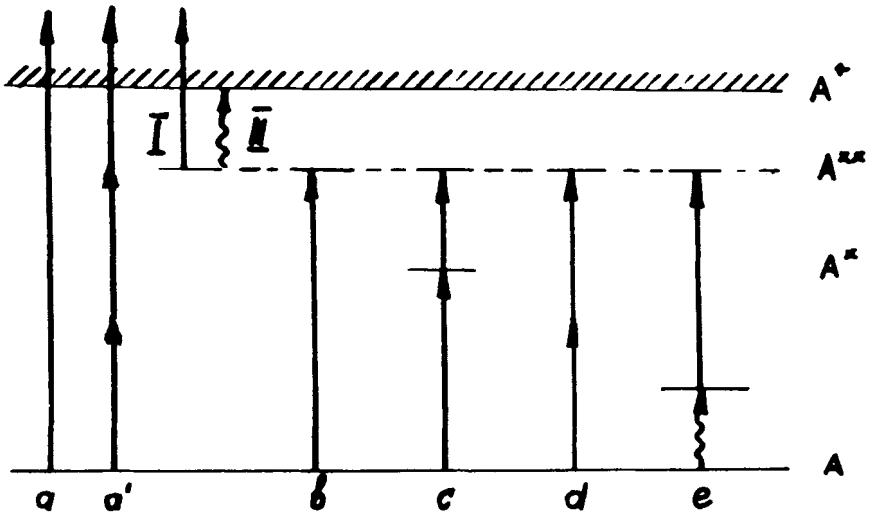

FIGURE 1. Basic excitation-ionization schemes for atomic ionization spectrometry; a, nonresonance photoionization (single-photon); a', nonresonance photoionization (multiphoton); I, photoionization from excited state A**; II, collisional ionization from excited state A**; b, optical excitation into excited state A**; c, two-step optical excitation through intermediate excitation state A*; d, multiphoton optical excitation into A** state; e, optical excitation into A** state from the state collisionally excited.

ionization of atoms and molecules can be detected in a laser-irradiated volume of a given gas.

Ionization of atoms or molecules takes place while absorbing $h\nu_i$ photons whose energy exceeds the ionization potentials of the particles (Figure 1a). This ionization is nonselective since all the atoms or molecules whose ionization potentials are lower than the photon energy are ionized. The method has found its application only in mass spectrometry (MS).[10] Nonselective ionization can also take place as a result of simultaneous absorption of several photons possessing equal energies (nonresonance multiphoton ionization, Figure 1a').

Selectivity of ionization can be provided by means of preliminary selective excitation of atoms before their ionization.[11] Because a spectral bandwidth of lasers being used may be fairly narrow, as in collimated beams, some isotopes of an element can be excited while other isotopes of the same element remain nonexcited.[12] Thus, use of narrowband lasers provides selectivity of optical excitation of one sort of atom. Atoms occupying the ground state interact with laser radiation, whose frequency matches the frequency of the $A \rightarrow A^{**}$ transition (Figure 1b), and populate the excited state A**.

Higher selectivity can be attained using successive resonance optical excitation of several intermediate states (Figure 1c). This stepwise excitation scheme is advantageous for elements possessing high ionization potentials. Schemes (b) and (c) in Figure 1 will be efficient when the energy densities of lasers are sufficient to transfer the greatest possible number of analyte atoms to an excited state. Attainment of these conditions (optical saturation of resonance transitions)[13] is possible with the aid of laser radiation. Atoms populating excited states can be also produced by multiphoton absorption (Figure 1d). When the population of some low-excited states becomes significant (e.g., in discharges or in media at high temperatures), photon absorption by atoms populating these states also leads to their selective excitation. One of the possible schemes of excitation for this case is shown in Figure 1e.

There are several ways to ionize atoms and molecules in excited states. Let us briefly discuss some of them. Ionization of atoms and molecules populating excited states can be accomplished when a photon is absorbed whose energy is enough to transfer them to a

nonbound state (Figure 1, I). It should be noted that the cross section of photoionization is smaller by several orders than the cross section of optically allowed bound-bound transitions.[14] Therefore, attainment of high efficiency of this process requires high densities (up to about 1 J/cm^2) of radiation energy.[15]

It has been suggested that the ionization cross section of excited atoms can be increased by the use of photoionization into autoionization states[16] or ionization of atoms excited to Rydberg states[17] by pulses of an electric field. Also of great importance are techniques of ionization of atoms from excited states in electric discharges or in flames (optogalvanic spectroscopy) due to collisions with electrons, atoms, and molecules (Figure 1, II) in the high temperature gas.[1,4] Basically, both photoionization (scheme I) and collisional ionization (scheme II) can take place.[18] Prevalence of one process over the other is determined by the means of excitation, the magnitude of ionization potential, the spectral density of energy of laser radiation as well as the density of a gas under investigation.

III. ATOMIC IONIZATION SPECTROMETRY IN FLAMES

A. General

Most studies on the atomic ionization (AI) analytical method have been carried out using sample atomization in flames since determination of elements in flames is fast, simple, and has good reproducibility. Freedom from conventional spectroscopic instrumentation and from interferences associated with laser radiation scattering, the possibility of collecting nearly 100% of resulting charged species enabling one to determine very low concentrations of species present in flames, and these concentrations' close agreement with the element concentrations of solutions introduced into flames make possible the determination of analyte concentrations in solutions at a level of 10^{-10} to 10^{-12} g/ml. Up until the present, more than 30 elements have been determined in flames, and their detection limits do not exceed, and often are much below, the limits used in conventional flame spectrometry techniques (atomic emission, atomic absorption, and atomic fluorescence). Application of the two-step atom excitation scheme has allowed a significant improvement of the detection limits for elements with high ionization potentials and of the selectivity of this method.

Changes in the impedance of the medium (as a result of photon absorption by medium components) are usually detected by voltage variations across electrodes between which the medium is placed, or by changes in a circuit current passing through the medium, which is one of the circuit's components. The flame experiments differ from atomic beam experiments or from MS experiments by the fact that measurements are of the impedance of medium changes rather than of separate charged species produced by laser radiation.

Dye lasers are used as sources of tunable radiation in broadband spectrum including both amplitude-modulated cw lasers[4,8,19] and pulsed lasers with flashlamp pumping,[6,20-22] N_2 laser pumping,[18,23-29] excimer laser pumping,[30] or Nd:YAG laser pumping.[26,31-34] Chaplygin et al.[35] studied the influence of the laser bandwidth on the magnitude of a measured AI signal. Pulsed lasers are the most commonly used ones and provide high peak power that allows one to reach easily the optical saturation of the resonance transition under investigation. Moreover, high peak power permits the attainment of high efficiency of conversion when it is necessary to provide radiation in the UV region of the spectrum whose exclusion from the investigation would make determination of many elements impossible.

When using flames, standard burners used in analytical atomic absorption spectrometry (AAS) are employed. These burners are usually equipped with a pneumatic nebulizer which allows the introduction of the solution being analyzed into the flame in the form of small droplets. These droplets are almost completely evaporated in the flame reaction zone at a height several millimeters from the burner head. The resultant vapors contain a mixture of various compounds and free atoms. The concentrations of analyte atoms depends on many factors, such as the nature of the element, the temperature of the analytical zone of the flame, the gas composition of the flame, etc.[36]

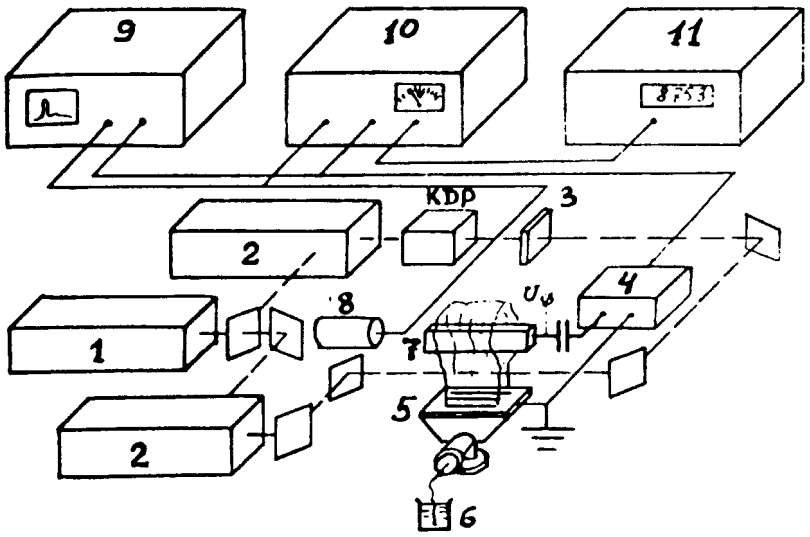

FIGURE 2. Scheme of a laser flame atomic ionization spectrometer: 1, pumping laser; 2, dye lasers; 3, filter; 4, amplifier; 5, burner; 6, sample solution; 7, electrode; 8, photodiode; 9, oscilloscope; 10, boxcar averager; 11, digital output of a signal.

The atomic ionization signal is measured by changes in a current passing through the flame at a voltage across electrodes, one of which may be the grounded burner head (see Figure 2) and the other either immersed directly into the flame or only touching the flame. The basic electrode configurations are shown in Figure 3.

A considerable number of studies have been dedicated to investigations of the effects of the material, shape, and positioning of electrodes on the magnitude of an AI signal. In the first such study,[4] the authors used tungsten-wire electrodes immersed directly into a flame. However, tungsten is easily corroded in the flame atmosphere, therefore in some subsequent works the electrodes were positioned so that the flame only touched their surfaces, providing electrical contact.[6] In other work, conditions and materials (nichrome, iridium, graphite) were selected which allowed the use of electrodes immersed into a flame.[24,26] Depending on its purpose, an electrode is either water cooled[39] or additionally heated by electric current.[40]

An AI signal-measuring system includes an amplifier and an electronic signal-processing system.[35,41]

B. Atomic Ionization Signal Detection in Flames

The perturbation of the electric properties (impedance) of a medium, e.g., flames, in response to the medium's absorption of photons is usually detected as changes in an electric current passing through the flame. This effect is achieved by the application of high voltage across the electrodes between which the medium under investigation is placed and is referred to as the optogalvanic (OG) effect.

It is this detection of the impedance of a medium rather than the detection of individual ions that differentiates OG effect experiments from experiments carried out in atomic beams, in vacuum, and in MS studies.[44,45]

Variations of the impedance of a medium are caused by variations of its complex permittivity. Resonance absorption leads to variations in static and dynamic polarizability as well as in medium conductivity. Polarizability contributions to variations in permittivity are negligible compared with conductivity variation contributions. Therefore, variations of charged species represent the basic contributions to impedance variations.

The OG effect in flames occurs when laser radiation interacts with some atomic or

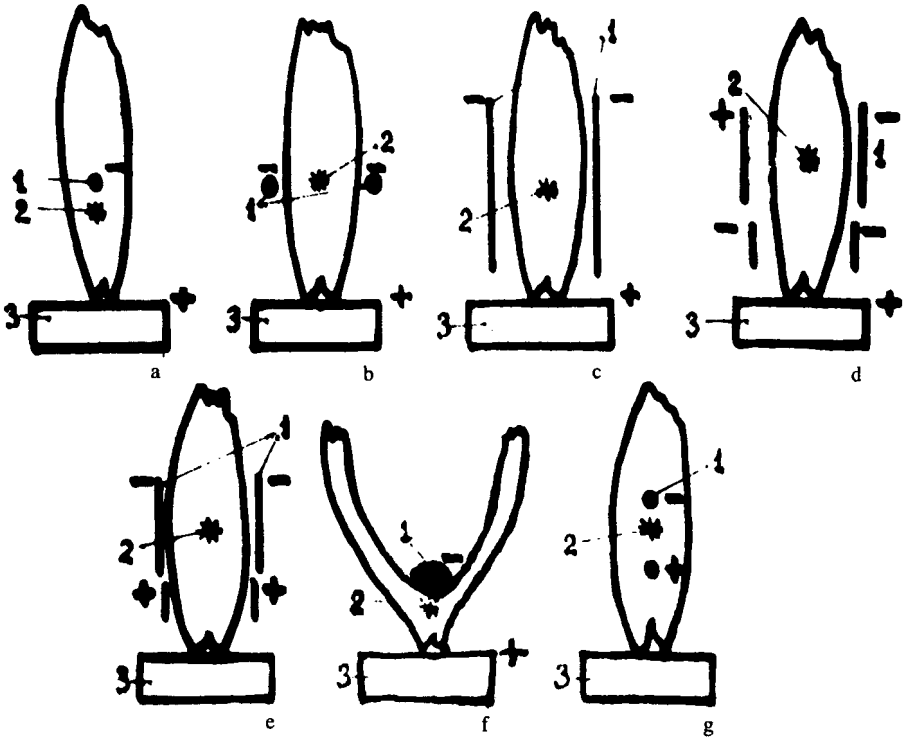

FIGURE 3. Basic electrode configurations used in flame atomic ionization spectrometry: a, wire electrode immersed into a flame,[4,26] b, U-shaped wire electrode outside a flame;[6,31] c, U-shaped plate cathode outside a flame;[37,42] d, multiple-electrode configuration outside a flame;[38] e, dual anode-cathode system outside a flame;[38] f, water-cooled cathode inside a flame;[39] g, wire cathode and anode inside a flame;[43] 1, cathode; 2, laser beam; 3, burner head.

molecular species in flames. A signal measured in this process depends on the laser pulse duration. When using modulated cw laser radiation and flashlamp-pumped laser radiation, the temporary AI signal waveform replicates the shape of a laser pulse.[6,19]

When a flame is irradiated by laser pulses of a nanosecond duration, the waveform represents a two-peak pulse.[46] The first peak appears immediately after an irradiation pulse (the delay time is about 10^{-7} s), and the delay time of the second peak reaches several microseconds and is proportional to the distance between the cathode immersed in the flame and the laser irradiation volume. Green and co-workers[37,38,47] studied the effects of electrode configurations on the magnitude of a signal as well as the dependance of an AI signal value on the voltage across electrodes. It has been found that the AI signal amplitude is a function of the electric field strength in an irradiation volume, which in turn depends on the laser beam position.

The presence of the saturation point on the signal magnitude-cathode potential curve permits the interpretation of an AI signal as the arrival of charges onto electrodes, and the saturation itself as the complete collection of charges resulting from irradiation.[22] The two peaks of an AI signal are associated with the arrival of electrons and positive ions onto electrodes, while the time shift between their occurrences is associated with different mobilities of electrons and positive ions in flames.

Detailed studies on the temporal shape on the first peak have found that it consists of two closely situated maximums; the first is attributed to capacitive coupling at the moment of the additional charge creation and separation, and the second is attributed to the arrival of electrons at the anode.[48,49]

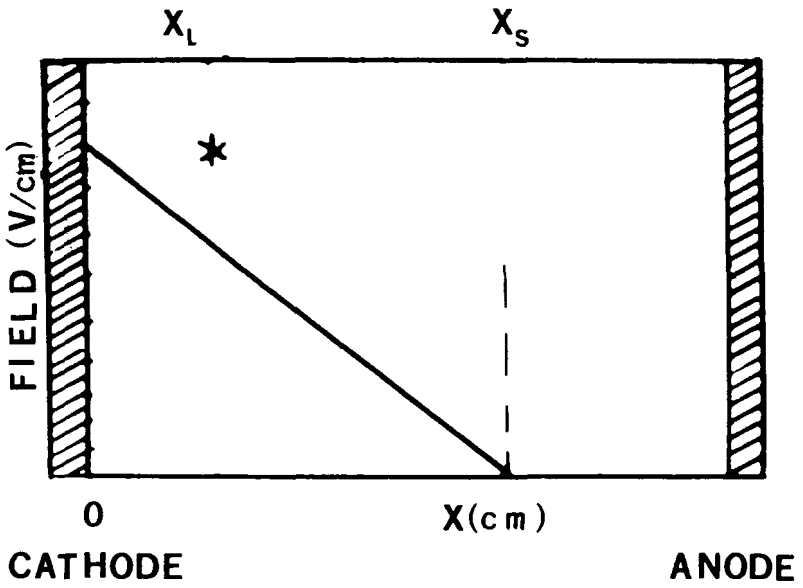

FIGURE 4. Distribution of electric field strength between plane electrodes in the point charge model.

The first attempt to quantify the temporal profile of an AI signal under conditions of optical excitation of analyte atoms by laser pulses of a nanosecond duration was made by Havrilla et al.[50] They employed a point charge model based on the assumption of independent motion of resulting charges possessing different mobilities in an external electric field. The motion of these charges induced a current in an external circuit that was measured as an AI signal. A one-dimensional case was investigated when weakly ionized plasma, e.g., a flame, filled the space between an idealized pair of infinite plane parallel electrodes across which voltage was applied. Figure 4 shows the electric field strength distribution between infinite plane electrodes which is assumed by a point charge model under common experimental conditions when using flames in analytical studies. The field distribution resulting from different conditions in which diffusion and charge interaction can be neglected is described in some detail by Lawton and Weinberg.[51]

In the idealized one-dimensional diffusion-free approximation of a flame under the influence of an applied potential, the field is found to be modified by a positive ion space charge or sheath, adjacent to the cathode. The space charge and the resulting field modification are natural consequences of the fact that electrons travel much faster than positive ions in response to a given electric field.

The point charge model assumes that the field-free region of the flame outside the near-cathode potential drop layer ($X > X_s$) behaves as an ideal electrical conductor and that the sheath boundary X_s becomes an effective anode. Charges are generated at the irradiated point $X = X_L < X_s$, and the current i(t) is induced by the charge motion in the external circuit at the time $t = 0$ due to the motion of ions $i_+(t)$ and electrons $i_-(t)$ in the flame:

$$i(t) = i_+(t) + i_-(t) \quad (1)$$

Havrilla et al.[50] gave the following expressions for these current components connected to ions and electrons:

$$i_+(t) = \begin{cases} \dfrac{Ne(X_s - X_L)}{X_s\tau_+} e^{t/\tau_+} & \text{at } t < t_{arr} \\ 0 & \text{at } t > t_{arr} \end{cases} \quad (2)$$

and

$$i_-(t) = \frac{Ne(X_s - X_L)}{X_s\tau_-} e^{-t/\tau_-} \quad (3)$$

where τ_- and τ_+ represent the characteristic times for electron pulse exponential decay and ion pulse exponential rise, respectively, determined by mobility and the electric field gradient; t_{arr} is the arrival time of a positive charge at the cathode, N is the number of charges generated at the irradiation point X_L, and e is the electronic charge.

For comparison with the experimental data, the authors take into consideration the time constant of an amplifier (risetime $-$ τ_r), and thus they obtain the following expression for $i_-(t)$:

$$i_-(t) = \frac{Ne(X_s - X_L)}{X_s(\tau_- - \tau_r)} [e^{-t/\tau_-} - e^{-t/\tau_r}] \quad (4)$$

Comparison of the pulse waveform of the current i(t) predicted by the point charge model with the experimental pulse waveform of an AI signal shows quite good correlation. There are, however, a number of discrepancies between theory and experiment, which the authors could not explain.

One of the reasons for this resides in the more elaborate relationship between an electric field strength and the distance from the cathode. Actually, the electric field strength profile is not linear, as is assumed by the point charge model, but has a more complicated nature, as was experimentally found out by Kuzyakov et al.,[52] who determined potential variations in the neighborhood of a cathode and, in more detail, for different voltages across electrodes and for different charge concentrations in a flame.[50,53]

Travis et al.,[54] advancing the point charge model, pointed out that this model could be applied when the concentration of charged species produced by laser action was significantly less than the concentrations of the flame background ions. For example, the laser-produced ion density should be much less than 10^9 cm^{-3} for an acetylene-air flame, or the solution concentrations should be much less than 10 ng/ml (if complete ionization is achieved).

It is known that for charged species concentrations in plasma exceeding 10^7 to 10^8 cm^{-3} in a region with linear dimensions of $L > r_D$ (where r_D is the Debye radius in plasma), concentration variations resulting from external effects are restored to a steady state at a rate of ambipolar diffusion.[55] As this takes place, relaxation of this concentration instability in plasma occurs as the quasi-stability is maintained.[56]

Taking this into consideration, Novodvorsky et al.[53,57] have suggested the following interpretation of an OG signal waveform in flames. When a sharp change in concentrations, e.g., an increase, occurs within the limited volume of a flame containing a sufficiently great number of charged species, then, under the action of an external electric field, the charges generated begin to move until an internal electric field is produced that opposes this motion. As a result of the movement, the region of higher charge concentrations is polarized, and the external electric field strength in this region is reduced. The distribution variations of

the electric field in the total circuit (the response to the charge concentration variations) are a result of the relaxation time of the electric field in the flame in response to an external action. Since the flame represents a collisional plasma (the motion of charges is defined by their collisions with neutral species), the rate of the field relaxation is defined by the flame conductivity. Therefore, the magnitude and the delay of the first peak of an AI signal depend on the steady concentration of charged species in the flame. The region of higher concentration of charges expands in space as long as the internal field between charges compensates for the action of the external field. Since this region is polarized, then in an inhomogeneous electric field it has an attraction for the cathode with a force $F = p\nabla E$, where p is the value of a dipole moment and E is the electric field strength. The motion of this region in space will be defined by the action of this force and by the motion of the surroundings gas flow.

Near the cathode surface at the distance of a free path of electrons, both a change from ambipolar diffusion mode into the free diffusion mode[58] as well as the simultaneous arrival of charged particles at the electrodes take place. This process defines the appearance of the second peak of an AI signal pulse and its shape corresponds to the profile of the charge concentration distribution in the above-mentioned region. The total AI signal pulse observed represents the current induced in the external circuit by the motion of laser-produced charges in the field supported in the flame by the external circuit.

C. Ionization Processes of Resonantly Excited Species in Flames

Atom/molecule absorption of monochromatic laser radiation results in a population of their excited states,

$$A + h\nu \rightarrow A^*$$

Several ways of atom/molecule ionization from excited states are possible

1. Collisional ionization,

$$A^* + X \rightarrow A^+ + e^- + X$$

2. Photoionization due to absorption of additional photons,

$$A^* + h\nu \rightarrow A^+ + e^-$$

3. Associative ionization,

$$A^* + X \rightarrow AX^+ + e^-$$

4. Energy transfer to other species with subsequent ionization,

$$A^* + X \rightarrow A + X^*$$

where X is any species in a flame.

Let us consider these processes of atomic ionization.

1. Collisional Ionization

In this case, excited atoms collide in flame with: (1) electrons, (2) laser-excited atoms, and (3) thermally excited species.

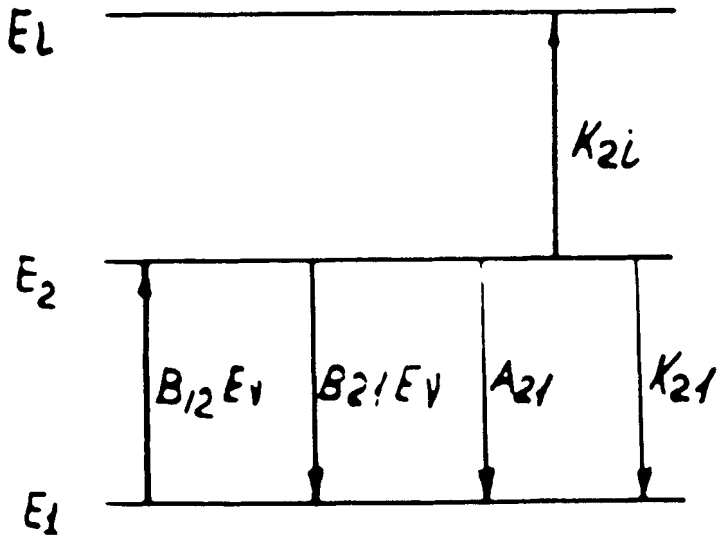

FIGURE 5. Diagram of energy levels and processes proposed by Travis et al.[21]

Electrons cannot make basic contributions to a rise in the degree of ionization because in that case an OG signal would be a linear function of electronic concentrations in a flame. Experiments have not revealed such an effect. Electron concentration in a flame can be increased significantly with addition of easily ionized atoms such as potassium or barium. However, no considerable rise of an OG signal is observed[59] in conjunction with this.

Mutual collisions of laser-excited atoms of the same element A* are also unable to make basic contributions to an OG signal because in such a situation a quadratic dependence would take place between the signal and the concentration A that is in contradiction with experimental results.

As for ionization by way of collisions with thermally excited atoms or molecules, even the very first studies on OG spectroscopy in flames[4,60] noted that just this kind of collision makes basic contributions to an enhancement of ionization of laser-excited atoms of alkali metals. In flames at atmospheric pressure, it is known that the number density of species is about 10^{18} cm^{-3} and the number of gas kinetic collisions between the species A* and other species in a flame is about 10^9 s^{-1}.[36] The most likely partners for the species A* are the atoms or molecules of combustion products as well as nitrogen molecules always present in flames at atmospheric pressure; these latter make up the major portion of the total concentration of species in flames.

Production of an OG signal under laser radiation is associated with the fact that species ionization in flames is more likely to occur from excited electronic states than from the ground state. This mechanism assumes that the OG effect will manifest itself most strongly in the case of excitation of an atom or a molecule to a state close to its ionization potential.[61]

In 1979, Travis et al.[21] investigated ionization kinetics. The authors examined four energy levels, each characterized by a definite energy E_q, population n_q, and multiplicity g_q (Figure 5):

1. The atomic ground state (E_0, n_0, g_0)
2. The lower level of optical transition used (E_1, n_1, g_1)

3. The upper level of optical transition used (E_2, n_2, g_2)
4. The ground state of an ion produced (E_i, n_i, g_i)

Ionization is assumed to occur only from the higher level of optical transition and it is postulated to be due to collisions in a flame. Under the influence of a sufficiently large electric field, the current density extracted from a flame is a direct measure of the rate of ion production per unit volume.[51] The rate constant of ion production from level j is calculated from the following expression:

$$k_{ji} = n_X\left[\frac{8kT(m_A + m_X)}{\pi m_A m_X}\right]^{1/2} \cdot Q_{jx} \cdot \exp[-(E_i - E_j)/kT] \qquad j = 0, 1, 2, \ldots \quad (5)$$

where k is the Boltzmann constant, T is the temperature, m_A and m_X are masses of an analyte atom and its collision partner, respectively, Q_{jx} is the ionization cross section of an analyte atom occupying the level j when colliding with its partner X, and n_X is the number density of the collision partner. As follows from Equation 5, the lesser the value of $E_i - E_j$ (i.e., the closer the laser-excited level is to the atom ionization limit), then the greater the ionization rate will be. For example, for a flame at T = 2500 K (kT = 1739 cm^{-1}), a decrease of the value ($E_i - E_j$) by 1 eV (1 eV ≈ 8000 cm^{-1}) will result in increase of the rate constant of collision ionization by a factor of 100.

Travis et al.[21] have taken into account only the processes shown in Figure 5, considering that electron-ion recombination in the presence of an electric field is negligible, as is thermal excitation from level 1 to level 2.

Following analysis of various radiation and collision processes, a semi-empirical formula has been suggested describing the sensitivity coefficient S_T (expressed in nA·ng^{-1}·ml) of atom determination in flames for a given atom transition,

$$S_T = C_1 X_B \beta_A [P B_{12} \cdot E_\nu^P]^{C_2} \quad (6)$$

where C_1 is the empirical constant, X_B is the Bolzmann population factor defining the population of the initial level of optical transition, β_A is the atomization efficiency factor for the analyte element in the flame being employed, $P = \exp[-(E_i - E_2)/kT]$ is a coefficient proportional to the probability of ionization due to collisions, B_{12} is the absorption coefficient for the optical transition used, E_ν^P is the laser spectral irradiance, and C_2 is an empirically determined constant which is a function of the laser pulse shape (C_2 = 1 for square wave pulses). The dimensions nA·ng^{-1}·ml mean that the current density across a flame is measured as a function of the concentration of a metal salt solution being aspirated into a flame whose metal atoms are excited by laser radiation.

The S_T values calculated from Equation 6 have shown quite good agreement with experimental data on electric current measurements. The worst deviation was equal to 100%.

Improvements of the model of collision ionization from excited states were made by Travis et al.,[54] who theoretically analyzed the efficiency of collision ionization for various excited states.

It is assumed that the total number density of species is equal to the sum of neutral and ionized species at any point in the flame at any time ($n_T = n_a + n_+$) and that $n_+ = 0$ at t = 0, i.e., the collisional ionization from the ground state produces only a negligible degree of ionization of metal analyte atoms compared with the degree produced by laser excitation.

When the laser is switched on at t = 0, the ionization rate (see Figure 5) can be expressed as follows:

$$dn_+/dt = k_{2i}n_2 - \alpha n_+ n_- \tag{7}$$

where α is the recombination factor.

When recombination is neglected, the equation takes the form,

$$dn_+/dt = k_{2i}n_2 \tag{8}$$

Assuming that the laser pulse has a square wave shape, i.e., E_{12} = a constant in the interval from t = 0 through t = τ_L, where τ_L is the laser pulse length. Defining the ratio

$$F = n_2/n_A = n_2/(n_T - n_+) \tag{9}$$

and substituting n_2 from this expression into Equation 8, we obtain,

$$dn_+/dt = k_{2i}F(n_T - n_+) \tag{10}$$

where only n_+ is a function of time.

Solving this equation, we get the following expression:

$$n_+(t) = n_T(1 - \exp[-k_{2i}Ft]) \qquad 0 < t \leqq \tau_L \tag{11}$$

and at the end of the laser pulse (t = τ_L),

$$n_+(\tau_L) = n_T(1 - \exp[-k_{2i}F\tau_L]) \tag{12}$$

It is obvious that n_+ can reach 100%, provided that

$$\tau_L \gg [k_{2i}F]^{-1} \tag{13}$$

This suggests that the possibility of complete ionization depends upon the laser pulse length and the effective collisional ionization rate constant. For pulsed lasers, the assumption of optical saturation and equality of statistical weights $g_1 = g_2$ brings about a value of F = 0.5. Then from Equation 13 we obtain the following condition:

$$k_{2i} \gg 2/\tau_L \tag{14}$$

which must be satisfied if a saturating laser pulse of length τ_L is to provide complete ionization. In order to obtain the maximum signal, Travis et al.[54] recommended selecting as high an energy level as possible, i.e., the difference $E_i - E_j$ should be minimized (see Equation 5).

When using short-pulse duration lasers, it is practically impossible to satisfy the condition of Equation 14. This pertains to commonly used dye lasers pumped by a N_2 laser or by a Nd:YAG laser (τ_L = 5 ns) when investigating elements with an ionization potential in excess of 7.5 eV. To overcome this difficulty in order to increase the sensitivity of element determination, it is necessary to employ stepwise optical excitation. If optical saturation is achieved for both transitions sharing a common energy level, then Equation 14 would be approximately valid when applied to the final (highest) level excited optically. It should be noted that, strictly speaking, instead of the factor 2 used in Equation 14, one should substitute another value reflecting the fractional population of this final level and the double saturation resulting from the statistical weights of the laser-mixed states.

Most of the above-mentioned considerations can be applied to the OG effect using cw

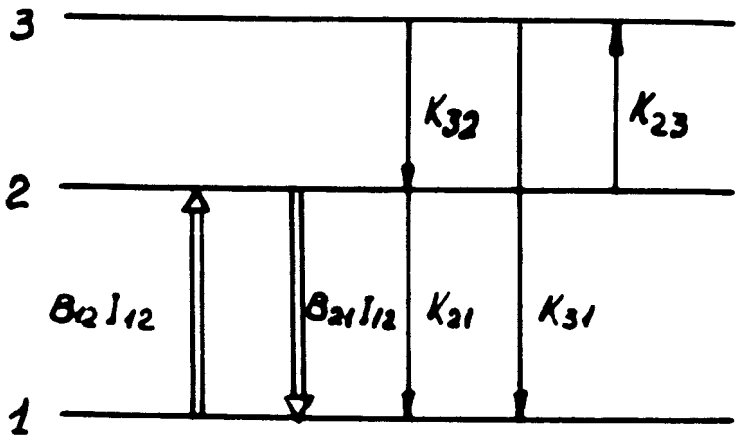

FIGURE 6. Diagram of energy levels and processes in the three-level system.[64]

lasers if the pulse length τ_L in the considerations is replaced by the residence time of an atom in a laser beam. For a flame velocity of about 10 m/s[62,63] and a beam diameter of 1 mm, this time may be about 10^{-4} s. Thus, in the case of cw lasers, the conditions of Equation 13 can be satisfied 100 times more easily than when using a flashlamp laser, and about 10^4 times more easily than when using dye lasers pumped by N_2 lasers or by Nd:YAG lasers. Even though for cw lasers the residence time of an atom in a laser beam is well over the residence time for pulse lasers, the disadvantage of the former is that they are not able to provide the achievement of saturated excited states, especially when using nonfocused radiation. And if the beam of a cw laser is focused to increase the value F, then the reduced beam diameter reduces the dwell time τ_L. The disadvantage of cw dye lasers is their limited wavelength range of operation.

A slightly modified model of collisional ionization was suggested by Swedish scientists.[59,64] These authors discussed the possibilities of all four methods of ionization of the excited atom A* and came to the conclusion that the most probable one is the collisional mechanism. In their opinion, photoionization is not the dominant process because, when using flashlamp-pumped dye lasers, they did not observe a quadratic dependence of the AI signal on the laser power. In principle, associative ionization may be one of the possible processes, particularly when the excited atom A* interacts with a species which is a component of flame combustion products. Thus, for example, the following process of associative ionization can take place for alkali elements,[65]

$$Ba + OH \rightarrow BaOH^+ + e^-$$

Nor do the authors reject an ionization mechanism involving energy transfer to other species, e.g., according to the following scheme:

$$A^* + CH \rightarrow A + CH^*$$
$$CH^* + O \rightarrow CHO^+ + e^-$$

However, it is rather difficult to take into account the contributions of associative ionization and the process of excitation energy transfer to other species, therefore Axner et al.[59] take into consideration only the mechanism of collision ionization, which they consider predominant.

Axner et al. developed a simplified three-level kinetic model (Figure 6) defined by (1) a

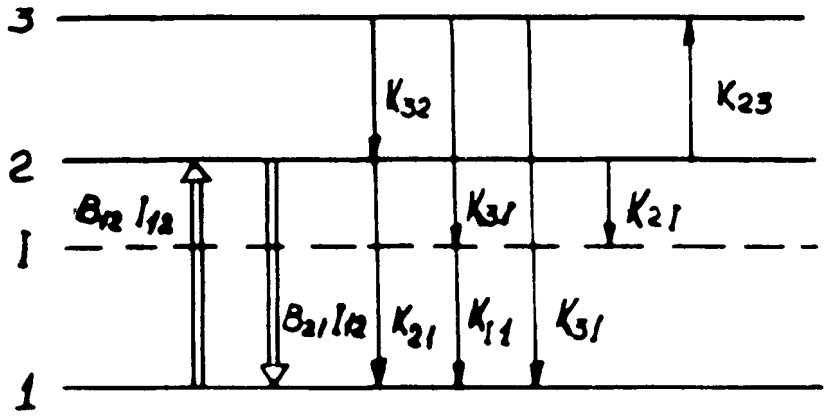

FIGURE 7. Diagram of energy levels and processes in the three-level system with intermediate level (I).[64]

lower level of optical transition, (2) a higher level of optical transition, and (3) a highly situated level from which ionization begins. The model is based on the assumption that atomic energy levels are populated according to a Boltzmann distribution, but the rates of collision excitation are defined by the conditions of detailed equilibrium. The model neglects both the rate of thermal ionization from level 1 and spontaneous radiation and takes into consideration only the processes shown in Figure 6, assuming that the ionization from level 3 is mainly collisional due to high temperature. In contrast to the results of Travis et al.,[21] however, the restoration of thermodynamic equilibrium in a medium is expected immediately after the passage of a light pulse, i.e., achievement of a new Boltzmann distribution over energy levels with regard to the population enhancement at level 2 under laser radiation. In the opinion of Axner et al., thermal ionization from level 2, which is populated because of the laser-induced transition, does not play a basic role in formation of the OG effect in flames. Instead, this role belongs to ionization from the higher energy levels (level 3) whose population is enhanced as a result of laser irradiation followed by a new thermodynamic equilibrium.

Since this three-level model is simplified and far from reality, the considerations also include one more intermediate level I (Figure 7). When the number of intermediate levels becomes fairly great, the AI signal then is reduced, a reduction which may be rather significant due to transitions which considerably reduce the population of levels 3 and 2. This model can be easily applied to two-step processes. In such processes, the number of intermediate levels is much greater and should be taken into consideration.

Based on this model, Axner et al.[59,64] calculated theoretically predicted sensitivities of determination of a number of elements, Σ_{theor}, with some simplifying assumptions. It was assumed that the lower level of optical transition was not the lowest atomic level. Since the authors did not know the constants of collision transition rate, it was assumed that these constants were proportional to the degeneracies of the highest transition levels, i.e.,

$$k_{ij} \propto g_j \tag{15}$$

The transition rate from level 2 (the quenching rate) was assumed to be 7 GHz, based on saturation measurements of the quenching rate for sodium. The thermal ionization rate was assumed to be $2 \times 10^{12}\ e^{-Ei/kT}$ Hz, based on the values available for ionization rates of alkalis[65] measured in an $H_2/O_2/N_2$ flame at the temperature of 2250 K.

Though Axner et al.[59,64] think that the measured values of Σ_{theor} correlate to a great extent

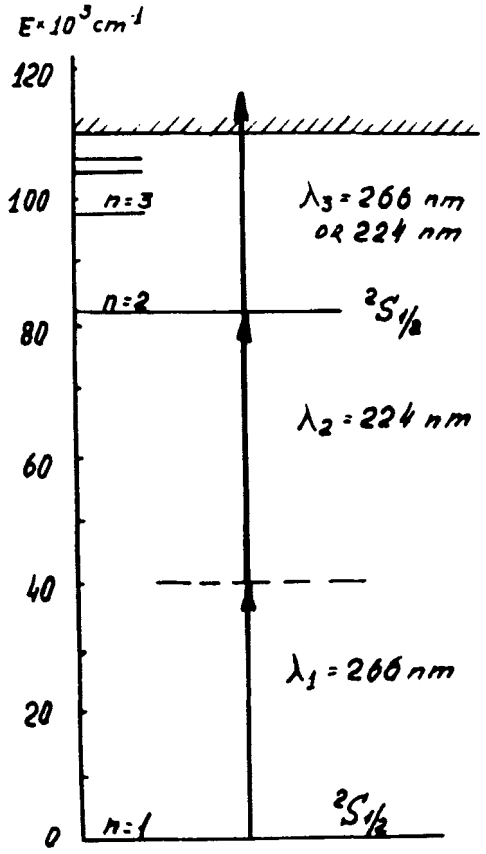

FIGURE 8. Diagram of energy levels and processes for multiphoton ionization of atomic hydrogen in flames.[31]

with the experimental values Σ_{ex}, the results indicate that the model they proposed is far from ideal. The authors also mention other possible ways of ionization, e.g., with the production of metal oxides at the intermediate stages, but they do not describe these mechanisms in detail.

Using the saturation regime during photoionization of atoms from excited states, Marunkov and Chekalin[66] measured the degree of collisional ionization, β_i, of indium and lead atoms in an acetylene-air flame. For indium, β_i, from the $5d^2D_{3/2,5/2}$ excited level, equals 0.07, and for lead during excitation of the $8p^3D_2$ level, β_i ranges from 0.4 to 0.65, depending on the flame.

2. Photoionization

In his studies, Goldsmith[31,67] obtained an AI signal from oxygen and hydrogen atoms as well as from OH radicals and NO radicals in flames. The multiphoton scheme of excitation and subsequent ionization of a hydrogen atom is shown in Figure 8. Excitation from the ground state, n = 1, into the excited state, n = 2, is accomplished by simultaneous absorption of two photons, λ_1 = 224 nm (doubling the dye laser radiation and then mixing it with the 1.06 μm first harmonic of a Nd:YAG laser) and λ_2 = 226 nm (the third harmonic of a Nd:YAG laser). Each photon of any beam has enough energy to accomplish photoionization from the excited state, n = 2. Moreover, since two-photon excitation of the n = 2 state is proportional to the product of the intensities of these beams, and the photoionization rate is to some extent proportional to their sum, then it is possible to check the rates of excitation

and ionization independently. Goldsmith proved that the observed AI signal in a hydrogen-oxygen flame is associated precisely with the photoionization of atomic oygen. The AI signal of hydrogen against a background of the multiphoton AI signals of hydroxide and nitric oxide occurs only when the flame is simultaneously exposed to two laser beams, $\lambda_1 = 224$ nm and $\lambda_2 = 226$ nm. Under the action of a single laser (e.g., with $\lambda_1 = 224$ nm), the peak related to atomic hydrogen disappears while the background signal related to the ionization of OH radicals survives. Considerable reduction of an AI signal of atomic hydrogen is observed when the distance between the laser-irradiated region and the burner head increases; this effect can be easily explained by a sharp reduction of the concentration of hydrogen atoms along the height of a flame due to their recombination.

3. Evaluation of Collisional Ionization and Photoionization in Atomic Ionization Signal Formation

When studying the mechanism of ionization of laser-excited 3P levels and 4D levels of sodium atoms, Crouch et al.[18] employed the nonresonant radiation of a nitrogen laser (337.1 nm). The energy gap between the ionization potential and the excitation energy was 3.04 eV for the first level and 0.86 eV for the second level. The authors revealed that in the case of 3P-level excitation by dye laser radiation the switch-on of a nitrogen laser increases the AI signal amplitude by 144 times. When using radiation of a single nitrogen laser, an AI signal is not observed at all. In the case of experiments with the 4D level, an increase of the AI signal is not observed.

Based on these experiments, the conclusion has been made that photoionization is the mechanism of the atomic ionization from the 3P level and in the case of 4D-level excitation it is collisional ionization. Investigations of the dependence of the AI signal on the sodium concentration, using a two-step scheme from the 3P level, have shown that the slope of the calibration curve is equal to 1 over a range covering more than two orders of concentrations, beginning with 0.1 μg/ml of sodium. From this, the conclusion reached is that associative ionization does not take place to any considerable extent since this mechanism requires two sodium atoms ($2Na^* + h\nu \rightarrow Na_2^+ + e^-$)[68,69] and in such a case the slope of the calibration curve would be equal to 2.

Later on, Crouch et al.[25] extended the number of elements under investigation by studying dual laser ionization processes in flames by resonance radiation of dye lasers and non-resonance radiation of a nitrogen laser. They examined various schemes for the excitation of atoms of lithium, sodium, potassium, calcium, strontium, indium, and cesium. For Li, Na, Ca, and Sr, the authors obtained an increase of the AI signal by two to three orders of magnitude compared with the excitation of these elements under the resonance radiation of dye lasers only. The authors think that the conditions chosen in these cases are such that photoionization from excited levels significantly predominates over collisional ionization. Among these conditions are a fairly great oscillator strength of resonance transition and a moderate (up to 0.7 eV) value of the excess of total energy, ΔE, received by an analyte atom above its ionization potential. The photoionization cross section declines with an increase of the value of ΔE. The authors emphasize, however, that the general form of the relationship between ΔE and the cross section of photoionization from an excited state is not as simple as it seems. For some elements, e.g., Cs, the computed curve plotted against ΔE for the cross section of photoionization from the 5D level has two minimums.[70]

This conclusion is also confirmed by Swedish scientists,[71] who note that high intensity of laser radiation increases the probability of photoionization. Also, when the value ΔE is small, the photoionization process can compete with or even predominate over collisional ionization processes. This is confirmed by the extremely low detection limits for Fe and Mg.

To confirm this hypothesis, Curran et al.[25] examined the results published in those papers[7,72]

which discussed the attempt to accomplish three-photon ionization of lithium atoms in flames. In these experiments, two dye lasers pumped by an Nd:YAG laser provided stepwise exitation of lithium to a 3d level whose energy was less than the ionization potential by 1.49 eV. A considerable increase of the AI signal was not observed under the action of the second harmonic of the Nd:YAG laser, which Curran et al.[25] explain by the significant value of $\Delta E = 0.84$ eV.

In the case of two-photon excitation of the 4d level of sodium and the 3d level of lithium, the AI signal does not increase under the additional action of a nitrogen laser, which the authors relate to the fact that with this additional action the atoms gain so much energy that the photoionization cross section sharply declines and in this case collisional ionization plays its role. Analogous considerations are valid for Cs (6s $\rightarrow$ 7p) and In (5p $\rightarrow$ 6s). A weak increase in the signal is observed in the latter case.

Axner et al.[73] compared the efficiencies of contributions of laser-induced photoionization and collisional ionization to the AI signal of Na, Tl, and Li in flames. For this purpose, they performed experiments either on atomic excitation into Rydberg states near the ionization potential or on their direct ionization. It was found that the ionization signal value changed smoothly with the excitation of an atom into the bound states near the ionization limit or into continuum. Good agreement was observed between calculated and measured values of the photoionization signal. Questions of the increase of noise with the introduction of atoms of easily ionized elements into a flame also were discussed.

Goldsmith[31] gives some estimates of the relative contributions of collisional and photoionization mechanisms. In the case of atomic oxygen experiments, a laser beam ($\lambda = 266$ nm) with an 1-mJ energy and 5-ns pulse length is focused onto a 200-μm spot, which corresponds to a peak power density of 0.2 GW/cm^2. Taking into consideration that the photoionization cross section of 2s-hydrogen state is equal to 7.5×10^{-18} cm^2,[74] the photoionization rate calculated is 1.7×10^9 s^{-1}, which is comparable to the frequency of gas kinetic collisions in flames. On the other hand, there are few species in a flame which have enough energy so that a hydrogen atom existing at the 2s level could obtain energy of about 3.4 eV and be ionized as a consequence of colliding with them. From this, it clearly follows that photoionization is the predominant mechanism in experiments involving hydrogen atoms. These assessments also indicate that it will be possible to attain 100% efficiency of ionization from the 2s level.

To evaluate the influence of various mechanisms on the efficiency of ionization, investigations on the value of an AI signal have been carried out[53,80] using resonance excitation of various n^2p states of potassium and rubidium atoms with known oscillator strengths of the main series transitions.[74,75] The wavelengths of the transitions from the ground state to many other n^2p states ($n > 6$ for potassium and $n > 8$ for rubidium) fall in the region of wavelengths easily obtained by doubling the radiation of dye lasers pumped by the second harmonic of a Nd:YAG laser. The frequency-doubled radiation, whose wavelength corresponds to the definite transition in a potassium atom or a rubidium atom, is directed into a propane-butane flame into which the solution of potassium and rubidium are aspirated, their concentrations being 50 μg/ml and 100 μg/ml, respectively. Since the population of a given level is proportional to the intensity of laser radiation, which changes with variations of the laser wavelength, the AI signals are then normalized to the appropriate laser power. The relative changes of an AI signal are measured when the unit photon flux is tuned to various atomic transitions.

The experimental results are shown in Table 1; they indicate that with an increase of the energy of the excited level the magnitude of the normalized AI signal falls much more than the oscillator strength of the appropriate transition.

From the assumption of the thermal nature of ionization,[21,54,64] it follows that the AI signal value A is proportional to the product of the transition oscillator strength and an exponential

Table 1
ATOMIC IONIZATION OF RUBIDIUM AND POTASSIUM WITH EXCITATION OF VARIOUS ELECTRONIC STATES

Transition	AI signal rel. unity	Oscillator strength (f)	$\Delta E = E_i - E_j$ (eV)	$f \exp\left(-\frac{\Delta E}{kT}\right)$
		Rubidium		
5s-9p	1	2.6×10^{-4}	0.336	2.7×10^{-5}
5s-10p	0.72	1.3×10^{-4}	0.251	2.4×10^{-5}
5s-11p	0.19	9.1×10^{-5}	0.194	2.5×10^{-5}
5s-12p	0.15	5.2×10^{-5}	0.154	1.9×10^{-5}
5s-13p	0.096	3.6×10^{-5}	0.126	1.5×10^{-5}
5s-14p	0.044	2.8×10^{-5}	0.100	1.4×10^{-5}
5s-15p	0.019	1.7×10^{-5}	0.088	9.5×10^{-6}
5s-16p	0.008	1.4×10^{-5}	0.076	8.4×10^{-6}
5s-17p	0.004	1.1×10^{-5}	0.065	7.1×10^{-6}
		Potassium		
4s-7p	1	2.1×10^{-4}	0.488	8.4×10^{-6}
4s-8p	0.53	8.1×10^{-5}	0.345	8.1×10^{-6}
4s-9p	0.134	3.9×10^{-5}	0.256	6.6×10^{-6}
4s-10p	0.026	2.2×10^{-5}	0.198	6.0×10^{-6}

factor increasing with the reduction of the difference between the excited level energy and the ionization potential

$$A \propto f \cdot \exp[-(E_i - E_j)/kT] \tag{16}$$

where E_j is the energy of an excited level, E_i is the atom ionization potential, and f is the transition oscillator strength for the state n. From this expression, it follows that the AI signal value should decline slower than the oscillator strength. However, the experimental relationship (Table 1) is inconsistent with these conclusions. Consequently, the assumption of a collisional mechanism of ionization from excited levels is not confirmed for these conditions.

Then the assumption of an optical mechanism of ionization of excited atoms was made because for all the schemes of excitation of potassium and rubidium listed in Table 1 the resonance photon energy is sufficient to ionize the atom by absorption of a second photon (especially assuming the rapid relaxation from the optical excited states to the lower electronic states[30,93] followed by absorbtion of a second photon). It is known[45,76,77] that the photoionization cross section, $\sigma(\epsilon)$, declines with the increase of ϵ during the ionization of alkali atoms populating the p states, where ϵ is the energy (carried away by the photoelectron) representing the difference between the energy of the ionizing photon and the energy necessary for attainment of the ionization limit from the excited p states. Since the value of ϵ increases with an increase of the energy of the excitation level, then the efficiency of photoionization, which is proportional to the product of $\sigma(\epsilon)$ and the oscillator strength of optical transition, f, will decrease more rapidly as a function of excitation energy level than f, as can be observed in this experiment (see Table 1). Thus, the assumption of an optical mechanism of ionization of these atoms corresponds qualitatively to the experimental data.

If one assumes that two-photon ionization of a species takes place, then the number of ions produced is a quadratic function of the number of incident photons, i.e., the power of the exciting radiation. Since the probability of these processes is proportional to the square

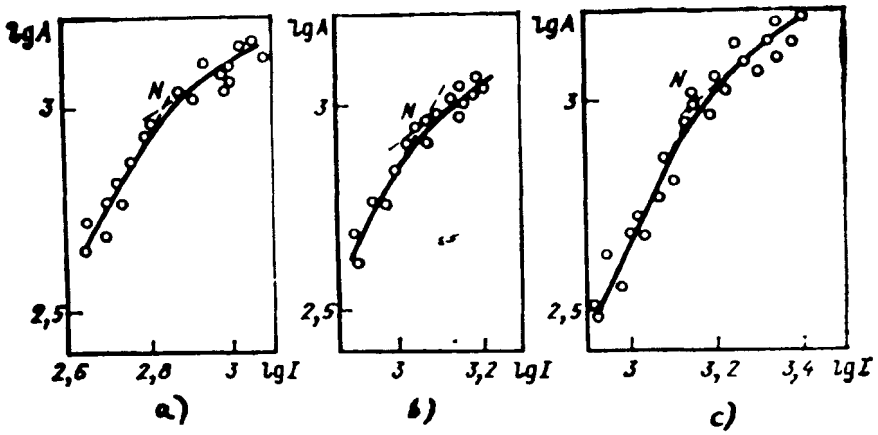

FIGURE 9. Dependence of AI signal in a flame on the laser power density when 4s-7p (a), 4s-8p (b), and 4s-9p (c) transitions in a potassium atom were excited (AI signals values are given in relative units; N is the point when the optical saturation occurred).

of the power density of the laser radiation,[78] a log-log plot of this dependence is represented by a straight line with a slope of 2. All the excitation schemes should yield this result when the energy of the second photon is sufficient to ionize the atom from an excited state (the energy of two photons exceeds the ionization energy) and first step saturation is absent. The effect of optical saturation of the bound-bound transition excited by a laser appears when there is sufficient power of exciting radiation and a low enough power of ionization radiation as, for instance, in a two-color experiment. When using the same frequency of radiation for the excitation and ionization steps, then saturation can be reached, provided that the cross section of transition between discrete levels is much larger than the cross section of ionization from an excited level.

A description of the kinetics of two-step ionization processes in the presence of optical saturation of the excitation transition with the use of pulsed laser radiation, when processes of deexcitation (or relaxation) can be neglected, requires the following relation:[79]

$$\tilde{n}_+ = n_o[1 - \exp(-\sigma_{ph}\tilde{F}_\nu/2)] \quad (17)$$

where $\tilde{n}_+$ is the total number density of resulting ions in the unit volume of excited atoms, n_o is the number density of nonexcited atoms, σ_{ph} is the cross section of photoionization of an excited atom, and $\tilde{F}_\nu$ is the total photon flux in a laser pulse (cm^{-2}).

Thus, when increasing the photon flux from a small magnitude (when in the first step optical saturation is absent), the slope of the AI signal curve in log-log coordinates is first equal to 2 and then declines and equals 1 when optical saturation is attained. During further enhancement of the flux, the slope should decline to zero in accordance with the above relation.

In order to study ionization mechanisms, Novodvorsky[53] and Zorov et al.[80] investigated, in log-log coordinates, the dependence of an AI signal value on the intensity of laser radiation. When exciting the transitions 4s-7p (321.7 nm), 4s-8p (310.2 nm), and 4s-9p (303.5 nm) in potassium atoms with small power densities of radiation, in all three cases the slope is first equal to 2 and then declines with an increase of the power density of laser radiation (Figure 9).

The values of power densities which correspond to changes of the slope also correspond to the optical saturation of resonance transitions. They are defined by the abscissa of the

intersection of tangents to the two sections of the curve before and after the saturation. For the transitions to the 7p, 8p, and 9p levels, these values are equal to 0.65, 1.2, and 1.6 MW/cm^2, respectively.

D. Analytical Applications

The main advantages of AI determinations are their high sensitivity and selectivity. Computation has shown that the minimum concentration of atoms which can be determined in flames amounts to 10^4 to 10^6 atom/cm^3 [33] or about 10^5 atom/cm^3.[81] The calculations were made assuming that the main factor restricting detection limits for various elements is the noise resulting from the fluctuations of background current in flames. The experimental detection limits for 32 elements are shown in Table 2. It should be noted that for most of the elements studied the values are lower by one to three orders of magnitude than the limits attainable with any other methods of atomic spectroscopy (atomic emission, atomic absorption, atomic fluorescence). The best values of detection limits are found at the picogram-per-milliliter level, corresponding to the minimal detected concentrations in flames, $n_{min} \approx 10^5$ atom/cm^3 (as is known,[82] the concentration of atoms in an acetylene-air flame, when aspirating into it a solution with an element concentration of 1 μg/ml, is $n_{at} \approx 10^{11}$ atom/cm^3 at the atomization efficiency of $\beta \approx 1$).

The detection limits shown in Table 2 relate to pure aqueous solutions of analyte elements. In the case of analysis of solutions with complex compositions, additional noise sources may appear which are associated with nonselective (thermal) ionization of elements with low ionization potentials as well as with multiphoton ionization of atoms and molecules of the sample matrix.[6,23,83,84] These processes reduce the signal-to-noise ratio and correspondingly increase the element detection limits for analysis of complex samples. In a number of cases, application of two-step scheme of excitation permits a reduction in the noise level when determining elements in real samples.[85] Thus, Axner et al.[86] note that for some elements they have obtained much better detection limits when using a two-step scheme of excitation (see Table 2).

As in case of other methods of spectroscopy, selectivity of AI technique depends on the bandwidth of the laser. At present, dye lasers have been developed which have a bandwidth of about 10^{-2} to 10^{-3} cm^{-1},[96,97] which is considerably narrower than the absorption linewidth of atoms in atmospheric pressure flames (0.1 to 1 cm^{-1}).[98] Thus, experimental resolution is restricted by the absorption linewidth of analyte atoms in flames. In the analysis of complex samples, the selectivity of the AI method is also limited by the possibility of coincidence of the lines of matrix elements and the lines of analyte atoms. Unlike conventional atomic spectroscopy techniques, AI determinations can be successfully employed with both resonance and nonresonance transitions as well as two-photon transitions (e.g., experiments with lithium described by Turk et al.[22]) which permit one to avoid spectral interferences. Spectral interferences can sometimes be avoided by spectra scanning when the laser is tuned across the transition being used.

Unique possibilities for an increase in sensitivity (in the case of determination of elements with high ionization potentials) and in selectivity using two-step ionization of atoms in flames were first demonstrated at Moscow State University.[26,27] Two-step schemes have also been successfully employed for AI determination of elements with high (up to 9.2 eV) ionization potentials (Au, Cd, Co, Cu, Ni, Pb, Sn).[25] The magnitude of a signal of two-step excitation is 35 to 1300 times greater than the amplitude of a signal of one-step excitation, depending on the analyte atom.

Two-step excitation considerably improves spectral selectivity since the probability of the simultaneous coincidence of two transitions used to excite an analyte atom and two transitions of a matrix atom is very negligible. The coincidence of one of the two analytical lines of Co (λ_1 = 252.136 nm) with the line of the matrix element In (λ = 252.137 nm), falling

Table 2
DETECTION LIMITS (ng/ml) OF ELEMENTS BY LASER ATOMIC IONIZATION SPECTROMETRY IN FLAMES

Element	Wavelength of 1st step dye laser (nm)	Wavelength of 2nd step dye laser (nm)	Pumping source[a]	Flame[b]	Detection limit	Ref.
Ag	328.1	421.1	Ex	A-A	0.05	87
Al	309.3		Fl	A-N_2O	0.1	9
As	278.02		Ex	A-A	3000	88
Au	242.8	479.3	Nd:YAG	A-A	1	32
Ba	307.2		Fl	A-A	0.2	22
Bi	306.8		Fl	A-A	2	22
Ca	300.7		Fl	A-A	0.1	22
Cd	228.8	466.2	Nd:YAG	A-A	0.1	32
Co	252.1	591.7	Nd:YAG	A-A	0.08	32
Cr	298.6		Fl	A-A	2	22
Cs	455.5		N_2	A-P	0.004	24
Cu	324.8	453.1	Nd:YAG	A-A	0.07	32
Fe	302.1		Ex	A-A	0.08	71
Ga	294.4		Ex	A-A	0.04	71
In	451.1	571.0	Nd:YAG	A-A	0.0004	89
K	404.4		N_2	A-P	0.1	90
Li	670.8	460.3	Ex	A-A	0.0002	91
Lu	308.2		Fl	A-N_2O	0.2	9
Mg	285.2		Ex	A-A	0.003	71
Mn	279.5	521.5	Nd:YAG	A-A	0.02	9
Mo	319.4		Fl	A-N_2O	1	20
Na	589.0	568.8	N_2	A-A	0.0006	92
Ni	300.2	576.5	Nd:YAG	A-A	0.08	32
Pb	283.3	600.2	Nd:YAG	A-A	0.0007	89
Rb	420.2		N_2	A-P	0.1	90
Sb	287.79		Ex	A-A	50	88
Sc	301.9		Fl	A-N_2O	0.2	9
Si	288.2		Fl	A-N_2O	40	20
Sn	284.0	597.0	Nd:YAG	A-H_2	0.3	32
Sr	460.7	554.3	Ex	A-A	0.2	93
Ti	318.6		Fl	A-N_2O	1	20
Tl	291.8	377.6	Ex	A-A	0.008	30
Tm	297.3		Fl	A-N_2O	200	9
V	318.4		Fl	A-N_2O	0.9	20
W	283.14		Ex	A-A	300	88
Y	298.4		Fl	A-N_2O	10	9
Yb	555.6	581.2	Nd:YAG	A-A	0.1	92
Zn	213.8	396.5	Nd:YAG	A-A	1	94

[a] Ex = excimer laser; Fl = flashlamp; Nd:YAG = neodimium laser; N_2 = nitrogen laser.
[b] A-N_2O = acetylene-nitrous oxide; A-A = acetylene-air; A-P = air-propane-butane; A-H_2 = air-hydrogen.

within 0.001 nm of each other, does not interfere with the determination of Co in the presence of the excessive amount of In.[32]

Magnusson et al.[85] examined ways for eliminating spectral interferences from matrix elements in solutions. They showed that selectivity can be much improved by the correct selection of experimental parameters. This is illustrated by the determination of low concentration of Mg in the presence of the Na matrix. Spectral interferences existing in the one-step scheme of excitation for AI determination of Mg decline 70 times when using a

two-step scheme. Spectral resolution is even more improved, in general 1300 times, by optimizing (reducing) the intensity of a laser without any particular loss in sensitivity. The experiments show that under these conditions Mg can be determined in solution, in the presence of a 10^5-fold excess of Na. They also show that spectral interferences arising from the presence of NO molecules in an acetylene-air flame can be reduced efficiently. Signals from the molecules can be suppressed using a lower intensity of laser radiation, e.g., by defocusing, and/or by using two-step excitation. Using these techniques, the authors have successfully carried out the determination of Mg in samples containing large quantities of Na, such as urine and tap water.

Several ionization signals were observed by Omenetto et al.[97] for strontium atoms in an acetylene-air flame when a single, pulsed dye laser was focused into it. These signals were clearly different from those obtained at exact single-photon or two-photon resonances. Some considerations were pointed out from these observations. The signals were attributed to near-resonance two-step excitation followed by collisional ionization with flame species. When a single dye laser is focused in a flame so that high photon irradiances are achieved, the radiative absorpion rate in the far wings can be sufficiently large so that the near resonance ionization can easily be observed. This can be a problem for analytical applications because the resulting spectrum can be very complex, especially when the analyte atoms are present as trace constituents in a solution containing large amounts of other concomitants. As a result, the possibility of observing spectral interferences becomes severe, and there appears to be "a threshold" for the maximum laser irradiance which is analytically useful.

Recently, the AI method has begun to be used for determination of low concentrations of molecules. The review of Webster and Rettner[98] summarizes the results of the AI spectroscopy of a number of molecules. The first study reporting observations of the ionization spectrum of molecules of LaO, SrO, and YO in a hydrogen-air flame dates back to 1978.[23] In their more recent study, Mallard et al.[99] investigated resonance two-photon ionization of NO molecules in a $H_2/O_2/N_2O$ flame within the 270- to 317-nm spectral region. They note the possibility of determining NO with the detection limit of 1 ppm. The same detection limit is attained in determination of NO molecules in methane-air flame.[83] The authors have employed four-photon ionization of NO in the 425- to 455-nm region. Two-photon ionization of PO molecules in an enriched acetylene-air flame has been first observed by Smyth and Mallard.[84] The detection limit turns out to be as good as 1×10^{-8} mol fractions. Novodvorsky et al.[34] measured phosphine impurites in acetylene at a level of 7×10^{-3}% of volume. Phosphine combustion in a flame provides PO molecules that can be detected from the AI spectrum within the 320-nm region.

In AI determination of elements in hydrocarbon flames, it is necessary to take into consideration the possibility of the emergence of spectral interferences associated with the multiphoton ionization of some molecules in flames, e.g., NO and PO.[85,94]

It should be noted that at higher temperatures at the surface of an electrode detecting the ionization of an analyte atom complex processes can occur with the result that, in the close vicinity of the electrode, free atoms of elements will emerge from the electrode material. Thus, for example, when using nichrome and stainless steel electrodes in a flame and working in the 537- to 560-nm region, it appears in up to 28 lines in an AI spectrum. It has been found that these lines correspond to the transitions of atoms of Fe, Ni, Mg, and Co.[100,101] All these atoms enter into the composition of electrodes used, and the AI signal obtained corresponds to their transitions from the excited atomic states. An AI signal depends on the fuel gas-oxidizer gas-consumption ratio, which has a significant effect on the temperature and composition of the combustion products in the immediate vicinity of the electrode surface. When developing analytical procedures for the determination of elements, chemical analysts should take into consideration the interferences resulting from possible occurrences of this effect due to evaporation of elements from the electrode surface.

In analytical practice, the most important and difficult case is the determination of element traces in the presence of a great excess of elements with similar properties. The AI determination of elements in complex samples at an atomization stage obviously is accompanied by all kinds of matrix interferences which are observed in conventional flame atomic spectroscopy methods. One of the advantages of the AI method is the absence of some interferences inherent in the methods of optical detection of a signal and related to light scattering, self-absorption, and flame radiation.

The first studies on the AI method have revealed strong depressing effects on an AI signal value of a matrix containing a great number of easily ionized elements.[6,102] These effects are due to ionization interferences specific to the AI method which are associated with the increase of the number of charged species in flames as a result of thermal ionization of easily ionized elements. An increase of the number of species leads to a change of the electric field distribution in flames as well as to a decrease of the response time of a medium (OG signal) to external action (laser radiation).

Ionization interferences and ways of eliminating them are being intensely discussed in the literature on the subject. Green et al.,[37] Trask and Green,[38] and Havrilla and Green[47] performed detailed investigations on the influence of various concentrations of Na and K on an AI signal of In in relation to the configuration of electrodes and their voltage, the height of the irradiation zone in flames, and the consumption of fuel gas and oxidizer. It has been found that aspiration of solutions containing Na and K at 1- to 10-μg/ml concentrations brings about the reduction of an AI signal to the vanishing point. Various schemes and configurations of electrodes have been investigated to reduce the ionization interferences (see Figure 3). In the three studies mentioned earlier, schemes (b) and (c) with the cathode placed outside the flame were employed. Green and colleagues[38,47] suggested a double system of electrodes (Figure 3d) in which the first cathode, situated closer to the burner (anode), serves as a collector of nonselective thermal ions, and the second pair of electrodes is designed to detect an AI signal. However, no noticeable reduction of ionization interferences is attained. The use of a U-shape flat cathode and anode placed outside the flame (Figure 3e) is not efficient either.[38]

The results obtained by Zorov et al.[33] in their study on ionization interferences with the use of an electrode (cathode) immersed into a flame (Figure 3a) show that this system has advantages and provides lower ionization effects on the AI signals compared with layouts where electrodes are positioned outside a flame. A little later, experiments were carried out with the use of a water-cooled cathode inside the flame[39] (Figure 3e) and cathodes of various configurations placed inside the flame of a total consumption burner;[103] these experiments confirm the advantages of this arrangement for reducing the ionization effects. Thus, for example, with a cathode placed in a flame, the suppression of an AI signal occurs when the concentrations of matrix elements are 100 times higher than with a cathode placed outside a flame (Figure 10). This means that when using the "cathode in a flame" setup, direct AI determinations can be performed in samples containing large quantities of elements with low ionization potentials.

The advantages of the "cathode in a flame" setup are easily explained on the basis of the experimental data on the potential distribution around a cathode immersed into a flame (Figure 11). It has been shown that the total potential drop between a cathode and anode (burner head) takes place in the region near the cathode.[52] Efficient detection of selectively produced ions comes about only in the region in which the potential value is not equal to zero. The space charge density of positive ions produced by thermal ionization of matrix atoms in flames increases with the increase of concentrations of matrix elements in solutions. Because of this, the radius of the nonzero potential zone, in which the laser beam must be brought closer to the cathode surface, declines. In the case of the "cathode-in-flame" setup, the distance between the laser beam and the cathode may be fairly small, down to tenths of a millimeter (it is limited only by the photoeffect onset when the laser beam touches the

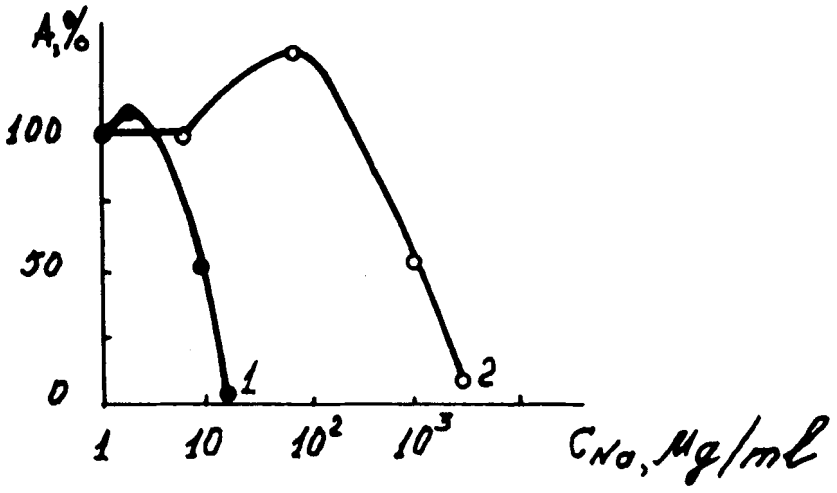

FIGURE 10. Effect of sodium concentration on the AI signal for: 1, determination of indium (electrode outside the flame);[37] 2, determination of cesium (electrode inside the flame).[52]

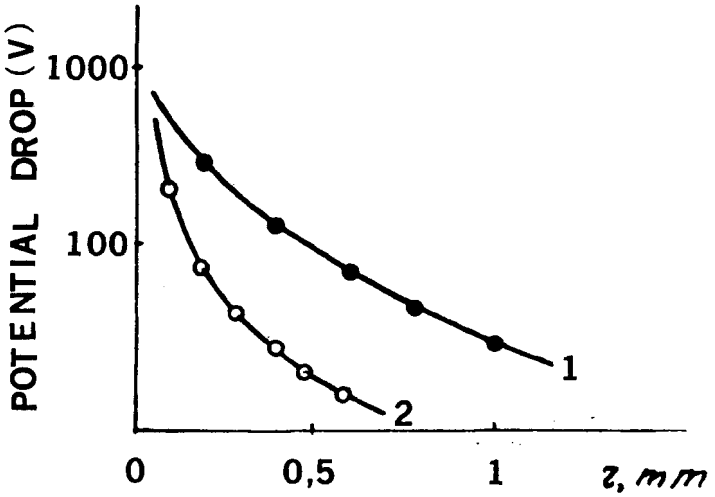

FIGURE 11. Potential drop near the cathode for various concentrations of charged species in a flame: 1, unseeded flame; 2, aspiration of sodium solution into the flame (C_{Na} = 30 μg/ml).

electrode surface). When the cathode is placed outside the flame, this distance becomes significantly greater and results in considerable ionization effects on an AI signal.

Introduction of an electrode (cathode) directly into a flame allows one to use the technique of analyte solution deposition onto an electrode itself. This technique has an advantage in that the excitation and ionization of atoms takes place in the sample atomization zone, and therefore the efficiency of sample utilization is very high. Due to this fact, low absolute detection limits have been obtained[104] (2×10^{-15} g for cesium). When depositing 10^{-14} g of sodium onto an electrode, the signal-to-noise ratio is 1000. Smaller quantities of Na cannot be deposited onto an electrode because of the sodium impurity of water used and the environmental atmosphere. However, the reproducibility of this technique is somewhat worse than in the case of aspiration of a sample solution into a flame, and its value is about 20 to 30%.

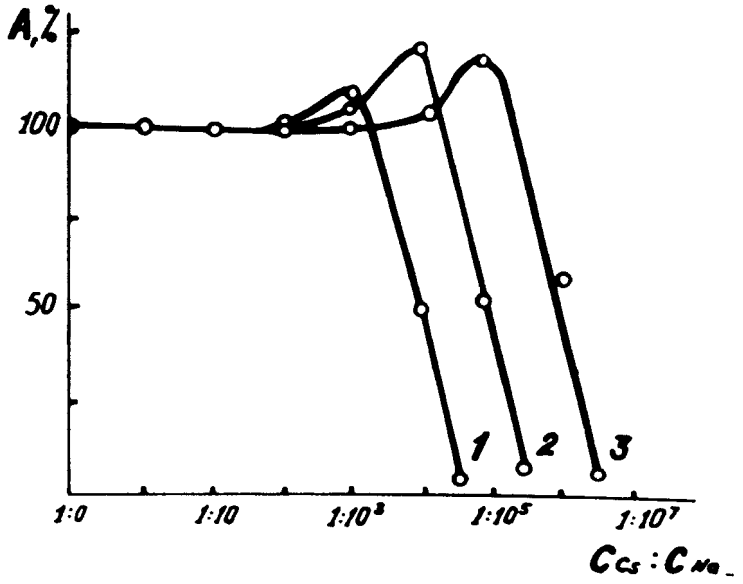

FIGURE 12. The effect of C_{Cs}/C_{Na} ratio on the cesium AI signal for various cesium concentrations: 1, 100; 2, 10; 3, 1 ng/ml; (the value of AI signal with no sodium additions is taken as 100%).

By studying the effects of various quantities of Li, Na, K, Rb, Ca, and Fe on an AI signal of Cs (with the content of Cs at a level of 1, 10, and 100 ng/ml), Chaplygin et al.[24] found that an AI signal is affected by the matrix element content of a sample rather than by the relation between its concentration and the concentration of an analyte. Thus, a Cs signal reduction by approximately 50% occurs when the Na concentration is about 1000 μg/ml, irrespective of the Cs concentration (Figure 12). In addition, the depressing effects of all other elements depend only on their total amount in the mixture. Therefore, to eliminate the ionization effects, it is sufficient to dilute the initial solution so that during its aspiration into a flame the concentration of thermal ions resulting from the sample matrix is insignificant. Nippold and Green[105] came to the same conclusion after investigating the ionization effects of K on an AI signal of In.

There is another way to reduce matrix interferences; reduce the quantity of a sample being analyzed, i.e., the use of micromethods. In order to solve this problem, an atomizer[106] has been developed which serves as a special burner (Figure 13). The central channel of the burner contains an electric heating wire loop or filament upon which the sample is deposited. Using this burner permits us to simultaneously solve several problems. Deposition of small quantities of a substance being analyzed onto the filament means that the sample matrix will contain only a small absolute quantity of easily ionized atoms which will interfere with the determination. The use of a Varian-Techtron CRA-90 programmed temperature-control unit for heating the filament allows separation of signals in temperatures and in times of appearance produced by different elements (namely, the analyte element and the sample matrix elements) due to the difference in the volatilization temperatures of the compounds of these elements. The results of application of this atomizer are presented in Figure 14. The detection limit of cesium is 5×10^{-13} g, and the reproducibility is better than 5 to 6%. Such a burner, providing separate vaporization and sample atomization, makes possible not only the reduction of reciprocal influence of elements but also the analysis of microsamples.

Curran et al.[106a] examined the effects of various amounts of K, Cs, Mg, and Zn on an AI signal of Na, Li, and Sr using a two-step scheme of ionization. It has been shown that this scheme provides ionization of excited atoms of Li, Na, and Sr, for the most part, by

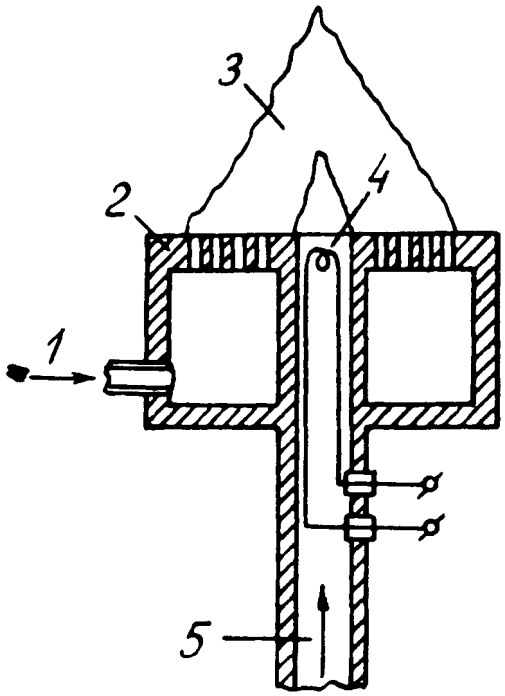

FIGURE 13. Atomizer with separate vaporization and atomization of sample: 1, introduction of fuel and air; 2, burner body; 3, flame; 4, electrically heated loop; 5, argon introduction.

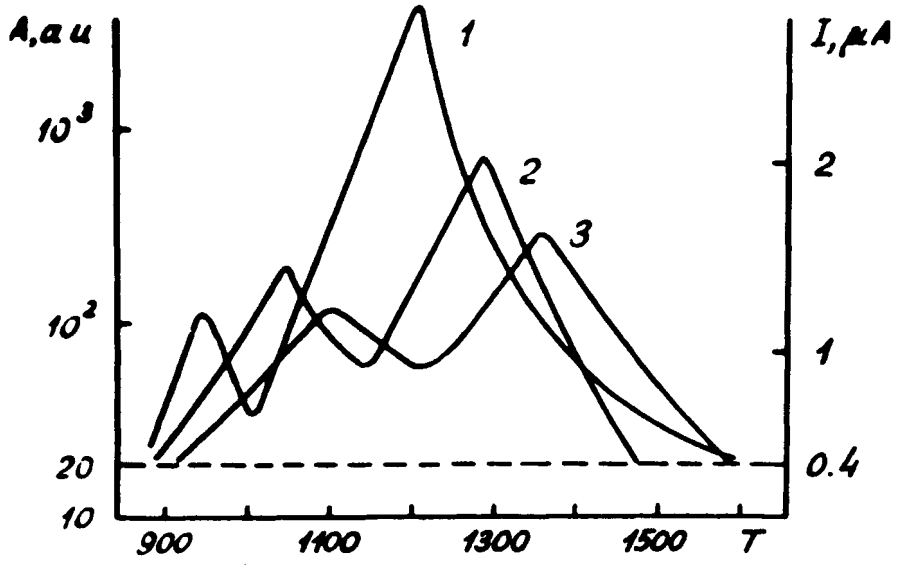

FIGURE 14. Temperature dependence of Al signal of cesium (A) and background signals (I) of Na and Rb: 1, cesium signal (m_{Cs} = 5 × 10^{-9} g); 2, background current of rubidium (m_{Rb} = 5 × 10^{-7} g); 3, background current of sodium (m_{Na} = 5 × 10^{-7} g). The noise level is 20 arbitrary units; flame conductance 0.4 μA for evaporation of 5 μl of high-purity water.

Table 3
EXAMPLES OF LASER ATOMIC IONIZATION ANALYSIS OF VARIOUS SAMPLES IN FLAMES

Sample	Element to be detected	Content (wt%)	Ref.
Cs metal, special pure, N1	Rb	$(3.3 \pm 0.6) \times 10^{-3}$	80
Cs metal, special pure, N4	Rb	$(8.4 \pm 1.1) \times 10^{-4}$	80
Rb_2CO_3, special pure	Cs	$(7.0 \pm 0.4) \times 10^{-4}$	80
K metal, N1	Cs	$(7.6 \pm 0.5) \times 10^{-3}$	80
K metal, N2	Cs	$(6.8 \pm 0.5) \times 10^{-3}$	80
Tap water	Rb	$(7.0 \pm 0.5) \times 10^{-7}$	80
Pine needles, SRM 1575	Rb	$(1.1 \pm 0.1) \times 10^{-3}$	108
RbCl, special pure, 16-2	Cs	$(1.3 \pm 0.1) \times 10^{-3}$	106
Tap water	Cs	$(6 \pm 1) \times 10^{-8}$	24
Ni alloy	In	3.5×10^{-3}	22
Steel, SRM 362	Sn	$(1.6 \pm 0.1) \times 10^{-2}$	32
Steel, SRM 363	Pb	$(2.2 \pm 0.1) \times 10^{-3}$	32
Steel, SRM 363	Ni	$(4.3 \pm 0.2) \times 10^{-4}$	32
Copper, SRM 396	Sn	$(6.7 \pm 0.5) \times 10^{-5}$	32
Semiconductor alloy	In	2.9×10^{-2}	28
Organo-silicon polymeric materials	K	$10^{-5} - 10^{-6}$	107
Tap water	Mg	—	85
Urine	Mg	—	85
Sn metal	In	$10^{-6} - 10^{-7}$	109
Al alloys	Na, K, Li	$10^{-1} - 10^{-4}$	110
Natural waters	Pb	$10^{-6} - 10^{-8}$	111
Pb metal	Tl	10^{-4}	30
Water, SRM 1643a	Zn	7.3×10^{-6}	94
Petroleum, SRM 1634a	Ni	2.8×10^{-3}	112
Heavy oil flash distillate	Ni	1.2×10^{-3}	112

the absorption of an additional photon (photoionization mechanism).[25] The authors have found that the presence of large amounts of easily ionized elements results mainly in an increase of the noise level due to multiphoton ionization of matrix atoms. Therefore, to reduce and eliminate ionization interferences in analysis of complex samples it would be promising to (1) immerse a cathode directly into a flame and pass a laser beam right up to its surface; (2) dilute a sample; and (3) use micromethods, i.e., to use small absolute quantities of substances for analysis.

Analytical practice often deals with samples having large quantities of silicon compounds whose aspiration in flames produces thermostable silicon dioxide. The latter is deposited onto the surface of the electrode detecting the AI-produced ion in flames to the point that eventually the AI signal of an analyte vanishes completely.[107] To eliminate such interference during the analysis of samples which have elements producing thermostable oxides in flames, we suggested[40] a procedure of additional electric heating of a cathode. When this is done, SiO_2 deposit onto the cathode surface is not observed. The technique is used to determine directly the contents of K in silicon-bearing samples at a level of 10^{-4} to 10^{-5}% without the time-consuming procedure of matrix separation.

Table 3 lists some examples of direct AI determinations of elements in complex samples in a number of cases, however, it would be useful to perform previous separation of easily ionized elements. Thus, Berglind et al.[113] connected an on-line laser AI detector with a high-pressure liquid chromatography (HPLC) system equipped with a UV absorbance detector. The feasibility of this combined detector system has been demonstrated for metal analysis in HPLC-separated compounds. In the situation where the compounds are not separated in the HPLC column, the AI detector can be used for selective detection of the

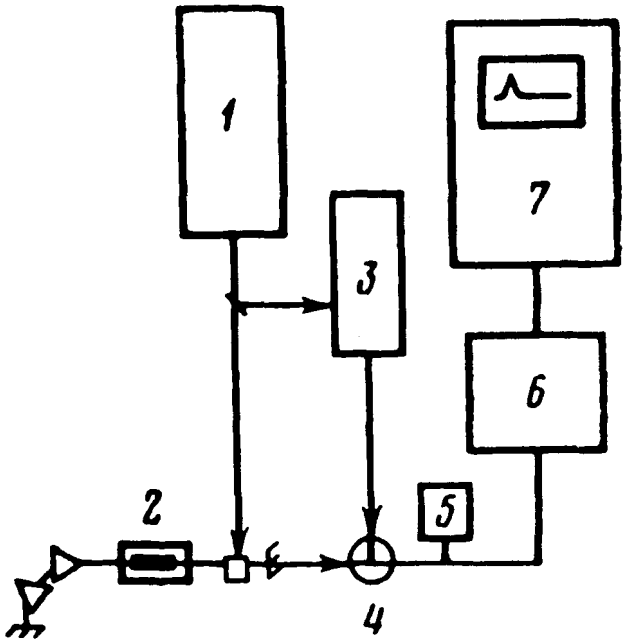

FIGURE 15. Experimental setup for intracavity laser spectroscopy with a resonance ionization photon detector: 1, pumping laser; 2, acetylene-air slot burner placed inside the resonator of the dye laser with the bandwidth of 20 cm^{-1}; 3, dye laser; 4, propane-butane flame (the resonance ionization photon detector cell with atomic vapors); 5, source of voltage applied to the electrode in flame; 6, amplifier; 7, oscilloscope.

compounds containing the metal. In these experiments, the detection limit of the system for metal determination was approximately 1 ng for Fe, but could easily be improved by orders of magnitude.

E. Photon Detectors Based on Atomic Ionization Spectroscopy in Flames

One of the most interesting applications of selective laser ionization of atoms in analytical spectroscopy is the detection of weak light fluxes bearing analytical information based on the use of resonance ionization photon detectors.[114] This detector was first used to detect weak absorption lines of Li atoms in intracavity laser spectroscopy.[72] The experimental setup is shown in Figure 15. The second harmonic of an Nd:YAG laser is used to pump two dye lasers, one (Figure 15, 2) tuned to the 670.8-nm wavelength and the other (Figure 15, 3) tuned to the 610.4-nm wavelength, and the Li atoms are excited to the 3^2D state. An acetylene-air slot burner is placed inside the resonator of the first laser, and lithium standard solutions are introduced into the burner flame. The radiations of both lasers are directed into the center of a propane-butane burner (Figure 15, 4) into which a lithium solution of 10-μg/ml constant concentration is aspirated. The flame of the propane-butane burner serves as a photon detector cell for the lithium resonance absorption line. While aspirating the Li standard solutions into the acetylene-air flame burner placed in the resonator, the calibration curve is plotted, whose characteristic concentration is equal to 0.03 μg/ml. The determination of Li up to a 10-μg/ml concentration using this method is found to be preferable to the determination of Li by a single-pass absorption technique since an absorption signal is several times higher in the first case.

Some other applications of resonance ionization photon detectors have been discussed by Matveev[115] and Dorofeev and Aidarov.[116]

F. Combustion Diagnostics

It should be noted that methods based on AI spectroscopy are becoming powerful tools for diagnosing combustion processes in flames.[117] These have been used for the determination of flame velocities[62,63] and temperatures,[118] for investigation of space distribution of neutral and charged particles, and for measurement of ion mobilities[33,46,119,120] and ambipolar diffusion coefficients[53,118] as well as the degree of ionization of various elements in flames.[91,121,122]

Schenk et al.[63] suggested employing laser-enhanced atomic ionization for the determination of the space distribution of gas velocities in flames. The idea behind the method of measurement of gas velocities is as follows. Two colinear beams of cw dye lasers are directed into a flame. The beams are vertically spaced 1 to 2 mm apart, and the wavelength of both lasers is tuned to the 3s-3p resonance transition of a Na atom. The local concentration of Na atoms in the ground state varies in the flame zone being irradiated by the lower beam. This variation can be made periodic by modulating the lower beam in a specific way. In this case, the intensity of the higher beam passing through the flame also varies periodically due to the periodic variation of the concentration of Na atoms resulting from their interaction with the lower beam. The time delay or phase delay in the intensity variation of the higher beam (the intensity variation is controlled by absorption or fluorescence) in relation to the lower beam carries information on the velocity of Na atoms in the gap between the two beams. The velocity of an acetylene-air flame is measured at 11 to 12 m/s. The space resolution of this method is ensured by only two coordinates, the vertical and the horizontal.

Kuzyakov et al.[62] suggested a simpler experimental method for the measurement of gas velocities in flames based on the use of pulsed dye lasers, which makes it possible to measure gas velocities in flames at any point. Two laser beams are directed into the flame. These beams are situated in a horizontal plane at an angle to each other so that they intersect at the point in the flame where the measurements of gas velocities should be taken. The wavelengths of the lasers are tuned to two succeeding resonance transitions of a sodium atom in order to excite it to the $3^2D_{5/2}$ state. The resonance excitation and ionization of Na atoms occur in the area of the beam intersection, and therefore the concentration of charged species becomes higher in this area than in the surrounding gas. Since the diffusion coefficient of electrons exceeds the one of Na atoms by more than two orders of magnitude, then a positive charge is produced in the center of the region. This charge is detected by a neutral probe electrode placed into the flame above the zone of excitation. The delay of the charge arrival to the probe electrode in relation to the instant of laser irradiation is caused by the flame-burning velocity and distance between the region irradiated and the probe electrode. The flame-burning velocity estimated for an acetylene-air flame is 11.5 ± 0.9 m/s, and for a propane-butane-air flame it is 7.3 ± 0.7 m/s.

There are few data on metal ion mobilities in flames[123] and they are often contradictory, but ion mobility is an important gas kinetic parameter. Ion mobility measurement procedure based on detection of AI signals is simple and fairly accurate. Zorov et al.[33] performed measurements for a propane-butane-air flame of ion mobilities of Li (μ_{Li^+} = 17.0 ± 3.2 $cm^2/V \cdot s$) and Cs (μ_{Cs^+} = 10.1 ± 2.1 $cm^2/V \cdot s$). The layout of electrodes and the laser beam is shown in Figure 16. A cylindrical anode made of a nichrome grid, r_a = 1.5 cm, is placed into a flame around a cathode made of nichrome wire, r_c = 0.5 mm. The anode is placed so that it disturbs the flame as little as possible. By focusing the two laser beams (a two-step excitation scheme is used for Li, λ_1 = 670.8 nm and λ_2 = 610.4 nm; and the single step excitation scheme is used for Cs, λ = 455.5 nm) at different distances r from the cathode, measurements are taken of the delay of the ion pulse arrival to the cathode in relation to the occurrence of the laser pulse τ. The ion mobility μ_+ is determined from the following expression:

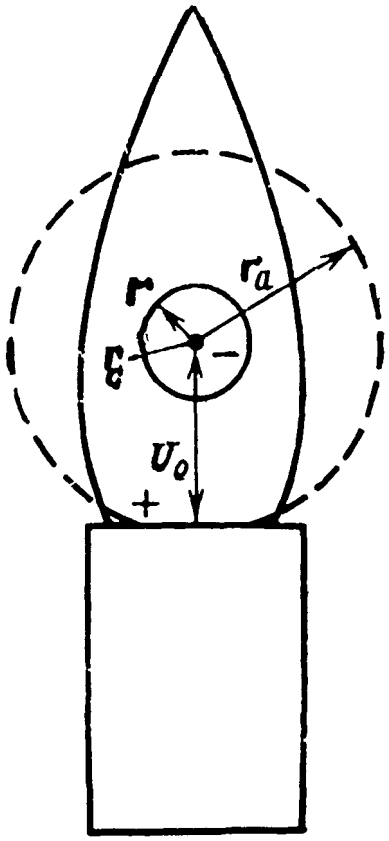

FIGURE 16. Electrodes and laser beam arrangement for ion mobility determination in flames.

$$\mu_+ = r^2 \ln(r_a/r_c)/2u_0\tau \quad (18)$$

where u_0 is the potential of the cathode.

The identical procedure has been used for the determination of the ion mobilities of Na, K, Rb, Ga, and In: 17.7, 15.8, 11.0, 18.3, and 10.1 $cm^2/V \cdot s$, respectively.[120]

Mallard and Smyth[119] developed a technique for the determination of ion mobilities (Li, Na, K, Ca, Fe, Sr, Ba, In, Tl, U) based on measurements of AI signals in an acetylene-air flame. In order to create a localized ion cloud, the authors used a nitrogen-pumped, tunable dye laser. The ion current pulses were detected by a cathode made of tungsten. The mobilities of metal ions were determined by measuring the change of the electric field strength and the laser beam-cathode distance, simultaneously measuring the delay of the arrival of an ion pulse to the cathode. Experimental mobilities do not differ from the values calculated by the Langevin theory by more than 50%.

Using a system made of two "floating" electrodes placed into a $H_2/O_2/Ar$ flame, measurements have been taken of diffusion coefficients (D) and mobilities (μ) of Na and Li ions[36] with the aid of AI signals. The excitation of Na atoms is performed using the two-step scheme, $\lambda_1 = 589.0$ nm and $\lambda_2 = 337.1$ nm (nonresonance radiation of a nitrogen laser); and the excitation of Li atoms is performed using the two-photon scheme, $\lambda = 639.2$ nm. The mobilities turn out to be 30.2 ± 0.6 and 38.6 ± 2.1 $cm^2/V \cdot s$, and the diffusion coefficients are 5.65 ± 0.30 and 6.70 ± 0.34 cm^2/s for Na and Li, respectively. In the

same study, the Einstein formula $T = gDk^{-1}\mu^{-1}$ (where g is the electronic charge and k is the Boltzmann factor) has been used to calculate the temperatures of a $H_2/O_2/Ar$ flame, which turn out to be 2171 ± 123 K for Na and 2014 ± 150 K for Li.

Turk and Omenetto[124] reported that they observed two different modes of Sr^+ decay in acetylene-air flame. The first one was a fast decay, occurring with an exponential decay time constant of 58 ns, caused by flame reactions between Sr^+ and flame species present under oxygen-rich conditions. The fast decay consumes 85% of the laser-produced Sr^+ ions before reaching equilibrium. The remaining 15% of the ions decay at a much slower rate, with an exponential time constant of 57 μs, caused by ion-electron recombination and/or gas flow and diffusion.

A little later, Turk et al.[125] studied the recombination kinetics between the strontium ions and the electrons in an inductively coupled plasma (ICP). The most significant difference between Sr^+ decay in the flame and the ICP is the absence of the fast decay caused by flame chemistry. It means that in argon ICP there is no complex chemical interactions, which are often the origin of interferences in flames and other excitation sources in molecular gas. The observed recombination rate (time constant was 15.5 μs) is somewhat faster in the ICP than in flame. This seems reasonable since the electron number density is much higher in the ICP, but comparison simply on the basis of electron number density is not justified since the detailed mechanisms of recombination are different. The absence of N_2 in the ICP as a third body collisional partner for recombination is particularly relevant.

G. Conclusion

From the present theoretical and experimental data, one must conclude that the selective laser atomic ionization of atoms seeded in a flame is a powerful technique for trace analysis of elements.

Detection limits of the flame AI method are superior to those obtained with existing flame spectrometric methods. The use of flames as an atomization source is a simple, reliable, cheap, and rapid method and obviously will be attractive to analytical chemists for a long time.

Despite the fact that low detection limits have been obtained (<1 pg/ml) with the use of a flame, there are some drawbacks intrinsic in this method. These include dilution of a sample by flame gas combustion products and the limited range of temperatures used. There also are some chemically active combustion products which react with analyte atoms, reducing their number density in the analytical volume.

Methods combining separate vaporization and atomization of a sample in a flame apparently make it possibile to avoid some drawbacks intrinsic to flames which result from ordinary pneumatic aspiration of a sample solution into a flame.[106,126]

Another drawback mentioned earlier, i.e., electrodes detecting the appearance of an additional number of ions, sometimes gives rise to interference.[100,101]

Ion detection devices based on the ability of ions to absorb microwave radiation have been suggested.[127,128] But, at present, results achieved by using such devices are not good enough to utilize them in analytical chemistry.

The flame version of the AI method has one more drawback. To reach optical saturation of the spectral transition under investigation, it is necessary to use high irradiance which, in some cases, might cause undesirable multiphoton ionization of matrix components.

The number of published papers devoted to applications of the flame AI method for trace element determination in real complex samples is increasing, indicating that the difficulties associated with the use of flames can be overcome.

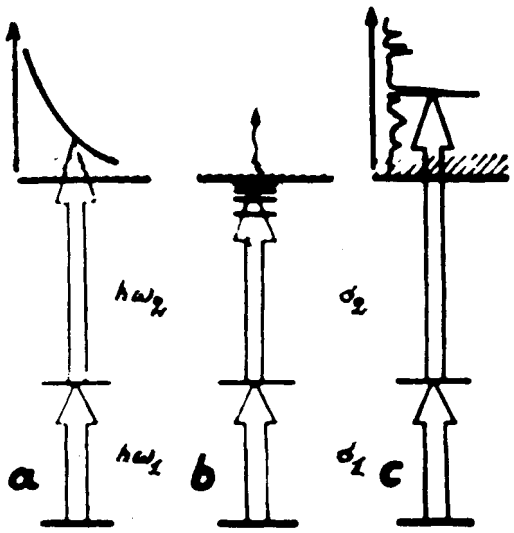

FIGURE 17. Ionization schemes used in atomic ionization spectrometry for determination of atoms.

IV. ATOMIC IONIZATION SPECTROMETRY WITH ELECTROTHERMAL ATOMIZERS

A. General

The employment of electrothermal atomizers has some advantages compared with flames. Besides the higher density of atom vapors in a laser-irradiated volume, these advantages include creation of a controlled atmosphere, continuous control of atomizer temperatures, and the possibility of creating conditions of analyzed substance vapors flowout from the atomizer into vacuum. Electrothermal atomizers provide higher densities of analyte atoms in the laser-irradiated analytical volume than can be attained using a flame. Among these atomizers are specially designed furnaces, crucibles, and atomizers of the Knudsen-cell type.

Using the laser atomization technique with electrothermal atomizers, it is possible to reach the best analytical possibilities — single atom detection.

In the atomic ionization method with electrothermal atomizers, the atoms are first excited by laser radiation to some intermediate state from which the ionization of these excited atoms is performed.

Depending on techniques of ionization of the last intermediate states, the following approaches can be used in the practice of AI spectrometry:

1. Nonresonance direct photoionization from the excited state into a continuum (Figure 17a)
2. Electric field ionization of an atom from high-lying Rydberg states (Figure 17b)
3. Resonance photoionization of an excited atom by its excitation into an autoionization state (Figure 17c)

Since each approach includes resonance interaction with laser radiation and subsequent atom transition to a specific excited state, then, for simplicity, the process is referred to as resonance ionization spectroscopy (RIS), although the ionization process itself may be nonresonant by its nature, as in Figure 17a.

Let us discuss in detail each approach.

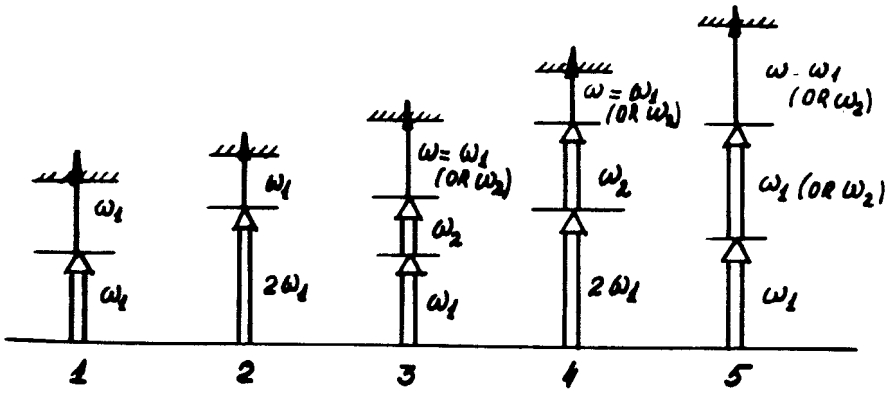

FIGURE 18. Possible schemes for direct photoionization of the elements into continuum.

1. Direct Photoionization into a Continuum

In this technique, an excited atom is ionized by additional laser radiation or by radiation used at one of the steps of resonance excitation (Figure 17a). This ionization technique was first suggested by Letokhov,[129] who employed it for separations of atoms, and was realized by Ambartsumyan et al.,[11] using Rb as an example.

Possible energetic pathways in the direct photoionization in RIS were considered by the researchers at the Oak Ridge National Laboratory,[130] who singled out the five basic schemes shown in Figure 18.

As illustrated in the figure, a simple RIS scheme consists in the absorption of two photons of equal energy through the resonant intermediate level, followed by subsequent photoionization (scheme 1). This scheme was realized by Hurst et al.[15] in one of the first studies on cesium determination. A possible version of this simplest scheme can be the transition using frequency (energy) doubling of a laser (scheme 2). The next is scheme 3, where photoionization is attained by using the energy of three photons of two different lasers. This scheme was employed for RIS determination of lithium.[131] If the first excited state is far from the ground state of a given atomic species, then the frequency of the first photon can be doubled (scheme 4). For atoms whose ionization potential and/or first excited state is very far from the ground state, the population of an excited state can be accomplished using two photons with the doubled frequency ω_1, followed by the consequent ionization due to absorption of the photon with the frequency ω_1. This scheme was used by Bjorklund et al.[132] for the RIMS determination of ^1H and ^2H. In the opinion of Young et al.,[130] the use of these five schemes allows detection of 98 of the first 102 elements of the periodic system.

The ionization schemes shown in Figure 18 will be efficient if the power densities of laser radiation, frequencies ω_1 and ω_2, are sufficient to transfer to an excited state and to ionize almost every analyte atom. Achievement of these conditions (optical saturation of transitions)[13] is possible using laser radiation. The power density required to reach optical saturation is derived from the expression

$$P_{sat} = \hbar\omega/2\sigma\tau \quad (19)$$

where ω is the frequency of laser radiation, σ is the cross section of laser excitation of energy levels, and τ is the lifetime of an excited state. While the cross section of atom transition from one discrete state to another is 10^{-11} to 10^{-14} cm^2, the cross section of (nonresonance) photoionization, σ_{ion}, is 10^{-17} to 10^{-19} cm^2.[16,133] This means that radiation power densities required to ionize excited atoms should be rather high. So, in the first experiment on two-step photoionization,[11] the output of photoionization of the Rb atoms,

η_{ion}, was equal to 10^{-3} due to the low energy of the ionizing laser pulse. In addition, only the significant increase of its energy provided η_{ion}, which was about unity.[13] The necessity of using high radiation power densities may lead to nonresonant multiphoton ionization[78] of any atoms or molecules occupying the analytical volumes which will result in selectivity losses. Other ionization methods such as electric field ionization of atoms excited to the Rydberg states and resonant photoionization into autoionization states, which will retain selectivity, will become increasingly important.

2. Electric Field Ionization from Rydberg States

In this method, suggested by Ivanov and Letokhov,[17] the atom is excited from an intermediate state to a high Rydberg state, which is then ionized by an electric field pulse. Studies[134-136] have demonstrated that such Rydberg states are easily ionized in the electric field, irrespective of the kind of atoms. Each Rydberg state has a characteristic threshold for field ionization. When the electric field strength exceeds the critical value for a given Rydberg state, the atoms excited to this state are ionized with close to unity efficiency.

The Rydberg state can be populated in two or three steps using radiation from synchronized dye lasers.[136-138] The choice of an excitation scheme depends on a particular atom.

The atom ionization through the Rydberg states has certain advantages when it is employed for analytical purposes. Since this method uses resonance excitation, optical saturation requires power densities that are three to four orders of magnitude less than those needed for direct, nonresonant photoionization into the continuum. The nonselective ion background is therefore greatly reduced. The atomic ionization through the Rydberg states makes possible the efficient detection of atoms in an atomic beam when the high pulse repetition rate is required. The maximum spectral resolution is attained and a matrix noise is reduced when a beam is used, and a high degree of selectivity can be attained in combination with a multistep excitation scheme.

3. Photoionization into Autoionization States

Autoionization states are discrete states corresponding to excitations of inner electrons of the atom; they lie above the first ionization limit of that atom. For multielectron atoms, these states can be fairly narrow and the cross section of this autoionization transition can exceed the cross section of nonresonance direct photoionization into continuum by several orders of magnitude.[137,139,140] The lifetime of an autoionization state with respect to the decay into a continuum is typically several nanoseconds. Thus, when using a laser pulse of 10^{-8} s, this state will decay during the laser pulse. This situation affords the limiting absolute yield of ionization $\eta_{ion} = 1$.

The technique of atomic ionization into autoionization states (Figure 17c) is particularily promising: it affords the advantages of resonance excitation and efficient ionization.

One of the difficulties of application of this method is the absence of data on these states for a significant number of elements. In analytical AI spectroscopy, photoionization into autoionization states has found application mainly for determination of lanthanides.[141,142]

4. Spectroscopy of Rydberg and Autoionization States

Laser AI spectrometry has been used in spectroscopic investigations of high-lying Rydberg and autoionization states of various elements. In the case of the lanthanides, it has been employed to measure ionization potentials,[143] to determine the positions of autoionization levels,[140,142,144-148] to measure atomic cross sections and state lifetimes,[146] and to investigate Rydberg states.[149,150] Knowledge of these characteristics along with the positions of high-lying Rydberg and autoionization levels is of great practical importance, e.g., in developing selective laser photoionization schemes for trace elemental analysis.

B. Single Atom Detection

Applications of laser AI offer unique opportunities in analytical chemistry as was indicated by Letokhov as early as 1970.[129] Hurst et al.[151] and, independently, Letokhov[152,153] further suggested that laser AI could provide sensitivity sufficient to detect single atoms and molecules.

The detection of single, charged species is a well-exploited field of experimental nuclear physics.[154,155] It is based on the fact that a charged species acquires substantial energy within an electric field. When such an energetic particle passes through a medium, it initiates ionization and excitation of a great number of atoms or molecules that can be easily detected. Examples of this type of detection device are a Geiger-Müller counter and an ionization chamber.

Detection of single, neutral particles such as atoms and molecules is more complicated. Recently, however, new laser techniques have been suggested and realized that have made possible the efficient ionization and detection of single atoms. The efficiency and selectivity of detecting a neutral species is therefore determined by the efficiency and selectivity of the ionization process.

Ambartsumyan et al.[11] were the first to implement stepwise AI by laser radiation, a method well suited for selective AI. In this approach, atoms are excited to an intermediate state by absorption of one or more photons; the excited atoms are then selectively photoionized. This process uses resonant excitation, and therefore requires only moderate laser intensities for optical saturation of the appropriate transitions.

Ambartsumyan et al.[13] and Hurst et al.[156] have demonstrated that with sufficiently intense laser beams the quantum yield of photoionization is close to unity, making it possible to efficiently detect single atoms.

The first experiments on detecting single atoms in a laser-irradiated volume were described by Hurst et al.[15,157] in 1977. They used a flashlamp-pumped dye laser with a bandwidth of 0.07 nm to ionize atomic cesium via the $6^2S_{1/2} \rightarrow 7^2P_{3/2}$ ($\lambda = 455.5$ nm) transition. The laser beam was directed into a chamber of a specially designed proportional counter which would be triggered when even a single electron bearing thermal energy appeared in the chamber. The proportional counter was filled with a gas mixture of Ar (90%) and CH_4 (10%) at 100-torr pressure. The laser radiation also served to ionize the cesium atoms in the $7^2P_{3/2}$ state by absorption of a second photon of the same wavelength. Under the action of the convection flow of a buffer gas, atoms from a special oven, which was heated electrically, arrived into the proportional counter chamber. The laser power was adjusted to achieve optical saturation of the cesium transitions. Under these conditions each cesium atom was ionized with unit efficiency, yet the gas mixture filling the counter was not ionized. A single atom of cesium could be selectively detected out of 10^{19} atoms of the gas filling the counter (Ar and CH_4). In this experiment, the residence time of cesium atoms detected in the irradiated volume is fairly long because it is determined by the time of atom diffusion in the buffer gas. However, at such high pressure, it is difficult to attain high spectral resolution because of collisional effects that lead to line broadening.

When high spectral resolution is required, the experiment can be conducted in an atomic beam. The results of the experiments[136,140,158] on the detection of single atoms of sodium and ytterbium in an atomic beam with a Knudsen-cell source were published in 1978. The atoms were excited into Rydberg states by radiation from three lasers whose power was sufficient to saturate each transition. The laser bandwidth was equal to 1 cm^{-1}. The ionization was accomplished by applying a pulsed electric field. The amount of ions produced was determined using an electron multiplier. With decreasing temperature of the Knudsen cell, the magnitude of an ionization signal decreased to a particular value and the signal disappeared when the atomic beam was cut off or when any of the laser beams were blocked. This minimum signal amplitude, which fluctuated in time, was associated with single-atom

detection. It should be noted that applications of atomic beams can provide selectivity sufficient for detection of rare isotopes.[159,160] The atomic beam technique can also be combined with the mass spectrometer allowing increased selectivity for detection of single atoms and isotopes.[161,162] A detailed discussion of problems associated with detection of single atoms by the technique of laser AI spectrometry is given in some reviews.[5,157,163-173]

An interesting idea related to detection of single atoms was expressed by Hurst et al.[174] They suggested use of the RIS technique with amplification (RISA). This approach incorporates the collisional processes occurring during a laser pulse in order to complete a photoionization cycle and therefore obtain more than one electron from each atom detected selectively. These cyclic processes occur by transfer of the atom charge to another species:

$$A^\circ + h\omega_1 + h\omega_2 \rightarrow A^+ + e^- \tag{20}$$

and

$$A^+ + M \rightarrow A^\circ + M^+ \tag{21}$$

where A° is the ground state of the atom of interest and M is some molecule.

Alternatively, these processes can take place by the Penning process involving an atom in a Rydberg state, A**, and a molecule M,

$$A^\circ + h\omega_1 + h\omega_2 \rightarrow A^{**} \tag{22}$$

and

$$A^{**} + M \rightarrow A^\circ + M^+ + e^- \tag{23}$$

Thus, a single atom can be repeatedly used as often as desired since, of course, atoms are not destroyed. The authors believe that many important applications of the RISA method will be forthcoming in the practice of single-atom detection.

At present, the methods of single-atom detection by laser AI can be used in various fields of science and technology. A detailed discussion of these problems is likely to be the subject of special review. Here, we briefly outline some examples of the application of techniques of single-atom detection.

1. Detection of Nuclear Reaction Products

In nuclear reactions, nuclei of new elements or short-lived isotopes of known elements are often produced in small amounts. The first experiment for detecting single daughter atoms was performed by Kramer et al.,[175] who employed the AI method to detect the number of daughter atoms of Cs resulting from the radioactive decay of ^{252}Cf implanted in a thin nickel foil. The foil was mounted in front of an apertured surface-barrier detector which sensed a fission fragment and signaled that the complementary fragment has been injected into the sample chamber. The heavy fragment was stopped in a gas mixture (90% Ar, 10% CH_4) at 317-torr pressure at a known position where the fragment intersected with a laser beam. The wavelength of the laser was tuned to ionize selectively the neutralized fission fragment of interest. In the case of cesium, the laser was tuned to either 4555 or 4593 Å in order to excite either the $7^2P_{3/2}$ or the $7^2P_{1/2}$ level, respectively. The experiment showed that 8 ± 2 atoms of cesium were produced for every 100 decays of ^{252}Cf.

The AI laser spectrometry of single atoms can help to identify exotic light nuclides[176] and other unstable nuclei resulting from interaction with accelerated particles.[146]

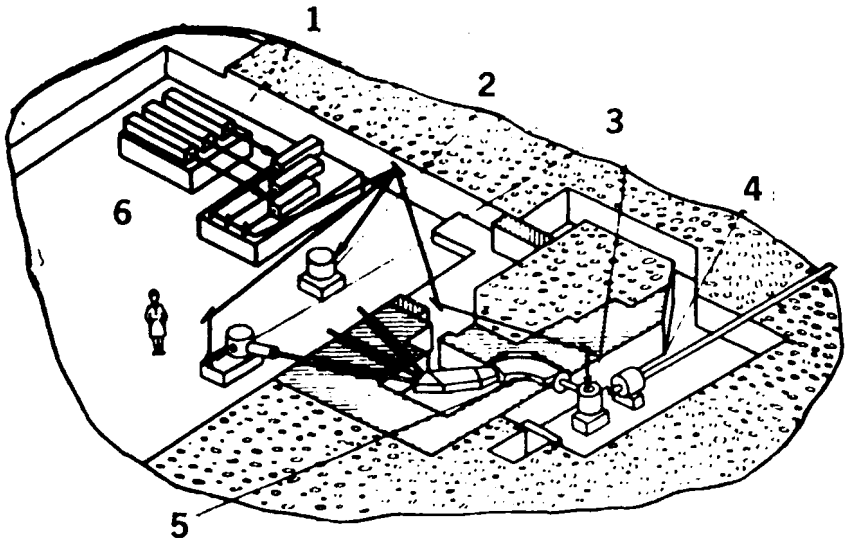

FIGURE 19. General view of a laser nuclear complex designed by the Leningrad Institute of Nuclear Physics and the Institute of Spectroscopy, U.S.S.R. Academy of Sciences: 1, dye lasers; 2, off-line chamber; 3, on-line chamber; 4, proton beam; 5, mass separator; 6, Cu lasers.

The high resolution of the atomic ionization method in combination with the maximum possible sensitivity is of particular value for investigations of the super-fine structure of spectral lines of atoms with short-lived nuclei that are only available in very small amounts (10^3 to 10^{10} atoms). This method has been successfully used for measuring the radii of nuclei of short-lived isotopes generated in the proton accelerator at the Leningrad Institute of Nuclear Physics named after B. P. Konstantinov. A laser nuclear measurement complex has been constructed which uses three-step AI technique[146,177] to detect radioactive nuclei. Experiments can be conducted on- or off-line. Figure 19 shows a general view of this complex. The proton beam (4) irradiates the target where short-lived isotopes are formed from nuclear reactions. These products are evaporated from the heated target and are ionized and separated in the mass separator (5). In the off-line mode, the isotopes under investigation are accumulated in the sample and then proceed into the chamber (2) where, on heating, they evaporate into the vacuum in the form of neutral atoms with radioactive nuclei. Once in the vacuum, they are excited by laser pulses. Investigations on short-lived isotopes and nuclear isomers are performed in the on-line mode where the flow of radioactive nuclei is steadily accumulated in the sample (3) and evaporated in the form of neutral atoms. In this case, because of low concentrations of resulting atoms with short-lived nuclei, maximum detection sensitivity and high spectral resolution are necessary.

Resonance AI follows a three-step scheme which simultaneously uses three laser pulses from three independent dye lasers (1). The dye lasers are pumped by a Cu vapor laser (6) at a high repetition rate (10 kHz). The high repetition rate is required to provide maximum "interception" of the rare atoms as they pass rapidly through the zone of laser irradiation. The sensitivity is very high. The method makes it possible to measure the spectra of isotopes generated in the target in the amount of 3×10^3 nuclei/s. Given a half-life of 10 s, this corresponds to a equilibrium population of only 3×10^4 nuclei in the target.

An interesting example of determination of rare radioactive elements is the study performed by Andreev and co-workers[178] on the radioactive isotope ^{221}Fr, which has a half-life of 4.8 min. The experiment was accomplished on a sample containing about 10^9 atoms of ^{225}Ra, implanted to a depth of about 100 Å into tantalum foil. Radioactive decay of ^{225}Ra atoms

produces a chain of elements $^{225}Ra \xrightarrow{\beta} {}^{225}Ac \xrightarrow{\alpha} {}^{221}Fr \xrightarrow{\alpha}$, with the element ^{221}Fr being one of them. The experiments were carried out with the flow of Fr from the sample equal to 8×10^2 isotopes/s. The photoionization of Fr was performed in two steps: excitation of Fr from the ground state was accomplished using a dye laser ($\lambda = 718.0$ nm), and the ionization was induced by radiation of a Cu vapor laser ($\lambda = 510.6$ nm), which was simultaneously used to pump the dye laser. The limiting sensitivty of detection of Fr in the sample was 10^4 atoms with minimum signal-to-noise ratio.

Letokhov[179] published a review of the application of multistep laser ionization for the high-resolution, high-sensitivity determination of isotopes of short-lived atoms of radioactive elements.

2. Determination of the Solar Neutrino Flux

An interesting example of laser AI detection of single atoms is the determination of the solar neutrino flux onto the earth, using neutrino detectors of various kinds.[180] One of these detectors[181,182] is based on a radiochemical scheme of neutrino detection by the reaction $^{81}Br(\nu,e^-)^{81}Kr$. In the proposed experiment it is necessary to count about 500 atoms of ^{81}Kr produced in a tank containing 862 tons of ethylene bromide. The long lifetime of the ^{81}Kr isotope would allow counting of these atoms before their disappearance by radioactive decay. The feasibility of a $^{81}Br(\nu,e^-)^{81}Kr$ solar neutrino experiment was described in detail by Hurst.[183]

3. Some Applications in Environmental Research

^{81}Kr is very useful in geological applications because of its long half-life (2.1×10^5 years) and because it is chemically inert. The long half-life causes exceptional difficulties for measurements of its radioactivity; the laser AI method, however, allows direct measurement of ^{81}Kr atoms. Geological applications include polar ice cap dating,[184] which can provide valuable information on climatic history, and the dating and possible circulation of groundwaters.[185-188] The procedure involves separation of noble gases from several liters of water. All isotopes of elemental krypton are concentrated and finally the ^{81}Kr atoms are counted using the RIS technique in combination with MS to attain the required sensitivity and selectivity.

Laser AI spectrometry for detection of isotopes resulting from cosmic radiation can address problems of isotope chronology. Provided that these isotopes accumulate at a certain rate in ocean deposits and that measurements are made of the content of the isotopes ^{10}Be, ^{14}C, and ^{26}Al, generated by action of cosmic rays on the content of stable isotopes, then one can determine time variations of the intensity of cosmic rays resulting from variations in solar activity.[172] As is noted later, determination of single atoms of the isotope ^{81}Kr in geological samples makes it possible to select sites for hazardous waste disposal.[184]

One-atom detection is of great importance for analytical chemistry because these experiments demonstrate that AI spectrometry can achieve extra-low detection limits in a substance. Research is needed to obtain more efficient techniques for sample atomization and better detection of analytical signals from ionization. Such advances will make it possible to realize the unique opportunities afforded by the laser.

C. Analytical Application of Atomic Ionization Spectrometry with Atomization in Vacuum

1. General

AI analyses are most efficiently conducted in an atomic-molecular beam in vacuum.[161] Under slow vaporization, the ions and electrons resulting from collisional processes are absent[140,169] and element detection limits are restricted only by unavoidable noise and back-

ground fluctuations. This noise arises from the multiphoton ionization process as well as from direct photoionization of atoms having ionization potentials that are less than the energy of the photon used for excitation or ionization of the analyte atoms. But the latter interferences do not occur for 82 elements even if the sample matrices contain sodium, the most widespread easily ionized element (IP = 5.14 eV, λ = 241 nm). Moreover, this noise can be reduced significantly using detecting schemes based on MS.[161] Recently it was shown that application of a stepwise excitation scheme and optimization of the laser output parameters could substantially reduce the noise level arising from nonselective multiphoton ionization of a sample matrix.[85]

Theoretical estimates that include the effects of noise[161,189] indicate that under conditions of complete sample atomization in an atomic beam the use of commercial lasers and mass spectrometric separation of matrix interferences can yield detection limits of $<10^{-12}$%.

Bekov et al.[190] estimated the minimum absolute amount of a chemical element necessary in order for a selective signal from its atoms to still be observable. Given an atom yield from a sample equal to 0.1 and a low pulse repetition rate (about 12 Hz), it is sufficient to have about 10^8 atoms of an element in a sample for detection of that chemical element. Thus, the detectable concentration of an analyte element (without the use of MS for background discrimination) is about 10^{-10} at.%. This value can be lower by three orders of magnitude for elements possessing excited levels which can be populated with the help of copper vapor laser-pumped dye lasers.

The most significant advantages of sample atomization in vacuum can be summarized as follows

1. Creation of a collimated beam of sample atoms enhances spectral resolution and allows use of reduced laser intensities.[45]
2. An atomic beam allows efficient elimination of noise arising from thermal ions of matrix using simple thermal ion-suppressing systems.[141]
3. An atomic beam precludes loss of analyte atoms by interactions with environmental atoms and molecules.[191]
4. Traces of analyte elements present in the atmosphere used in sample atomization are eliminated.[192]
5. Background signals related to thermal ionization and chemionization during interactions with atmospheric atoms and molecules are eliminated.[161]
6. Separation of thermal ions and ions results from direct laser photoionization of matrix atoms and molecules using mass spectrometers.[161]
7. Collisional deexcitation processes of the analyte atoms are minimized thus allowing use of lower laser powers.[193]

2. *Instrumentation and Procedures*

a. Laser Systems

An analytical laser ionization spectrometer includes a pulsed, tunable dye laser system for resonance excitation of atomic transition and subsequent ionization of excited atoms. The laser system consists of a pumping laser (N_2, excimer, or Nd:YAG laser) and two or three dye lasers which are simultaneously excited by the pumping laser.[137,194] The dye lasers are usually characterized by extremely high peak power, fairly narrow linewidth, and widely tunable wavelength range of operation (217 to 870 nm). If a high pulse repetition rate is required (10 kHz and more), it is advisable to use a copper vapor laser to pump the dye lasers.[177] In this case, a wavelength range down to 530 nm is available directly, and with the use of KDP doubling crystals, the range can be extended to higher energies. The choice of optimal laser systems is determined by each particular analyte and by the experimental conditions.

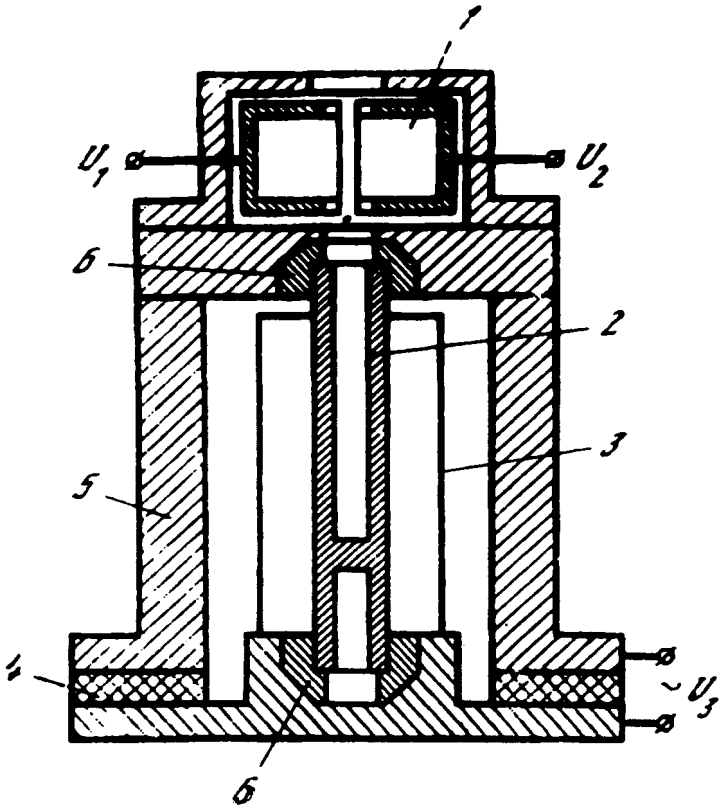

FIGURE 20. Design of the electrothermal high-temperature atomizer for producing collimated atomic beam in a vacuum: 1, thermal ion suppressor; 2, graphite tube crucible; 3, thermal screen; 4, insulator; 5, water-cooled copper housing; 6, graphite electrodes.

b. Atomization Technique

The main requirements for atomization systems are the attainment of temperatures up to 3000°C, the possibility of quick change of samples, the ease of operation and reliability, and compatibility with AI and ion detection systems. Figure 20 shows the design of the high temperature electrothermal atomizer that was used in the experiments of the Institute of Spectroscopy, U.S.S.R., Academy of Sciences.[141,195] A special ion-suppressing system was installed above the outlet channel of the tube crucible to suppress strong backgrounds from thermal ions and electrons. The sample of a substance being analyzed (up to 100 mg) was placed into the graphite crucible of the atomizer. Aqueous samples were evaporated first at 90°C in order to obtain dry residues. Then, the crucible was placed into the atomizer, and after evacuation to a pressure of 10^{-6} torr the crucible was heated stepwise up to the working temperature. The evaporating atoms and molecules were formed into an atomic-molecular beam which was irradiated at an angle of 90° simultaneously by all the laser pulses. For fine tuning of laser radiation to the transition of an element being excited, an additional oven was placed in the atomizer chamber to produce a reference atomic beam of this element. Both the sample and reference beams intersected the laser beams in the same region in front of a slit in one of the electrodes where an ionizing pulse of an electric field was applied.

Despite having found wide application in the analysis of various samples,[196] this atomizer possesses a number of disadvantages. One is a failure to provide complete atomization of a sample. In order to increase the efficiency of sample atomization, and consequently decrease

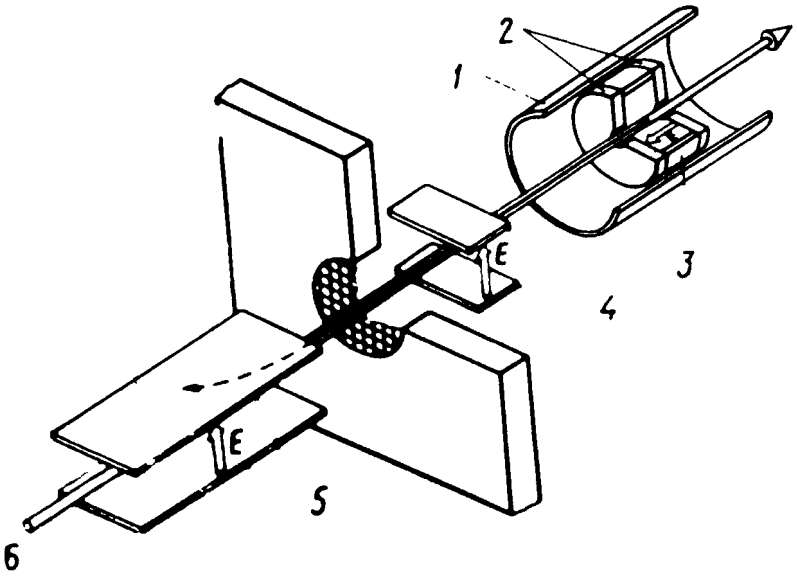

FIGURE 21. Laser resonance ionization setup using a hot cavity as an atomization source: 1, cavity heater; 2, ejecting metal plates (electrodes) in a hot cavity; 3, insulator; 4, filtering capacity (to reduce the thermal ions background); 5, plates collecting ions; 6, laser beams.

the detection limit as well as improve the accuracy of determination, an atomization system in vacuum was suggested where sample evaporation is accomplished by heating to a temperature providing effusive outflow: atomization is performed by heating to a temperature providing complete dissociation of all molecules that include analyte atoms.[197] This is accomplished by a temperature gradient along the atomizer's graphite tube crucible which increases towards the outlet. Local irradiation by light beams can be used to ensure heating of the graphite tube, offering, the added advantage of a significantly smaller volume of the analytical chamber and, consequently, an increased rate of analysis.

In an effort to increase the efficiency of the AI technique with the use of pulsed lasers, Andreev et al.[198] proposed carrying out atomization and ionization in a hot cavity contained in the vacuum with subsequent extraction of the generated ions by an electric field (Figure 21). The laser beam was passed along the channel of the hot cavity thus achieving multipass interaction of the analyte atoms with the laser beam. It was shown that with realistically achievable laser parameters (pulse duration is about 15 ns, repetition rate is about 10 kHz) a cavity configuration can be chosen so that the efficiency of particle interception exceeded 50%. The possibility of high efficiency ionization of Sr atoms inside a hot cavity with lasers of high pulse repetition rate (about 10^4 Hz) was studied by Andreev et al.[199] The Sr atoms were excited to a Rydberg state by three copper vapor-pumped dye lasers. The ionizing electric field was used at the same time to extract the resulting Sr ions from the cavity for analysis and counting.

c. Detection of Selective Atomic Ionization Signals

After excitation of analyte atoms to a Rydberg state, an ionizing electric field pulse with a duration of 10 ns and an amplitude of up to 15 kV is fed to the electrodes (Figure 22) with a delay of 20 to 50 ns. The ions resulting from field ionization of the Rydberg atoms, and being in the field of this pulse, acquire a velocity component normal to that of their thermal velocity in the atomic beam; the value of this component is two orders of magnitude larger than the mean atomic velocity in the beam. The ion therefore follows a path that is

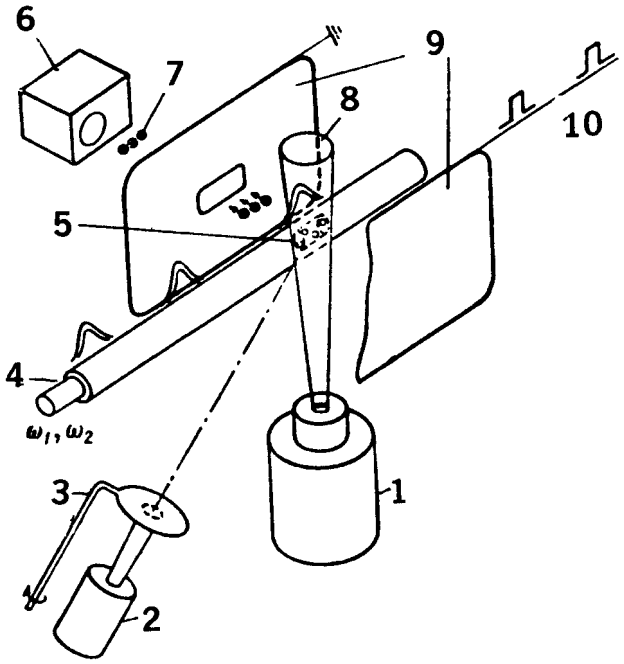

FIGURE 22. Detection of atoms in a beam produced under sample atomization in vacuum: 1, atomizer; 2, an oven to produce a reference atomic beam; 3, shutter; 4, laser beams; 5, zone of excitation; 6, electron multiplier; 7, ions; 8, investigated atomic molecular beam; 9, electrodes; 10, an ionizing electric-field pulse.

practically normal to the axis of the beam. The ion passes through a slit in the electrode and enters a secondary electron multiplier which detects it with an efficiency close to 1. The signal from the multiplier is processed by conventional methods: it is amplified and fed to a gated boxcar averager and then to a recorder or an amplitude analyzer for registration.

Bekov et al.[200] suggested an interesting method of AI signal detection which provides simultaneous elimination of noises caused by both thermal ions and ions resulting from nonselective photoionization. This method is based on the sharp threshold relationship between the degree of ionization of Rydberg atoms and the pulse amplitude of the ionizing electric field, and on the very weak dependence of the degree of ionization of Rydberg atoms on the pulse duration. A negative-going pulse of the electric field with an intensity lower than the critical one for ionization of the Rydberg state of interest is delivered to the electrodes: all foreign ions begin to move towards the slitless electrode. The effect of this pulse on Rydberg atoms is negligible.[201] A positive-going pulse is then delivered to the electrodes (the delay between pulses and their duration is chosen much less than the lifetime of a Rydberg state and equal to 10 to 50 ns). The amplitude of this pulse exceeds the threshold conditions and thus completely ionizes the Rydberg atoms. The effect of the second pulse on the nonselective ions is only to slow down their movement towards the slitless electrode, where the analyte ions produced from Rydberg atoms acquire a significant velocity component in the direction to the secondary electron multiplier to pass through the slit in the electrode. The selectivity is therefore increased by three to four orders of magnitude, even in analysis of complex samples.

The nonselective ion background can be also efficiently removed using a mass spectrometer.[161,196]

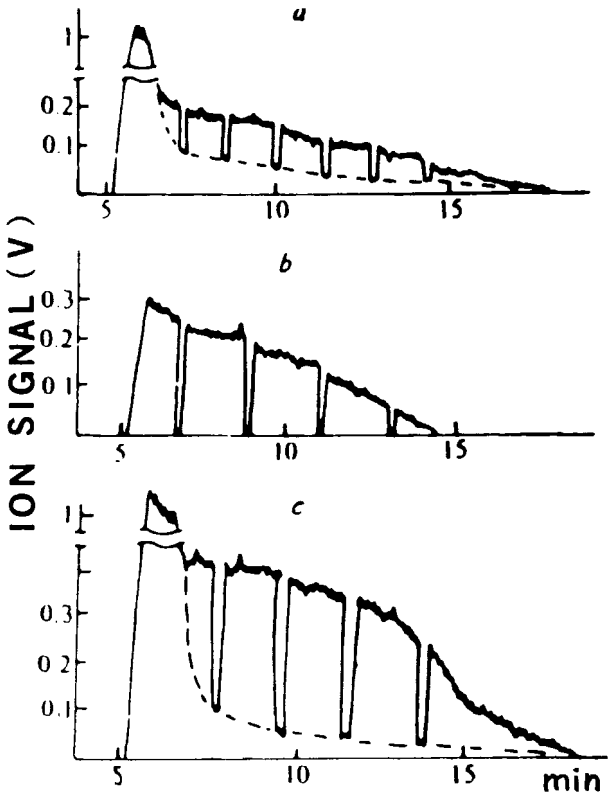

FIGURE 23. Dependence of an ion signal on the time of sample atomization at 1750°C: a, 40 μl of seawater; b, 40 μl of standard $AlCl_3$ solution in deionized water (concentration of Al is 100 μg/ml); c, 40 μl of solution containing of 9 parts of seawater and 1 part of standard $AlCl_3$ solution with an Al content of 1000 μg/l. The total yield of Al is equal to the sum of the yields from a and b.

For correction of a signal caused by both thermal ions and ions resulting from nonselective photoionization, Bekov et al.[141] suggested periodically detuning one of the lasers by about 2 cm^{-1} to both long and short wavelenths. Although this method of noise reduction makes it possible to come into resonance with a transition of a foreign atom or to change the order of a multiphoton ionization process, it has been effectively used for determination of aluminum in sea waters.[191,192] In order to discriminate the selective ion signal of aluminum from the total ion signal, the wavelength of the first step laser is periodically detuned 3 to 5 cm^{-1} from the $3^2P_{3/2} \xrightarrow{\lambda_1} 4^2S_{1/2}$ aluminum transition. The dips in Figure 23 are a consequence of detuning λ_1 from resonance, resulting in a drop in the ionization efficiency by more than two orders of magnitude. The total yield of aluminum in this case is defined by the area lying between the curve of the total ion signal and the dashed line.

The addition of standard solutions has shown that the matrix composition does not distort the results. A composite solution was prepared consisiting of nine parts seawater and one part standard solution of $AlCl_3$ with an Al content of 10^3 μg/l. This corresponds to the additional concentration of Al equal to about 100 μg/l in seawater. The dependence of the ion signal on evaporation time for a 40-μl sample of this mixture is presented in Figure 23c. The total signal from aluminium equals the selective signal from aluminium in seawater (Figure 23a) plus the signal of aluminium from the standard solution (Figure 23b).

The same technique has been used in the determination of Al traces in human blood.[202]

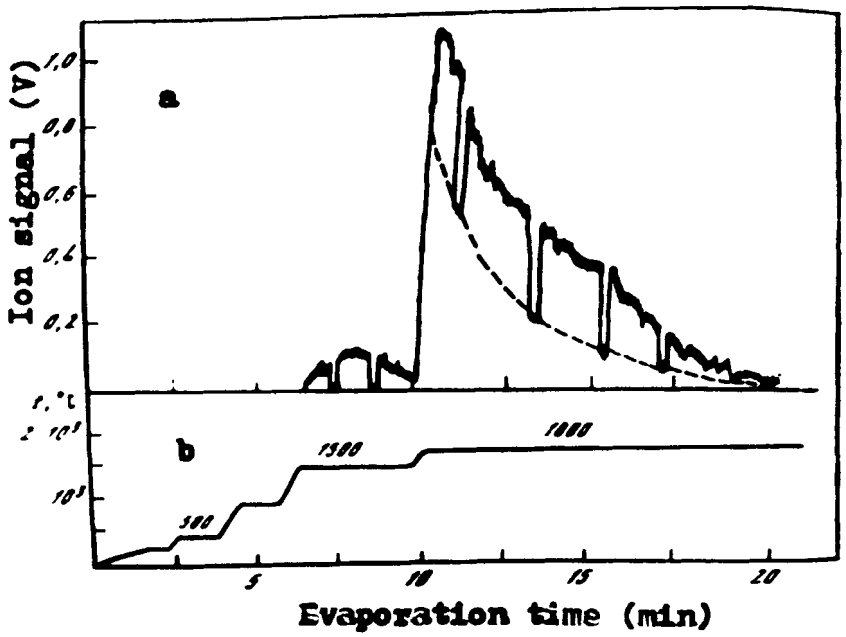

FIGURE 24. (a) Time dependence of the ion signal of Al during stepwise heating of the 40-μl blood sample. (b) Time dependence of the crucible temperature.

The total aluminum signal from the blood sample under investigation is determined by the total "selective" area (the difference between the observable and background signals) under the signal curve (Figure 24a). The value of the aluminum concentration corresponding to this signal is found from the calibration curve plotted for aluminum aqueous solutions. This procedure has been verified by the standard addition method. In this case, 40 μl of blood and 40 μl of standard $AlCl_3$ having a 100 ng/ml content of aluminum were introduced into the crucible. The aluminum signal produced by this mixture turns out to be additive within the limits of error equal to 10%. This result proves the absence of blood matrix influence on the aluminum yield during thermal atomization in vacuum.

Bekov et al.[203] also demonstrated that during determination of traces of Ru in natural subjects it is possible to calibrate analytical signals from solid samples atomized thermally using a calibration chart based on aqueous standard solutions of Ru. As an example, Figure 25b presents an analytical curve which is plotted using standards solutions of $RuCl_4$ and correlated with the analytical curve in Figure 25a plotted using Cu standards. This calibration is justified since there is coincidence between the analytical signals from the aqueous standard solutions of $RuCl_4$ and those from the Cu standards with the same Ru content.

3. Determination of Trace Elements in Real Samples

The experiments described have confirmed the versatility of analytical laser AI spectrometry with atomization of a sample in vacuum. Table 4 lists the results of the laser AI analysis of element traces in various samples whose composition are sometimes very complex, e.g., seawater and geological and biological subjects. The detection limits of these elements for real samples of complex composition that have been reported in various studies are also presented in the fourth column of Table 4.

One of the most important problems is to avoid of contamination in trace element analysis by RIS. Thus, Zilliacus et al.[213] have reported the main sources of contamination in RIS analysis and listed some measures which should be taken to improve the accuracy of

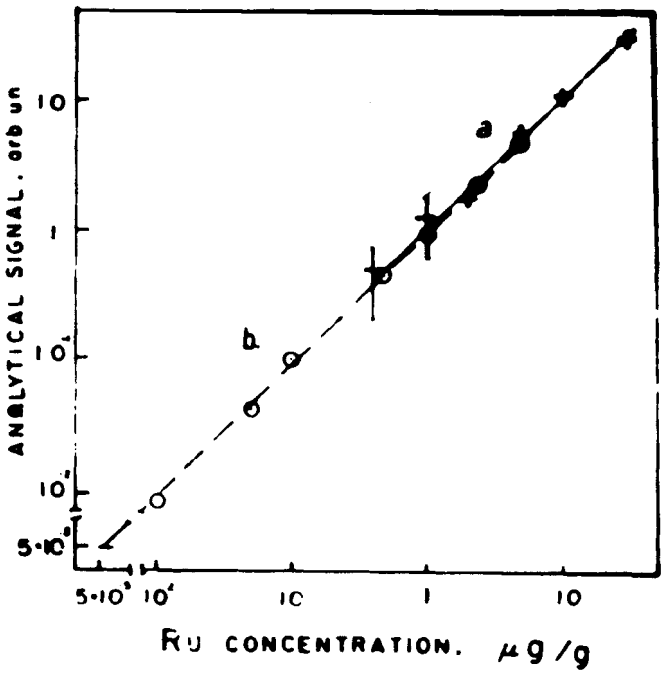

FIGURE 25. Analytical curve for Ru based on (a) Cu standards and (b) standard solutions of $RuCl_4$ in deionized water.

Table 4
RESULTS OF LASER ATOMIC IONIZATION ANALYSIS OF ELEMENT TRACES II VARIOUS SAMPLES (ATOMIZATION IN VACUUM)

Element	Sample	Element concentration (wt%)	Detection limit (wt%)	Ref.
Na	CdS crystal	$2 \times 10^{-6} - 6 \times 10^{-5}$	2×10^{-10}	204
	Ge crystal	2×10^{-8}	5×10^{-9}	205
	Pb metal	10^{-2}	10^{-6}	193
B	Ge crystal	$2 \times 10^{-8} - 2 \times 10^{-7}$	5×10^{-9}	200
Al	Aqueous solution of $AlCl_3$	2×10^{-7}	2×10^{-10}	206
	Ge crystal	5×10^{-7}	2×10^{-9}	207
	Water taken in the mouth of the Kura River (the Caspian Sea)	$3.6 \times 10^{-5} - 7.8 \times 10^{-4}$	1×10^{-7}	192
	Surface waters of the Mediterranean	$(6.5 \pm 0.7) \times 10^{-7}$	1×10^{-7}	191
	Human blood	$(2.3 \pm 0.5) \times 10^{-5}$	2×10^{-7}	202
Ga	High-purity Ge	10^{-5}	10^{-13}	208, 209
In	Ge crystal	$1.7 \times 10^{-6} - 2.5 \times 10^{-5}$	10^{-10}	210
Yb	Aqueous solution of $YbCl_3$	5×10^{-7}	2×10^{-9}	141
Ru	Geological materials (ore)	10^{-5}	10^{-10}	211
	Seawater	$(1.3 - 3.0) \times 10^{-10}$	3×10^{-12}	212
	Metalliferrous sediment (Red Sea, Discovery deep)	7.6×10^{-8}	3×10^{-12}	138

analysis. For example, gallium, which is not a widely spread contaminant in air, could be determined at the femtogram level in the blank samples without working in a clean room.

The AI spectrometry method has a potential for reduction of detection limits by one to two orders of magnitude by improving the atomizer design, increasing the efficiency and selectivity of ionization, discriminating the nonselective background, etc.

Moreover, the laser AI spectrometry in vacuum can be combined directly with MS or other methods of selective ion discrimination for isotopic studies. This problem is discussed in Section V.

D. Analytical Applications Involving Atomization in a Buffer Gas

In most cases, graphite crucibles, cells, and furnaces heated by electrical current to temperatures of 2000 to 3000°C are used in the process of sample evaporation into a buffer gas. The basic function of the buffer gas is to suppress expansion of the vapors of the evaporable substance, thus generating a sufficient local concentration of analyte atoms. The zone of local concentration is used as the analytical volume, i.e., laser radiation is directed into this volume for ionization of the analyte atoms existing in this volume element. An electric field is applied across the region for detection of the charged species produced by the laser radiation. When the buffer gas is at high temperature, ionization processes take place by collisions of laser-excited analyte atoms or molecules of the buffer gas. This method is relatively simple and fast (vacuum is not required) but requires that high purity gases be used as buffers. It is also necessary to consider the possibility of chemical reactions between analyte atoms and atoms or molecules of the buffer gas.

The first attempts to use a graphite tube atomizer at atmospheric pressure for AI determinations of elements failed.[214] Then Gonchakov et al.[215] reported the successful application of thermal atomization at atmospheric pressure for determination of small amounts of Na which were ionized by the three-step scheme. The dye lasers were pumped by radiation of the second harmonic of a Nd:YAG laser. A graphite cup in an argon atmosphere was used as an atomizer. The detection limit of Na is 1×10^{-15} g. Salsedo Torres[216] investigated a scheme of AI analysis using a Varian Techtron CRA-90 electrothermal atomizer. The first experiments were carried out for the determination of Cs because it is an easily ionized element (the temperature of atomization was about 1800°C). The detection limit of Cs was 5×10^{-12} g.

However, the determination of In with this atomizer failed because the temperature required for efficient atomization of In is about 2500°C. At these temperatures, an AI signal was not observed because of a high noise level from thermoionic emission of the atomizer material. Another disadvantage of this method is the possibility of arc formation between the ion-detecting electrode and the surface of the graphite atomizer. The requirements of careful cleaning or replacement of a graphite atomizer to reduce memory effects of the system when analyzing real samples can become significant. In the case of electrothermal atomization, the influence of sample matrices on the result of an analysis is also important.[217]

Bykov et al.[92] reported the determination of Na and In at a level of 10^{-14} to 10^{-15} g with the use of electrothermal atomizers of different kinds. The experiments were carried out at atmospheric pressure directly in air or in nitrogen. Determinations of Cs and Yb in aqueous solutions were also made. The AI signal was 10 to 100 times stronger than when using a flame as an atomizer, but reproducibility of the determination was not very good.

Magnusson et al.[218] reported successful applications of a graphite furnace for atomization of substances in the AI method. They reported good reproducibility and almost complete absence of memory effects. The AI signal was linear over a range of five orders of concentrations of analyte.

With a modified electrode arrangement, Magnusson et al.[219] were able to measure AI signals at an atomization temperature of 2600°C without interferences from the electric heating current. The two-color scheme of laser AI analysis in graphite furnace was used for the determination of traces of Co, Cr, Mn, Ni, and Pb. Detection limits in the picogram range are reported for all these elements. The reproducibility was estimated by performing ten consecutive measurements of 500 pg Cr. The relative standard deviation of the corresponding signals was 10%.

Minova et al.[220] have used a heated cavity for production of Tl vapors. The Tl atoms were ionized using the two-step scheme. The first photon transferred Tl atoms into the $7^2S_{1/2}$ state, and the second photon of the same energy induced ionization. The ions were detected by a proportional counter filled with Ar. A sensitivity of one atom of Tl per 10^{13} atoms of Ar was attained.

V. OTHER ATOMIZATION AND SIGNAL DETECTION SYSTEMS IN ATOMIC IONIZATION SPECTROMETRY

A. Laser Ablation, Ion Sputtering, Hollow Cathode Discharge

1. Laser Ablation

A unique property of focused lasers resulting in the evaporation of a sample from a very small area, determined by the laser beam cross section, gave birth to the development of new analytical methods based on investigations of emissions of laser plumes alone, emission of the plumes with additional excitation in spark discharge, atomic absorption, or fluorescence spectroscopy of laser-atomized samples.[98]

Mayo et al.[221] used laser ablation as an atomization source in the AI technique. The laser pulse evaporated the sample layer about 1 μm thick. Analysis has been done in a proportional counter operated with slowly flowing P-10 gas (90% argon and 10% methane by volume) at 95 torr. The ablated volume expands into this atmosphere, becoming thermolized within a very short distance from the crater. Two dye lasers were tuned to coincide with atomic transitions of analyte atoms. The authors detected sodium in single-crystal silicon plates. The diameter of the laser beam allowed the evaporation of the sample from the spot of the surface 30 to 100 μm in diameter on ablating laser irradiance about 10^7 W/cm^2. Three RIS schemes have been used to ionize sodium atoms via different resonantly excited levels. The estimated sodium concentration in the silicon sample was 5×10^{11} atoms/cm^3. No sodium was detected in this silicon bulk by neutron activation because the detection limit of the latter technique was only 1.5×10^{13} atoms per cm^3.

2. Ion Sputtering

Since 1983, several articles have been published which discuss the determination of traces by the AI technique in combination with the evaporation and atomization of a solid sample under irradiation with a beam of charged particles (usually Ar^+). As this takes place, a certain amount of material from the surface of a sample is sputtered by an energetic ion beam. The technique has been termed sputter initiated resonance ionization spectroscopy (SIRIS). In the SIRIS technique, ion sputtering is used to atomize the solid; sputtered secondary ions are electrostatically removed and the remaining neutral atoms are probed with the appropriate laser beam. This procedure occurs in a vacuum and the resonantly ionized atoms are then accelerated, detected, and counted. Usually, a mass spectrometer is included in the path to the detector for isotopic identification.

Parks and co-workers[222-224] pointed out that the SIRIS technique can be used to detect all elements of the periodic table except He and Ne. They have determined traces of Ga and In in Si, and also Al and V in stainless steel with a sensitivity limit of 2 ppb. The results were presented[255] for measurements of B concentrations down to the parts-per-million level in standard samples of steel and Si. Some preliminary results were also presented for U and U compounds in a complicated sample such as urine. The SIRIS technique has been described as being fairly accurate in the determination of Si in GaAs standard samples[226] and for determination of U, Pu, and Th[227] in urine down to levels of ≦0.05 μg U/l.

Fairbank et al.[228,229] suggested using the SIRIS technique for detecting rare exotic atoms, such as quark atoms or super heavy atoms. It has the potential of detecting concentrations of 10^{-15}. First results reached the 10^{-12} level. Searches for exotic atoms, which may exist

at very low concentrations in stable matter, using SIRIS were reported.[230] Preliminary concentration limits of 2×10^{-11} and 5×10^{-12}, respectively, were obtained for fractionally charged atoms in niobium and tungsten and for super heavy isotopes of lithium.

Parks et al.[231] presented results and described progress in the development of SIRIS measurements for the analysis of materials in varied fields, including semiconductors, medical, bioassay, health physics, and basic science communities.

SIRIS has been used for the detection of Ga isotopes in Si[232]. The advantages and disadvantages of this technique have been discussed.

Gorbunov et al.[233] observed ion sputtering of polycrystal indium solid samples in a study of the surface property.

3. Hollow Cathode Discharge

This atomization method has not been widely applied until now, but its possibilities were noted in a paper by Keller and Zalevski.[234] Under steady-state conditions of the discharge, a detection limit at the level of 10^6 atoms/cm^3 was reached. AI determination of the isotopic ratio of ^{238}U and ^{235}U has been demonstrated on atomization in a hollow cathode discharge.[235] The isotope U concentrations were 1×10^{12} and 3×10^9 atoms/cm^3, respectively, with a detection limit of about 1×10^8 atoms/cm^3 for ^{238}U. A great number of impure elements of cathode material[236] and filled gases[3] have been detected with the help of AI spectra in versatile hollow cathode lamps. The authors of these works, however, pointed out the observation of a higher noise level than that obtained with determinations in commercial hollow cathode lamps.

Hollow cathode as an atomization method has been widely applied in the resonance ionization MS technique.

B. Laser Resonance Ionization Mass Spectrometry

1. General

Laser sources are generally used in MS to produce ions when laser radiation interacts with a sample target; this technique is applied for conventional analysis. However, the properties of laser radiation — time and space coherence, high radiance, and high monochromaticity — provide the combined laser ionization-MS system with capabilities that are far from conventional. These properties allow using lasers as the selective ionization sources for elemental or isotopic analysis, and the resonance ionization MS (RIMS) technique offers some important advantages over conventional methods of ion production in MS, providing new possibilities for chemical analysis.

First, the resonance ionization process as described earlier has an inherently high elemental selectivity. The high monochromaticity provides a means for the removal of isobaric interferences in conventional MS (when isotopes of the same masses belong to different chemical elements). Mass spectrometric detection provides increased selectivity which is a practical necessity in order to eliminate nonspecific background ionization which may be caused in the process of nonlinear interaction of laser radiation with the matrix of a sample. This resonance ionization process results in a high selectivity in the determination of various isotopes.

Second, the high photon flux and radiance of a laser source result in a high ionization efficiency of analyte atoms, which in turn results in the high selectivity of RIMS.

2. Vaporization and Atomization Processes

As it was mentioned previously, the resonance ionization technique requires free atoms. A variety of sample atomization approaches have been employed in the RIMS technique, but most of the studies were conducted with the use of thermal (surface) vaporization.[237-253] With this technique, a solution of the element is deposited on a metal ribbon and dried according to a set procedure. The resulting deposit is heated to produce atoms or ions.

The thermal ionization process is usually described by the Saha-Langmuir expression:

$$n^+/n^o = \exp[e(\psi - E_i)/kT] \quad (24)$$

where n^+/n^o is the ratio of the charged to neutral species; e is the electronic charge; Ψ is the work function of the surface in eV; E_i is the ionization potential of the elemental species in eV; k is the gas constant in eVK^{-1}; and T is the absolute temperature in K.

The real analytical conditions of thermal ionization diverge considerably from the ideal conditions that the theory describes (the chemical form in which a sample is applied to the filament will affect the ionization yield). For example, the ionization efficiency for cesium as the chloride salt is on the order of 10^4 poorer than for its sulfate salt. The vaporization of even simple binary alkali halides, such as potassium chloride, results in an equilibrium vapor-phase mixture of K, Cl, K^+, Cl^+, KCl, and K_2Cl_2.[254] Chemical interactions with the host substrate can produce complex vapor-phase species. For example, $Ca(NO_3)_2 + Re \rightarrow Ca_xRe_yO_z$.[254,255] A generic approach to increase the atomization efficiency has been developed by means of reduction techniques, including heating the sample in hydrogen gas or drying the sample on a graphite substrate.

The sources providing atomic beams are used to increase the atom/ion ratio. In the work of Krönert et al.,[256] the element under investigation, e.g., uranium or plutonium, was depositied onto a rhenium filament of 25-μm thickness. The filament was directly heated up to 1800°C by a current of 30 A. Thermal ions and secondary ions produced by electron impact ionization from emitted electrons are suppressed by an electric field of 200 V/cm perpendicular to the filament. Uranium and plutonium atoms passed through a diaphragm into a region where they interacted with resonance laser radiation.

These thermal sources (hot filaments, ribbons) have a number of excellent attributes, including good reproducibility and stability. A significant disadvantage of these sources, however, is the low efficiency of interaction between the analyte and the laser beam, especially when pulsed lasers are used for resonance ionization of analyte atoms. The short pulses and relatively low repetition rates of most pulsed lasers, coupled with the constant evaporation of the sample from the thermal sources, results in a low (typically $\leqq 10^{-4}$) effective duty cycle and a substantial loss (nonuse) of analyte. This inefficiency can prove a substantial burden when the sample is difficult to obtain or when sample size must be minimized, as for radioactive materials.[256] One possible solution to this problem is the use of a pulsed sample heating and evaporation process.

Pulsed atomization sources, including laser ablation or pulsed particle sputtering, appear to offer a higher duty cycle, but generally this question is still under discussion.[257,263] Some authors contend that the wide spread in velocities of sputtered or ablated material makes it impossible to overlap the laser temporally and spatially with all the atoms emitted into the gas phase. For example, calculations and experiments of Kimock et al.[257] with sputtering indicate a sampling duty cycle of 3×10^{-4}, at best, with a 30-Hz laser.

Successful experiments have been described by Nogar et al.,[264] who used a pulsed Nd:YAG laser (1.06 μm) to desorb tantalum atoms from a sample filament maintained at a base temperature of 1200°C. These atoms were subsequently detected by pulsed resonance ionization and time-of-flight MS. The temperature of 1200°C was slightly below the temperature needed to produce a detectable resonance ionization signal without laser desorption. The Nd:YAG laser intensity was about 10^8 W cm^{-2}.

The pulsed desorption described in these experiments appears to be a quasi-thermal rather than a plasma-driven process. Initial evidence of this fact is provided by the absence of primary ions produced solely by laser impact as opposed to the presence of such ions in the laser microprobe technique.[265]

Overlap of the atomic tantalum pulse and the probe dye laser pulse was excellent with a

$\leqq$10% effective duty cycle. The total number of atoms removed from the surface was about 10^5 per pulse. The variable time delay between the desorption and interrogation pulses arrival and the use of ion lens between extractor and the flight tube maximized the transmission of ions to the detector and minimized the transmission variation due to the ion velocity components perpendicular to the flight tube.

By this means, the selective and efficient ionization of the flux of atoms ejected by sputtering or ablation has the potential for RIMS because of its higher sensitivity and lower susceptibility to matrix effects than secondary-ionization MS, which analyzes the ejected ions.

For example, Moore and co-workers[266] have shown that the microscopic amount of carbon on the rhenium filament probably has a lower vapor pressure than pure carbon in bulk. Because of this, the authors believe the direct analysis of carbon in solids using RIMS with sputtering or ablation techniques appears feasible and highly sensitive.

Laser ablation was used in resonance ionization for trace determinatin of sodium in high-purity silicon.[221] Beekman and Callcott[253] coupled a time-of-flight mass spectrometer with a laser microprobe and made thermodynamic measurements of the laser-ablated atoms.

Apel et al.[267] showed that laser desorption MS is a useful method for interrogating materials and events at or near surfaces. RIMS diagnostics for laser desorption/laser ablation was used for analysis of conventional analytical samples, like tantalum, and as a monitor of the interaction between lasers and some dielectric materials (optical damage on uncoated CaF_2 substrates).

Possible sources of pulse evaporation of a sample could be pulsed sputtering[257-261,268] or pulsed thermal ion sources.[245]

Harrison et al.[269] demonstrated the possibilities of a versatile glow discharge (as an atomization source) coupled with a tunable dye laser (for selective ionization), using a simple quadrupole mass spectrometer as the measurement system. Discharge plasma has been estimated to ionize less than 1% of the sputtered atoms in a general, nonspecific mode. That is why the glow discharge can be used as an atomization source. The probe laser radiation was directed just in front of the ion exit orifice of the glow discharge ion source, thus interacting with a population of neutral atoms sputtered from the adjacent sample cathode. Potassium was selected as an element under investigation. A small amount of potassium chloride was mixed with high-purity graphite and an electrode was formed with a hydraulic press. The laser pulse created a packet of ions which appeared at the detector approximately 60 μs later. Use of a delayed data gate in the counter/processor permitted the detection of these ions, while a background gate set to open between laser pulses provided a stripping mode to subtract ions formed from modes other than the laser pulse. These preliminary experiments demonstrated that the glow discharge was an effective atomization source which, at least for potassium, created ground state atoms capable of being ionized by multiphoton absorption. The glow discharge can be used as a simple and efficient source to be coupled with a tunable laser for direct multiphoton ionization of solids. The authors obtained $^{39}K^+$ and $^{41}K^+$ ion peaks, and the ionization selectivity and difference mode resulted, at least in part, from the stripping of large peaks at masses $^{40}(Ar^+)$ and $^{41}(ArH^+)$.

Hess and Harrison[270] used a glow discharge as an atomization source to study various metallic samples. The discharge parameters, such as discharge current and the inert gas pressure, were optimized to produce a high output of low energetic neutrals among the population of sputtered species and to reduce the number of excited particles or ions. The latter especially should be minimized to reduce the contribution to the analytical signal of background, nonresonant ions. The output from a tunable dye laser, pumped by an excimer laser, was directed and focused into the discharge chamber where the photons interacted with the sputtered atoms, causing ionization. The ions were then extracted and focused into a quadrupole mass spectrometer for analysis.

3. Ionization Processes

Pulsed dye lasers are ideally suited for RIMS experiments, especially with time-of-flight mass filtering. As was mentioned earlier, however, the pulsed lasers lose their efficiency when they are coupled with the constant evaporation of samples from thermal sources due to a duty cycle mismatch between the atomization and ionization processes. This duty cycle limits the sensitivity of the measurement process in RIMS because it depends on the geometries of the laser and atomization beam, the velocity of the atomic beam, the and the repetition rate of the laser. The atoms usually have thermal velocities of 10^4 to 10^5 cm/s, which define a limitation of the duty cycle of the measurement. For example, each pulse of the Nd:YAG pumped dye laser produces an ion packet whose shape is defined by interaction volume of the laser beam and atom plume or beam. Usually such an ion population produced in the atom population requires 1 to 10 μs to be replenished with the new atoms in the atomic flux. For a laser repetition rate of 10 Hz, the duty cycle is in the range of 10^{-4} to 10^{-5}.

To solve this problem, a pulsed thermal source has been used that produces an atom population with a full width at half-maximum approaching 1 ms, thus improving the efficiency of the duty cycle by a factor of 30.[245]

Different pulsed laser sources have been used in the practice of RIMS. RIMS has been demonstrated with dye lasers pumped by Nd:YAG lasers,[243-247,271] nitrogen lasers,[237,251] excimer lasers,[250,264] flashlamps,[239,249] and also by a copper vapor laser.[272]

While most works in RIMS have utilized pulse lasers, providing the appropriate high power densities to attain optical saturation of atomic transition and effective ionization from excited atomic levels, Miller and Nogar have suggested[262] and confirmed[248] that continuous wave lasers may prove to be a viable alternative. These authors and collaborators[273] believe there are several reasons for this choice. First, most RIMS work to date has utilized thermal atom sources,[237,243,248,249,274] which produce gas-phase atoms continuously. Continuous lasers obviously will exhibit a better temporal overlap with such a continuous source. Second, cw lasers are better suited for use with pulse-counting electronics since pulsed laser ionization typically produces ions in such short time intervals that the counter dead-time and pile-up could become serious problems. Last, cw lasers produce ions at the highest rate when the laser focal volume is very small ($\leq 10^{-4}$ cm^3), in contrast to pulsed lasers where ionization efficiency is greatest when a relatively large volume (1 cm^3) is saturated. This smaller ion source volume should lead to better extraction efficiency and resolution in the mass spectrometer. It has been shown experimentally that cw ionization rates are $>10^3$ times that observed with a flashlamp-pumped dye laser.

However, ionization with cw lasers is not without drawbacks. The range of wavelengths used is more limited than with pulsed lasers. As mentioned previously, the rather low powers available dictate that the laser must be focused in order to have an appreciable probability of analyte atoms ionization. The volume sampled is thus quite small. In order to increase RIMS efficiency with cw lasers, Nogar and co-workers have proposed the other methods.

With relatively low peak power flashlamp-pumped and cw dye lasers, the laser power circulating within the cavity is usually much larger than the power coupled out. That is why workers of the Los Alamos National Laboratory[242] have carried out experiments to exploit intracavity spectroscopy for resonance ionization (intracavity RIMS). The cavity of a flashlamp-pumped dye laser was extended to contain the source region of a time-of-flight mass spectrometer. Experiments were carried out with uranium, using three-photon doubly resonant ionization at 591.5 nm. The authors received a 3.3-fold increase of the intracavity RIMS signal when compared with the extracavity RIMS signal. When using the cw dye laser, workers at Los Alamos[273] proposed a gas-dynamic focusing to significantly reduce the cross-sectional area of a sample stream from a thermally heated filament surface. The gas-dynamic focusing for sample concentrations has considerable potential for increasing the sensitivity of the RIMS technique.

As a rule, common ionization schemes for RIMS have departed from those recommended for RIS[130,168] and usually allow single-laser ionization of elements for which two lasers were originally proposed. Such compromises are often made for practical reasons. In this case, however, the resulting power densities exceed optical saturation by orders of magnitude, resulting in an increase in linewidth known as power broadening.[243] The loss of spectral resolution due to power broadening, however, is largely offset by the addition of mass selectivity.

Apel et al.[275] have made several observations regarding the utility of the 2 + 1 (photons to resonance plus photons to ionize) ionization process for analytical RIMS. They showed that it is feasible to approach saturation for the two-photon absorption process, bringing 2 + 1 ionization to comparable ionization efficiencies as 1 + 1 ionization for pulsed lasers. The resonance-excited process is not dramatically oversaturated as is often the case with one-photon resonant excitation. This allows better spectral definition and higher isobaric selectivity. Some other advantages of 2 + 1 ionization compared with the more widely used 1 + 1 process are also discussed.

4. Ion Separation and Detection

As previously mentioned, the resonance ionization process has an inherently high elemental selectivity. Mass spectrometric detection provides increased selectivity, which is a practical necessity for analytical problems when nonspecific background ionization takes place and must be separated from the analytical signal. Resonance ionization is ideally suited to MS because the ionization is well defined in both time and space. The ions, produced under resonance ionization of atoms, have almost the same thermal velocity distribution as the atoms removed from a sample. It allows, with the help of moderate electric fields, the formation of a collimated ion beam, which can be a good ion source for any mass analyzers of ions. The use of high-transmission ion optics coupled with the ability to detect single-ion events with extremely low noise means that the mass spectrometer will not impair either the selectivity or sensitivity of the resonance ionization process.

Different types of mass spectrometers have been used in the RIMS technique. Starting with the first publications concerning RIMS, magnetic selectors[237,243,248,249] have mostly been used. A tandem mass spectrometer of ORNL design was used for detection of actinide elements. It consisted of two 90° magnetic sectors of 30-cm radius.[239,240]

For the detection of a small number of ions, and especially for analytical applications, the most important characteristics of the mass spectrometer are the mass resolution and the transmission coefficient. The most suitable instruments for this purpose are quadrupole and time-of-flight mass spectrometers.

The two major advantages of quadrupole mass spectrometers, which are important in the detection of weak ion fluxes, are that spectrometers are small in size, thus providing a means for a connection with the laser resonance ionization system, and that they have high reliability. Despite their moderate mass resolution ($M/\Delta M = 10^3$ to 10^4), quadrupole mass analyzers coupled with selective laser ionization of atoms are very promising for application in analytical spectrometry of traces.[269,270,276,277]

For pulse lasers which produce a temporally defined ion pulse, time-of-flight MS is a simple and reliable method for mass filtering.[241,256,264,268] The time-of-flight method makes use of the mass-dependent time of flight of ions accelerated in the electric field. These ions are moved in the direction perpendicular to the atoms' movement in the atomic beam.

The Bruker-Fanzen Company (Germany)[278] has developed a resonance ionization time-of-flight mass spectrometer. Mass spectra are shown, demonstrating the spectrometer's analytical capabilities, i.e., the possibility of soft and hard ionization, wavelength selectivity, and a mass resolution as high as 6500 (50% valley) at mass 96.

Ions of a given mass not produced by the laser radiation can be excluded by time-gated

integration (with the help of a boxcar averager) of the output of the electron multiplier, providing the detection of ions.

Bekov et al.[279] described a laser resonance photoionization spectrometer which was used for ultrasensitive trace chemical analysis. For its operation, the spectrometer depends on the thermal evaporation and atomization in a vacuum ($\leqq 10^{-4}$ Pa) of the substance to be analyzed, followed by the stepwise laser resonance excitation and field ionization of the atoms released, the ions thus produced being detected by an electron multiplier after time-of-flight mass separation. The analysis capability of the system is some ten samples per hour. This, coupled with the capability for direct analysis of many types of samples without any need for sample pretreatment, makes it feasible to analyze a large number of samples in a reasonable time.

5. Analytical Applications

The combination of a selective laser resonance ionization of analyte atoms and mass spectrometric ion separation and detection, as already noted above, opened new possibilities for chemical analysis.

The use of a laser as an ionization source for a mass spectrometer received attention in a 1972 paper by Ambartsumyan and Letokhov,[280] suggesting the combination of lasers and mass spectrometers for more selective and sensitive molecular spectroscopy.

Researchers at the Oak Ridge National Laboratory[281] were the first to propose an idea to use resonance ionization of analyte atoms for the improvement of selectivity of a mass spectrometric system. They have shown experimentally the feasibility of using RIS as an ion source for MS.

In order to make use of the RIMS technique in analytical laser spectrometry, it was necessary to verify that signals, obtained under laser excitation of atoms, in fact, are caused by resonance ionization. Thus, Donohue and Young[274] posed the following questions in the determination of Pu. First, did the observed signal at the given wavelength of excitation accurately represent the mass positions of the Pu isotopes present and in the approximate ratios expected (as determined by thermal ionization)? Second, did the signal for a given mass (i.e., ^{242}Pu) appear only at discrete wavelengths and were these wavelengths characteristic of allowed Pu electronic transitions?

The first question was answered satisfactorily by using an excitation wavelength of 431.1 nm (an expected RIS transition for Pu) and sweeping through the mass spectrum in the range of 238 to 250 mass units. Mass peaks for ^{239}Pu, ^{240}Pu, and ^{242}Pu appeared at approximately the same abundance as the thermal ionization spectrum obtained from the sample. The second question verifying that the resonance ionization was the source of the signals was addressed by setting the mass spectrometer to monitor ^{242}Pu ions while scanning the laser wavelength. The resulting spectrum showed a good match with the predicted spectral line positions of resonance ionization wavelength for plutonium. Thus, it has been demonstrated that RIMS would be applicable to isotopic measurements and could define the analytical parameters of such measurements.

Following are listed examples of the determination of isotopes of various periodic table elements by RIMS.

a. Potassium

Harrison et al.[269] used a Knudsen cell and glow discharge as atomization sources for the determination of potassium. For the Knudsen-cell potassium beam, a wavelength ionization spectrum taken between 400 and 410 nm showed two peaks (representing sharp increases in $^{39}K^+$) at 404.4 and 404.7 nm, consistent with previous observations.[282] Furthermore, the Knudsen cell was replaced with a glow discharge, the laser was tuned at 404.4 nm, and a mass spectrum was taken over the 1 to 70 mass range. Because the discharge source also

formed ions by electron impact and by collisions with metastable atoms, the ion counter/processor was set to the difference mode so that only those ions produced by the laser pulse were displayed in the resultant spectrum. As a result, only the ion peaks for $^{39}K^+$ and $^{41}K^+$ were taken. These experiments have shown that the glow discharge can be an effective atomization source for RIMS.

b. Strontium and Barium

The possibilities of using an ultrasensitive mass spectrometer for the determination of strontium were discussed in the work of Lucatorto et al.,[283] where chemical and isotopic selectivity were achieved due to the combination of laser resonance ionization and MS. Selectivity and sensitivity, limited by the processes of ions recharging and by effects of line-broadening as a result of high laser power densities, were considered as an example with isotopes $^{88}Sr/^{90}Sr$, which are of particular interest and provide the most difficult task for any conventional mass spectrometric method.

Considerable advances have been made by Cannon et al.[284] in the highly sensitive and highly selective Ba determination using two low-power, single-mode cw dye lasers and a high-power cw Nd:YAG laser as an atomization source for MS. The sensitivity for half of the upper states investigated was greater than using electron impact ionization. Isotopic selectivity of 800 was observed.

The determination of Sr and some other elements has been studied in the work of Moore et al.,[247] where systematics of multielement determination with RIMS and thermal atomization have been developed. Different aspects of atomization, ionization, and signal detection are discussed for 19 elements. The potential for multielement analysis with RIMS and thermal atomization has been demonstrated for the sample containing 1 μg of each specific element — V, Fe, Co, Ni, Lu, Pb, and U. For Co and Ni, transitions were used only from metastable excited levels. To increase spectral selectivity, a defocusing laser beam was used. Despite the fact that the ionization process was not under saturation conditions, an increase of analytical volume with an unfocused beam gives only a small loss in absolute intensity of the analytical signal. As this takes place, a considerable analytical gain was achieved due to the independent background reduction of the laser wavelength.

c. Indium

Kimock et al.[259] compared multiphoton resonance ionization of sputtered neutrals to low-dose secondary ions mass spectrometry (SIMS). The ion and neutral yields from the bombardment of the analyzed surface of polycrystal In with a primary beam of Ar^+ ions were studied via the chemisorbtion of O_2 on the sample surface. The In and In_2 yields decrease with oxidation, while the In^+ and In_2^+ yields increase dramatically. This means that the sample composition influences the yield of neutrals under bombardment with primary Ar^+ ions.

d. Iron

Fassett et al.[244-246,263,271,285] used RIMS to study the formation of iron ions. Rhenium filament was used as an atomization source.[244,263,285] Iron was thermally vaporized from a filament at 1250 K. A one-wavelength, two-photon ionization scheme was employed which utilized the tunable UV light provided by a Nd:YAG-pumped dye laser with frequency doubling. Experimental results were also presented for the elements Ni, Mo, V, and Re, but not iron, to study atom plumes produced by thermal vaporization.[244,263] A 30-fold improvement in sample utilization efficiency was demonstrated for the pulsed thermal source relative to a continuous thermal source.[245] That system has been tested by using the element iron.

Savicas et al.[276] used a glow discharge as an atomization source for RIMS. Fe and Cu

were ionized by two photons from excimer-pumped dye lasers, which provided the UV light of the same frequency. A quadrupole mass spectrometer was used to detect the RIMS signals.

Fassett et al.[246] used resonance ionization isotope dilution MS for the determination of iron in standard samples of blood serum (SRM 909), water standard samples (SRM 1643), and copper samples (SRM 458). The precision and accuracy of the measurement were typically 2 to 3%.

e. Copper

The atomic population of copper produced by a glow discharge was used for RIMS.[270] In this work, NBS reference materials were analyzed. The use of resonance ionization of atoms allowed the avoidance of some interferences in MS with conventional ion sources. Thus, in the analysis of zinc reference samples, the copper peak at 0.058% was difficult to recognize at m/e 63 due to an overlap with a huge intensity peak from $^{64}Zn^+$. Using laser resonance ionization of copper at 324.75 nm, these interferences were avoided. The copper isotopes $^{63}Cu^+$ and $^{65}Cu^+$ appeared in a proper ratio, even in the presence of a great excess of zinc.

f. Silver and Gold

Becker and Gillen[268] described surface analysis by multiphoton ionization of desorbed or sputtered atoms by a probe Ar^+ beam. The secondary ions were accelerated, focused, and detected into a high resolution time-of-flight mass spectrometer. Isotopes such as ^{197}Au, ^{209}Bi, ^{206}Pb, as well as isotopes of Ag, Sb, and Pt, were detected in NBS standard reference copper samples. About 10^{-10} g (about 10^{-2} monolayer over 10^{-1} cm^2) of material was removed for parts-per-million analysis.

g. Carbon

Moore et al.[266] demonstrated the possibilities of RIMS for the determination of carbon. A two-photon resonant excitation in the region of 280 nm, three-photon ionization scheme provided large ionization signals from carbon atoms obtained by heating microgram samples of graphite. These results show that elemental carbon vapor can be detected at densities at least as low as 10^7 atoms/cm^3. Thus, it appears feasible to carry out direct analysis of carbon in solids using RIMS with a sputtering or ablation technique and to develop a new approach to the measurement of ^{14}C in microgram samples of carbon. The same conclusion about RIMS potential for the highly sensitive determination of ^{14}C was made by Clark[286] in his theoretical work.

h. Lanthanides

In one of the first papers on the analytical application of RIMS, the workers of the Los Alamos National Laboratory showed that RIMS can be used for analysis of different samples and for analysis of aqueous solutions, which is very important for analytical chemistry.[249] The aqueous samples of lanthanide chlorides or their mixtures were deposited on the surface of a conventional filament source of the mass spectrometer and then vaporized. It has been demonstrated that the two-photon ionization process was extremely selective for the determination of Lu. If the equimolar mixture of Lu and Yb were measured under thermal ionization, then the Yb signal would be several orders of magnitude larger than that from Lu, due to the large difference in volatilities of the two elements. With the resonance photoionization of the same sample, under conditions in which thermal ionization was minimized, a dramatic enhancement was shown in the Lu signal. No laser-generated Yb ions were detectable, affording a selectivity S of the photoionization process S of $\geqq$50,000 for N_{175}/N_{174}, where N_{175} is the number of photogenerated Lu ions and N_{174} is the background signal of Yb at mass 174.

Such a high selectivity is connected with the absence of resonances in the Yb atom for one or two photons, used for Lu ionization, and with relatively soft laser radiation ($I \leqq 30$ kW/cm^2). The accuracy of laser photoionization in MS was also high. The observed ^{175}Lu/^{176}Lu ratio was in a good agreement with thermal ionization, to within 1%. Preliminary experiments showed that samples $\leqq$1 ng can be detected. Matrix and charge exchange effects did not seriously degrade the selectivity of the determination process.

Donohue et al.[237,251,287] showed that RIMS eliminated isobaric interferences for the determination of the rare-earth elements Nd and Sm with masses 144, 148, and 150. The sensitivity was not as good as with conventional (pulse counting) mass spectrometers primarily because of the low duty cycle of the N_2 laser used. To increase the number of atoms interacting with the laser radiation, Miller and Nogar[248] used a cw laser. The selectivity of cw ionization was demonstrated by the fidelity of the ^{175}Lu/^{176}Lu ratio in mixed lutetium/ytterbium samples in spite of isobaric ^{176}Yb interferences. The accuracy of the measurement was about 5%. The isotopic ratios for Nd and Sm in binary mixtures were measured without any chemical separation. Accuracy of these isotopic ratio measurements was considerably better than with conventional MS using a thermal ionization source. The isotope ratios of lutetium were accurately determined in 60-ng samples containing trace amounts of ^{173}Lu, ^{174}Lu, and a 1000-fold excess of the isobaric interfering isotopes ^{173}Yb and ^{174}Yb. The ratio ^{173}Lu/^{175}Lu was measured to be $(0.44 \pm 0.07) \times 10^{-6}$ on a sample containing only 10^8 atoms of ^{173}Lu.[288]

Miller et al.[289] showed that RIMS was an excellent technique for acquiring high-resolution optical spectra of rare isotopes. To demonstrate the potential of this technique, hyperfine spectra for ^{176}Lu, ^{175}Lu, ^{174}Lu, and ^{173}Lu were presented. The high sensitivity was documented by the fact that the total amount of the latter two rare isotopes in the sample was 2×10^{-10} and 3×10^{-11} g. In this work, it was also pointed out that power broadening is a serious problem in using single-color, 1 + 1 photoionization when the laser power is increased to attain reasonable ionization efficiency, the resonance transition is optically saturated by many orders of magnitude, resulting in power broadening and a reduction in isotope selectivity. A two-color, 1 + 1 process would result in a much better spectral resolution since the power in the ionization step could be kept at a high level.

Young et al.[238] evaluated the feasibility of using RIMS in the mass analysis of europium. They found that many more RIMS-active optical transitions appeared than could be predicted. These extra RIMS transitions for Eu arise from initial states well above the ground state (>13,000 cm^{-1}). It was proposed that these states are populated by hybrid resonant transitions involving dimer molecules, demonstrating a general phenomenon in RIMS. If so, there is the possibility of more spectral interferences in RIMS than had originally been expected. The true mechanism of population of the initial states of Eu atoms in the range of this study, however, requires further definition.

i. Actinides

RIMS was used successfully by Donohue et al.[239,274,287] for the determination of uranium and plutonium isotopes. The latter is very important for safeguarding the nuclear fuel cycle, for the quantitative determination of the degree of environmental pollution, and also for the determination of its isotopic composition and thus of the origin of the plutonium in the sample under investigation (e.g., fallout of Pu from nuclear weapons tests, pollution by nuclear power plants, or natural pollution). This is why the highly sensitive thermal ionization MS methods have been extensively studied at the Oak Ridge National Laboratory. However, such measurements have suffered in the past from isobaric interferences due to U (atomic mass 238) and Am (atomic mass 241). The former was found in samples of spent reactor fuel at a concentration 10^2 to 10^3 times higher than Pu, while the latter isotope is a decay product of ^{241}Pu. Donohue and Young[274] showed that RIMS was applicable to Pu isotopic

measurements and also to the determination of the analytical parameters of such measurements in a sample consisting of a mixture of Pu isotopes containing 1 μg of ^{242}Pu (99% pure) and 30 to 50 ng of NBS SRM 947e containing the isotopes of Pu from mass 238 to 242. The sample was depositied on a Re filament and thermally heated. Three-photon, doubly resonant ionization was used. The dye lasers were pumped by a N_2 laser. The same results were received for U and Pu in order to eliminate isobaric interferences at mass 238 and at mass 241 (due to Am). The measurements were made on nanogram-size samples loaded on resin beads.[287]

The isotope analysis of uranium and plutonium mixtures was carried out by RIMS with the use of flashlamp-pumped dye lasers and the pulsed thermal atomization technique.[239,290] Sample sizes of 10 ng for each element were adequate for measurement of the $^{240}Pu/^{239}Pu$, $^{241}Pu/^{239}Pu$, and $^{235}U/^{238}U$ isotope ratios. Sensitivity was enhanced by using a pulsed thermal atomization technique, which resulted in a tenfold improvement in a sample usage compared with continuous atomization. Precision and accuracy were about ± 1%. The requirements of laser and atomization sources discussed in the paper of Donohue et al.[290] improved the efficiency of the technique.

Researchers at the Los Alamos National Laboratory[242,273] suggested the intracavity laser ionization technique in order to improve the efficiency of ionization of uranium. That technique was particularly effective for uranium because three-photon, doubly resonant ionization at 591.5 nm (and thus a single laser) can be used to ionize uranium through sequential resonances.

RIMS was applied to a spectral study of Th, U, Np, Pu, Am, and Cm in the wavelength region of 580 to 607 nm, which was chosen before for the determination of Pu and U, to assess any spectral interferences among these elements.[240] Several RIMS peaks were observed in that region for all these actinides except Cm. The presented spectral data demonstrated that RIMS measurements can be made on the actinides with the use of relatively low-energy photons.

RIMS has been tested for the isotope-selective determination of trace amounts of plutonium.[256] An atomic beam was formed by evaporating plutonium atoms from a rhenium filament heated to 1800°C. Radiation from a pulsed dye laser excited the Pu atoms in a two-photon process (λ = 595.2 nm) followed by a photoionization of the excited atoms with the same photon. Mass selectivity was obtained by use of a time-of-flight spectrometer. A resonant signal of ^{239}Pu was measured with 10^{13} atoms deposited on the rhenium filament. The detection limit achieved in this experiment can be improved by reducing the background signal due to the nonresonant ionization of the chemical compounds UO, UF, and UO_2, increasing the duty cycle up to 1 by using a laser system with a high repetition rate, and producing a pulsed atomic beam with the same repetition rate as the laser used for RIMS. In addition, the increase of the diameter of the laser beam and the use of stepwise excitation and ionization can improve the detection limit.

Recommendations for the use of a high repetition rate laser system coupled with stepwise excitation and ionization were realized in the determination of plutonium in the work of Peuser et al.,[272] where a copper vapor laser-pumped dye laser system was used. The stepwise excitation and ionization of plutonium atoms were achieved in turn by three photons of 586.5, 688.2, and 578.2 nm. The method allowed the detection of about 10^8 atoms of Pu in a sample. The background signal became gradually smaller as the repetition rate was increased up to several kilohertz.

RIMS has also been applied to the measurement of U and Sm by utilizing the argon ion-sputtering technique for atomization of a sample.[258] The CMX-4 flashlamp-pumped dye laser was used for the ionization of atoms.

j. Technetium

The use of RIMS for the selective detection of technetium was studied by Nogar et al.[291]

The optimum wavelengths for the selective ionization of Tc were also studied. Samples were prepared by electroplating technetium onto Re filaments, which were then heated. Tc ions were generated via a simple photoionization scheme using two photons of the same wavelength. In the next work,[241] three-photon, two-color resonance ionization was described for Tc determination by RIMS. An unknown fraction of the sample of Tc was vaporized in molecular form and could not be addressed by normal atomic photoionization methods. Obvious candidates include Tc_2 and TcO. This RIMS work showed promise as a way of greatly reducing isobaric interferences in isotope-ratio measurements of Tc in samples containing molybdenum and ruthenium.

Rimke et al.[292] reported on their experiments with technetium. They identified a number of autoionization states of this element. For the strongest states observed, the ion current increased by a factor of 200 compared with ionization into a continuum. They predicted a detection limit of 10^6 to 10^7 atoms for this element.

k. Rhenium, Osmium

Walker and Fassett[293] measured the isotopic composition of microgram quantities of Re and Os. The high sensitivity necessary for these measurements was achieved by optimizing the conditions for atomization of the sample and for ionization of the resulting vapor.

Re and Os were absorbed from a chloride solution onto anion exchange beads as a means of purifying and concentrating the sample, and then were loaded onto a miniaturized Ta filament. The molecular species of Re and Os were reduced to metal in a vacuum of the mass spectrometer by gradual heating in the presence of collodion and graphite. Os atomization was optimized by pulse heating of the filament to coincide with the repetition rate of the laser system. Accuracy and precision of microgram quantities measurements were about 1%, although for picogram quantities they ranged from 1 to 5%, measured by counting statistics.

l. Noble Gases

A combination of RIS and the quadrupole mass spectrometer was proposed by Chen and co-workers[184,277] for isotopic analysis of noble (inert) gases. A quadrupole mass filter was introduced to reduce the background ions in the RIS determination of Xe. When the mass filter was tuned to pass amu = 131 and the resolution ($M/\Delta M$) was approximately 300, a background signal was not observable, thus permitting the detection of single ions. Hence, for a heavy ion such as Xe^+, a relatively simple mass filter can be used to eliminate background ionization due to multiphoton ionization of the residual gases at power densities where the ionization probability for a rare gas atom at the focus is close to unity. It was shown that detection of a single rare gas atom was extremely difficult without a mass filter to reject the residual gas ionization.

Kramer et al.[186] investigated a RIS ion source in conjunction with a quadrupole mass spectrometer to count 1000 individual ^{81}Kr atoms. This technique was demonstrated for the first time with a groundwater analysis in which about 1000 atoms of ^{81}Kr were counted after the processing of a gas extraction from only a few liters of water. This new method can be used for groundwater dating.[187] The capabilities of RIS in combination with MS as an analytical tool in isotope geophysics were discussed in the review of Lehmann,[188] who pointed out that present research makes it possible to count single atoms of radioactive noble gases if the RIS technique is combined with a quadrupole mass spectrometer.

The detection of ^{81}Kr, ^{85}Kr, ^{37}Ar, and ^{39}Ar in environmental samples (water, sediments, ice) by the RIS technique has distinct advantages compared with the low level decay-counting technique.[185] Geological applications include the dating of polar ice and the possibility of determinating groundwater circulation.[184] The use and application of these techniques is important not only in the study of geology, but also in site selection for hazardous waste disposal containing ^{239}Pu or other fissionable atoms.[294]

6. Interferences in RIMS

The combination of mass spectrometers and lasers as excitation sources provides new capabilities for chemical analysis. Such a combination allows the selection of analytes on isotopic levels after the selection on atomic levels; as a result, isobaric interferences are practically eliminated. Some interferences in RIMS, however, still remain. When the scheme of multiphoton ionization is used, requiring a UV light, a compromise exists between resolution and ionization efficiency and may provide unwanted background ionization of matrix species or organic vacuum contaminants. Such background ions may often be identified by their mass, but many peaks due to organic fragment ions overlap critical elemental isotopic masses.[252]

If rhenium or tantalum filaments are used as the atomization source, nonselective ionization of filament material can be detected. Thus, in the course of a RIMS investigation of technetium,[241] a persistent RIMS signal at mass 181 was observed. This signal was found to be generated via laser ionization of the tantalum filament material. The signal was observed at a wide variety of wavelengths under moderate irradiation and evaporation conditions. Investigations of multiphoton ionization of Ta have shown that a wide variety of spectral processes exist and can be observed.[250] Thus, considerable care must be taken in choosing resonance ionization schemes to ensure maximum selectivity in RIMS analysis. Nonselective ionization can be detected not only from filament atoms, but also similar ionization processes can occur from matrix elements or molecules such as TaO. This problem may be considerably reduced by using low-peak power lasers.

Nogar and Keller[295] studied the effect of very weak laser sidebands on optical spectra involving saturable intermediate states of matrix atoms. The authors reported that the occurence of weak sidebands on the laser output at some levels is a relatively common phenomenon, but it is only observable under special circumstances. These sidebands may result in a significant loss in analytical selectivity when a matrix atom has a transition close to the analytical transition used. This remains a very important consideration in isotope analysis.

VI. CONCLUSION

AI spectrometry represents a revolutionary advance in methods for the determination of elemental compositions of substances. The main advantage of the atomic ionization method is its extremely high sensitivity. In principle, the method can attain the limiting value; each atom existing in resonance with laser radiation can be detected. This effect is associated with the fact that using a laser allows transferring practically every atom into an excited state and detecting an ion with an efficiency equal to 1.

The high spectral selectivity of this method is related, on one hand, to the narrow band of a laser and, on the other hand, to the use of stepwise excitation and succeeding ionization of atoms which results in an increase of selectivity by several orders of magnitude. Combining resonance ionization with the MS detection method permits the isotope analysis of substances. The selectivity is of particular value for the elimination of matrix effects. The multiphoton mechanism of matrix ionization restricts the selectivity of the method. However, selection of experimental conditions in relation to the power density of laser radiation, required for more efficient ionization of an analyte element in comparison with a sample matrix, helps avoid these restrictions.

The main problem of AI spectrometry resides in the provision of high efficiency sample atomization, a problem common to any other method of analytical atomic spectrometry.

Depending on the problems being solved, the analytical atomic ionization method has a broad range of possibilities for the use of various systems of sample atomization. Recently, atomizers such as ICP plasma[125,296] and microwave helium plasmatron[297] have been tried. However, some disadvantages remain relative to flame atomizers.

When using simple and widespread atomization methods, e.g., a flame, the high sensitivity of the method allows the achievement of low detection limits and the detection of micro quantities of complex samples. Recently, AI spectrometry in flames has experienced ever-expanding applications for analysis of various real samples whose number is constantly increasing. It should be noted that before the introduction of AI spectrometry as a method these analyses were not performed in analytical flame spectrometry.

The AI method has found its application in various fields of human practice. For example, the AI method can help in determining Hg in the gaseous phase with a detection limit of 220 fg,[298] in measuring the influence of neutron radiation at a level below 1 mrad, in diagnosing bone diseases,[184] in detecting solar neutrino[232] and short-lived radioactive isotopes,[299] and in many other determinations.

Even though analytical AI spectrometry is relatively young (about 10 years old), the number of publications, including reviews,[300-306] is steadily increasing. At the same time, the number of publications devoted to investigations of processes occurring in a medium under the action of laser radiation and to studying the production of AI signals[53,54] is also increasing. An understanding of all phenomena taking place will make it possible to develop highly efficient, highly sensitive, and selective methods of determination of traces of elements with the use of AI spectrometry.

Up to now, broad application of the AI method has been restricted by the absence of inexpensive commercial tunable lasers posessing certain required characteristics, as well as by the absence of a sufficient number of qualified analytical chemists handling laser technology.

Recently, the method based on the determination of the number of ions resulting from the action of laser radiation has been efficiently used for the selective determination of molecules,[307] and this offers further promising prospects for analytical ionization spectrometry.

REFERENCES

1. **Green, R. B., Keller, R. A., Luther, G. G., Schenk, P. K., and Travis, J. C.,** Galvanic detection of optical absorption in a gas discharge, *Appl. Phys. Lett.*, 29, 727, 1976.
2. **Bridges, W. B.,** Characteristics of an opto-galvanic effect in cesium and other gas discharge plasmas, *J. Opt. Soc. Am.*, 68, 352, 1978.
3. **Feldman, D.,** Optogalvanic spectroscopy of some molecules in discharges: NH_3, NO_2, H_2, and N_2, *Opt. Commun.*, 29, 67, 1979.
4. **Green, R. B., Keller, R. A., Schenk, P. K., Travis, J. C., and Luther, G. G.,** Opto-galvanic detection of species in flames, *J. Am. Chem. Soc.*, 98, 8517, 1976.
5. **Alkemade, C. Th. J.,** Single-atom detection, *J. Appl. Spectrosc.*, 35, 1, 1981.
6. **Turk, G. C., Travis, J. C., DeVoe, J. R., and O'Haver, T. C.,** Analytical flame spectrometry with laser enhanced ionization, *Anal. Chem.*, 50, 817, 1978.
7. **Zorov, N. B., Kuzyakov, Yu. Ya., and Matveev, O. I.,** Atomic-ionization analysis by tunable lasers, *Zh. Anal. Khim.*, 37, 520, 1982.
8. **Travis, J. C., Turk, G. C., and Green, R. B.,** Laser-enhanced ionization spectrometry, *Anal. Chem*, 54, 1006A, 1982.
9. **Turk, G. C., Travis, J. C., and DeVoe, J. R.,** Laser-enhanced ionization spectrometry for trace metal analysis, *J. Phys. (Paris)*, 44, C7-301, 1983.
10. **Sysoev, A. A. and Chupakhin, M. S.,** *Introduction to Mass Spectrometry*, Atomizdat, Moscow, 1977, 302.
11. **Ambartsumyan, R. V., Kalinin, V. P., and Letokhov, V. S.,** Two-stage selective photoionization of rubidium atoms by laser radiation, *Pis'ma Zh. Eksp. Teor. Fiz.*, 13, 305, 1971; Selective two-photon photoionization of Rb atoms by laser radiation, IEEE *J. Quantum Electron.*, 7, 305, 1971.
12. **Letokhov, V. S. and Moore, C. B.,** Laser separation of isotopes. I, *Kvantovaya Elektron (Moscow)*, 3, 248, 1976; Laser isotope separation, Part II, *Kvantovaya Elektron (Moscow)*, 3, 485, 1976.

13. **Ambartsumyaan, R. V., Apatin, V. M., Letokhov, V. S., Makarov, A. A., Mishin, V. I., Puretskii, A. A., and Furzikov, N. D.,** Selective two-step ionization of rubidium atoms by laser radiation, *Zh. Eksp. Teor. Fiz.*, 70, 1660, 1976.
14. **Letokhov, V. S.,** Laser selective determination of single atoms, in *Chemical and Biochemical Application of Lasers*, Moore, C. B., Ed., Academic Press, New York, 1980, chap. 1.
15. **Hurst, G. S., Nayfeh, M. H., and Young, J. P.,** A demonstration of one-atom detection, *Appl. Phys. Lett.*, 30, 229, 1977.
16. **Letokhov, V. S., Mishin, V. I., and Puretskii, A. A.,** Selective photoionization of atoms by laser radiation, in *Khimia Plasmy*, 4th ed., Smirnov, B. M., Ed., Atomizdat, Moscow, 1977, 3.
17. **Ivanov, L. N. and Letokhov, V. S.,** Selective ionization of atoms by light and electric fields, *Kvantovaya Elektron. (Moscow)*, 2, 589, 1975.
18. **Van Dijk, C. A., Curran, F. M., Lin, K. C., and Crouch, S. D.,** Two-step laser assisted ionization of sodium in a hydrogen-oxygen-argon flame, *Anal. Chem.*, 53, 1275, 1981.
19. **Schenk, P. K., Travis, J. C., Turk, G. C., and O'Haver, T. C.,** Collection of ions produced by continuous wave laser-enhanced ionization in a hydrogen/air flame, *J. Phys. Chem.*, 85, 2547, 1981.
20. **Messman, J. D., Schmidt, N. E., Parli, J. R., and Green, R. B.,** Laser-enhanced ionization of refractory elements in a nitrous oxide-acetylene flame, *Appl. Spectrosc.*, 39, 504, 1985.
21. **Travis, J. C., Schenk, P. K., Turk, G. C., and Mallard, W. G.,** Effect of selective laser excitation on the ionization of atomic species in flames, *Anal. Chem.*, 51, 1516, 1979.
22. **Turk, G. C., Travis, J. C., DeVoe, J. R., and O'Haver, T. C.,** Laser-enhanced ionization spectrometry in analytical flames, *Anal. Chem.*, 51, 1890, 1979.
23. **Schenk, P. K., Mallard, W. G., Travis, J. C., and Smyth, K. G.,** Absorption spectra of metal oxydes using optogalvanic spectroscopy, *J. Chem. Phys.*, 69, 5147, 1978.
24. **Chaplygin, V. I., Zorov, N. B., and Kuzyakov, Yu. Ya.,** Laser atomic ionization determination of cesium in flames, *Talanta*, 30, 505, 1983.
25. **Curran, F. M., Lin, K. C., Leroi, G.E., Hunt, P. M., and Crouch, S. R.,** Energy consideration in dual laser ionization processes in flames, *Anal. Chem.*, 55, 2382, 1983.
26. **Gonchakov, A. S., Zorov, N. B., Kuzyakov, Yu. Ya., and Matveev, O. I.,** Determination of picogram concentrations of sodium in flame by stepwise photoionization of atoms, *Anal. Lett.*, 12, 1037, 1979.
27. **Zorov, N. B., Kuzyakov, Yu. Ya., and Matveev, O. I.,** Stepwise photoionization of atoms in analytical flame spectrometry, in *Abstr. III All Union Conf. Anal. Chem.*, Vol. 2, Minsk, 1979, 192.
28. **Salcedo Torres, L. E., Zorov, N. B., and Kuzyakov, Yu. Ya.,** Determination of indium by laser stepwise photoionization in flame, *Zh. Anal. Khim.*, 36, 1433, 1981.
29. **Turk, G. C., Mallard, W. G., Schenk, P. K., and Smyth, K. C.,** Improved sensitivity of laser enhanced ionization spectrometry in flames by stepwise excitation, *Anal. Chem.*, 51, 2408, 1979.
30. **Omenetto, N., Berthoud, T., Cavalli, P., and Rossi, G.,** Analytical laser enhanced ionization studies of thallium in the air-acetylene flame, *Anal. Chem.*, 57, 1256, 1985.
31. **Goldsmith, J. E. M.,** Resonant multiphoton optogalvanic spectroscopy of radicals in flames, *J. Phys. (Paris) Colloq.*, 44, C7-277, 1983.
32. **Turk, G. C., DeVoe, J. R., and Travis, J. C.,** Stepwise excitation laser enhnaced ionization spectrometry, *Anal. Chem.*, 54, 643, 1982.
33. **Zorov, N. B., Kuzyakov, Yu. Ya., Matveev, O. I., and Chaplygin, V. I.,** Determination of lithium and cesium by step atom photoionization in flame by dye lasers, *Zh. Anal. Khim.*, 35, 1701, 1980.
34. **Novodvorsky, O. A., Zorov, N. B., and Kuzyakov, Yu. Ya.,** Use of a holographic-grating laser with a grazing incidence for trace determination of phosphorus as phosphorus oxide (PO) molecules by optogalvanic spectroscopy, in *Proc. 4th All Union Conf. Tunable Laser Materials*, Novosibirsk, U.S.S.R., 1984, 382.
35. **Chaplygin, V. I., Novodvorsky, O. A., Matveev, O. A., Zorov, N. B., and Kuzyakov, Yu. Ya.,** Optimization of conditions for atomic-ionization laser determination of elements in a flame, *Deposited Doc. VINITI*, 2597, 83, 1983.
36. **Alkemade, C. Th. J., Hollander, T., Snelleman, W., and Zeegers, P. J. Th.,** *Metal Vapors in Flames*, Pergamon Press, Oxford, 1982, 1033.
37. **Green, R. B., Havrilla, G. J., and Trask, T. O.,** Laser-enhanced ionizaion spectrometry: characterization of electrical interferences, *Appl. Spectrosc.*, 34, 561, 1980.
38. **Trask, T. O. and Green, R. B.,** Evaluation of electrode configuration for high voltage interferent removal in laser-enhanced ionization spectrometry, *Spectrochim. Acta*, 38B, 503, 1983.
39. **Turk, G. C.,** Reduction of matrix ionization interference in laser-enhanced ionization spectrometry, *Anal. Chem.*, 53, 1187, 1981.
40. **Zorov, N. B., Kuzyakov, Yu. Ya., Novodvorsky, O. A., Chaplygyn, V. I., and Volchkov, I. V.,** U.S.S.R. Patent 1,155,919, 1985.
41. **Havrilla, G. J. and Green, R. B.,** Pre-amplifier for laser enhanced ionization spectrometry, *Chem. Biomed. Environ. Instrum.*, 11, 273, 1981.

42. **Travis, J. C. and DeVoe, J. R.,** The optogalvanic effect, in *Lasers in Chemical Analysis,* Hieftje, G. M., Travis, J. C., and Lytle, F. E., Eds., Humana Press, Clifton, NJ, 1981, 93.
43. **Van Dijk, C. A.,** Two-Photon Excitation of Higher Sodium Levels and Population Transfer in a Flame, Ph.D. thesis, University of Utrecht, Utrecht, 1978.
44. **Hurst, G. S.,** Resonance ionization spectroscopy, *Anal. Chem.,* 53, 1448A, 1981.
45. **Letokhov, V. S.,** *Nonlinear Selective Photoprocesses in Atoms and Molecules,* Nauka, Moscow, 1983, chap. 3.
46. **Smith, K. C. and Mallard, W. G.,** Laser induced ionization and mobility measurements of very small particles in premixed flames at the sooting limit, *Combust. Sci. Technol.,* 26, 35, 1981.
47. **Havrilla, G. J. and Green, R. B.,** Evaluation of plate electrodes for laser-enhanced ionization spectrometry, *Anal. Chem.,* 52, 2376, 1980.
48. **Berthoud, T., Lipinsky, J., Camus, P., and Stehle, J.-L.,** Electron pulse shape in laser-enhanced ionization spectrometry, *Anal. Chem.,* 55, 959, 1983.
49. **Berthoud, Th., Drin, N., Lipinsky, J., and Camus, P.,** Mechanisms of production and collection of charges in LEI spectroscopy, *J. Phys. (Paris) Colloq.,* 44, C7-67, 1983.
50. **Havrilla, G. J., Schenk, P. K., Travis, J. C., and Turk, G. C.,** Signal detection of pulsed laser enhanced ionization, *Anal. Chem.,* 56, 186, 1984.
51. **Lawton, J. and Weinberg, F. J.,** *Electrical Aspects of Combustion,* Clarendon Press, Oxford, England, 1969.
52. **Kuzyakov, Yu. Ya., Zorov, N. B., Chaplygin, V. I., and Novodvorsky, O. A.,** Trace analysis by laser optogalvanic spectroscopy, *J. Phys. (Paris), Colloq.,* 44, C7-335, 1983.
53. **Novodvorsky, O. A.,** Mechanisms of Ionization and Optogalvanic Signal Formation in Flames under Interaction with Resonance Radiation, Ph.D., thesis, Moscow State University, Moscow, 1984.
54. **Travis, J. C., Turk, G. C., DeVoe, J. R., Schenk, P. K., and Van Dijk, C. A.,** Principles of laser-enhanced ionization spectrometry in flames, *Prog. Anal. At. Spectrosc.,* 7, 199, 1984.
55. **McDaniel, E. W. and Mason, E. A.,** *The Mobility and Diffusion of Ions in Gases,* John Wiley & Sons, New York, 1973.
56. **Smirnov, B. M.,** *Introduction to Plasma Physics,* Nauka, Moscow, 1982, 177.
57. **Novodvorsky, O. A., Zorov, N. B., and Kuzyakov, Yu. Ya.,** Nature of the pulsed optogalvanic effect in a flame, *Vestn. Mosk. Univ. Khim.,* 26, 221, 1985.
58. **Allis, W. P. and Rose, D. J.,** The transition from free to ambipolar diffusion, *Phys. Rev.,* 93, 84, 1954.
59. **Axner, O., Berglind, T., Heully, J. L., Lindgren, I., and Rubinsztein-Dunlop, H.,** Improved theory of laser-enhanced ionization in flames: comparison with experiment, *J. Appl. Phys.,* 55, 3215, 1984.
60. **Alkemade, C. Th. J.,** Laser and flames, in *Proc. 20th Coll. Spectrosc. Int. and 7th Int. Conf. At. Spectrosc.,* Prague, 1977, 93.
61. **Smyth, K. C., Schenk, P. K., Mallard, W. G., and Travis, J. C.,** Optogalvanic spectroscopy: a new look at atoms and molecules, in *Proc. 10th Mater. Res. Symp. Characterization of High Temp. Vapours and Gases,* Washington, D.C., 1978, 188.
62. **Kuzyakov, Yu. Ya., Matveev, O. I., and Novodvorsky, O. A.,** Determination of flame velocity using selective laser-enhanced ionization of atoms, *Zh. Prikl. Spektrosk.,* 40, 145, 1984.
63. **Schenk, P. K., Travis, J. C., Turk, G. C., and O'Haver, T. C.,** Laser enhanced ionization flame velocimeter, *Appl. Spectrosc.,* 36, 168, 1982.
64. **Axner, O., Berglind, T., Heully, J. L., Lindgren, I., and Rubinsztein-Dunlop, H.,** Theory of laser enhanced ionization in flames — comparison with experiments, *J. Phys. (Paris) Colloq.,* 44, C7-311, 1983.
65. **Willer, W. J.,** Ions in flames. Evaluations and prognosis, in *Proc. 14th Int. Symp. Combustion,* Academic Press, New York, 1973, 307.
66. **Marunkov, A. G. and Chekalin, N. V.,** Determination of the degree of collisional ionization from exited levels of atoms in a flames, *Opt. Spectrosc. (USSR),* 61, 461, 1986.
67. **Goldsmith, J. E. M.,** Resonant multiphoton optogalvanic detection of atomic hydrogen in flames, *Opt. Lett.,* 7, 437, 1982.
68. **von Hellfeld, A., Gaddick, J., and Weiner, J.,** Observation of laser-induced Penning associative ionization in lithium-lithium collisions, *Phys. Rev. Lett.,* 40, 1369, 1978.
69. **Bearman, G. H. and Leventhal, J. J.,** Ionization and energy pooling in laser-excited sodium vapor, *Phys. Rev. Lett.,* 41, 1227, 1978.
70. **Msezane, A. and Manson, S. T.,** Effects of minima of the generalized oscillator strength on the total ionization cross section, *J. Phys. B,* 8, L5, 1975.
71. **Axner, O., Lindgren, I., Magnusson, I., and Rubinsztein-Dunlop, H.,** Trace element determination in flames by laser enhanced ionization spectrometry, *Anal. Chem.,* 57, 773, 1985.
72. **Matveev, O. I., Zorov, N. B., and Kuzyakov, Yu. Ya.,** Intracavity spectroscopy with a photon detector based on stepwise atoms photoionization, *Talanta,* 27, 907, 1980.
73. **Axner, O., Berglind, T., and Sjoestrom, S.,** Laser-enhanced ionization spectroscopy around the ionization limit, *Phys. Scr.,* 34, 18, 1986.

74. **Wise, W. W., Smyth, M. W., and Miiles, B. M.,** *Atomic Transition Probabilities. Sodium through Calcium*, Vol. 2, National Bureau of Standards, Washington, D.C., 1969, 228.
75. **Calicbe, E. and Niemax, K.,** Oscillator strengths of the principal series lines of Rb, *J. Phys. B*, 7, 1244, 1974.
76. **Aymar, M., Lue-Koenig, E., and Parnoux, P. C.,** Theoretical investigation of photoionization from Rydberg states of lithium, sodium and potassium, *J. Phys. B*, 9, 1279, 1976.
77. **Shevelko, V. P.,** Oscillator strengths and photoionization cross sections of alkali metals, *Prepr. Phys. Inst. Akad. Nauk S.S.S.R.*, N1, 30, 1970.
78. **Delone, N. B.,** Many-photon ionization of atoms, *Usp. Fiz. Nauk*, 115, 361, 1975.
79. **Klyucharev, A. N. and Bezuglov, N. N.,** *Excitation and Ionization of Atoms during Light Absorption*, Leningrad University, Leningrad, 1983, 272.
80. **Zorov, N. B., Kuzyakov, Yu. Ya., Novodvorsky, O. A., and Chaplygin, V. I.,** Optogalvanic effect in atmospheric pressure flames, in *Chemistry of Plasma*, Vol. 13, Smirnov, B. M., Ed., Atomizdat, Moscow, 1986, 131.
81. **Travis, J. C.,** Limits to sensitivity in laser enhanced ionization, *J. Chem. Educ.*, 59, 909, 1982.
82. **Omenetto, N. and Winefordner, J. D.,** Atomic fluorescence spectrometry (basic principles and applications), *Prog. Anal. At. Spectrosc.*, 2, 1, 1979.
83. **Rockney, B. H., Cool, T. A., and Grant, E. R.,** Detection of nancent NO in a methane/air flame by multiphoton ionization, *Chem. Phys. Lett.*, 87, 141, 1982.
84. **Smyth, K. C. and Mallard, W. G.,** Two-photon ionization processes of PO in C_2H_2/air flame, *J. Chem. Phys.*, 77, 1779, 1982.
85. **Magnusson, I., Axner, O., and Rubinsztein-Dunlop, H.,** Elimination of spectral interference using two-step excitation laser enhanced ionization, *Phys. Scr.*, 33, 429, 1986.
86. **Axner, O. and Magnusson, I.,** Determination of trace elements in water solutions by laser enhanced ionization using coumarine 47, *Phys. Scr.*, 31, 387, 1985.
87. **Omenetto, N., Smith, B. W., and Hart, L. P.,** Laser-induced fluorescence and ionization spectroscopy: theoretical and analytical consideration for pulsed sources, *Fresenius Z. Anal. Chem.*, 324, 683, 1986.
88. **Axner, O., Magnusson, I., Peterson, J., and Sjoestroem, S.,** Investigation of the multielement capability of laser-enhanced ionization spectrometry in flames for analysis of trace elements, *Appl. Spectrosc.*, 41, 19, 1987.
89. **Marunkov, A. G. and Chekalin, N. V.,** Experimental studies of the limiting capabilities of a flame atomic ionization spectrometer, *Zh. Anal. Khim.*, 42, 638, 1987.
90. **Chaplygin, V. I., Kuzyakov, Yu. Ya., and Zorov, N. B.,** Determination of alkali metals in different samples by laser atomic ionization in flames, *Spectrochim. Acta*, Suppl. 38B, 386, 1983.
91. **Smith, B. W., Hart, L. P., and Omenetto, N.,** Measurement of the laser-induced ionization yield for lithium in an air-acetylene flame, *Anal. Chem.*, 58, 2147, 1986.
92. **Bykov, I. V., Skvortsov, A. B., Tatsii, Yu. G., and Chekalin, N. V.,** Metal trace analysis by flame/graphite furnace OG spectroscopy, *J. Phys. (Paris) Colloq.*, 44, C7-345, 1983.
93. **Hart, L. P., Smith, B. W., and Omenetto, N.,** Laser induced stepwise and two-photon ionization studies of strontium in air-acetylene flame, *Spectrochim. Acta*, 40B, 1637, 1985.
94. **Havrilla, G. J. and Choi Kee, Yu.,** Detection and spectroscopic study of zinc by laser-enhanced ionization spectrometry, *Anal. Chem.*, 58, 3095, 1986.
95. **Marowsky, G.,** Principles of dye laser operation and dye laser tuning methods, *Opt. Acta*, 23, 855, 1976.
96. **Novodvorsky, O. A., Korn, G., Zorov, N. B., Kuzyakov, Yu. Ya., and Polze, S.,** Investigation of emission characteristics of a grazing-incidence longitudinally pumped laser with a holographic grating, *Kvantovaya Elektron. (Moscow)*, 10, 1997, 1983.
97. **Omenetto, N., Hart, L. P., Smith, B. W., and Turk, G. C.,** Near resonance effects in the laser induced ionization of Sr in air-acetylene flame, *Opt. Commun.*, 62, 86, 1987.
98. **Webster, C. R. and Rettner, C. T.,** Laser optogalvanic spectroscopy of molecules, *Laser Focus*, 19, 41, 1983.
99. **Mallard, W. G., Miller, J. H., and Smyth, K. C.,** Resonantly enhanced two-photon photoionization of NO in an atmospheric flame, *J. Chem. Phys.*, 76, 3483, 1982.
100. **Novodvorsky, O. A., Zorov, N. B., Kuzyakov, Yu. Ya., and Palivoda, A. P.,** Investigation of evaporation products from the surface of electrode by optogalvanic spectroscopy method, in *Abstr. XIX All Union Spectroscopy Congress*, Part 5, Tomsk, U.S.S.R., 1983, 17.
101. **Novodvorsky, O. A., Zorov, N. B., and Kuzyakov, Yu. Ya.,** Opto-galvanic effect in a flame on evaporation of the probe material, *Vestn. Mosk. Univ. Khim.*, 25, 114, 1984.
102. **Travis, J. C., Turk, G. C., and Green, R. B.,** Laser-enhanced ionization for trace metal analysis in flames, in *New Applications of Lasers to Chemistry*, Hieftje, G. M., Ed., ACS Symp. Ser., N 85, American Chemical Society, Washington, D.C., 1978, 91.
103. **Hall, J. E. and Green, R. B.,** Laser-enhanced ionization spectrometry with a total consumption burner, *Anal. Chem.*, 55, 1811, 1983.

104. **Zorov, N. B., Kuzyakov, Yu. Ya., Novodvorsky, O. A., and Chaplygin, V. I.,** Laser atomic ionization spectrometry for determination of traces, in *Determination of Low Concentration of Elements*, Zolotov, Yu. A. and Ryabukhin, V. A., Eds., Nauka, Moscow, 1986, 233.
105. **Nippold, M. A. and Green, R. B.,** Pulse signal collection for laser-enhanced ionization spectrometry, *Anal. Chem.*, 55, 554, 1983.
106. **Chaplygin, V. I., Zorov, N. B., Kuzyakov, Yu. Ya., and Matveev, O. I.,** Determination of cesium in flames by laser excited ionization of atoms with differential sample vaporization and atomization, *Zh. Anal. Khim.*, 38, 802, 1983.
106a. **Curran, F. M., van Dijk, C. A., and Crouch, S. R.,** Dual laser ionization in flames: search for electrical interferences, *Appl. Spectrosc.*, 37, 385, 1983.
107. **Chaplygin, V. I., Zorov, N. B., Kuzyakov, Yu. Ya., and Matveev, O. I.,** An application of selective ionization by laser to determination of potassium in flame, *Vestn. Mosk. Univ.*, 24, 168, 1983.
108. **Havrilla, G. J., Weeks, S. J., and Travis, J. C.,** Continuous wave excitation in laser enhanced ionization spectrometry, *Anal. Chem.*, 54, 2566, 1982.
109. **Bykov, I. V., Chekalin, N. V., and Tikhomirova, E. I.,** Determination of indium traces in special purity tin by laser atomic ionization, *Zh. Anal. Khim.*, 40, 1991, 1985.
110. **Gorbatenko, A. A., Zorov, N. B., and Kuzyakov, Yu. Ya.,** Determination of alkali metal traces in aluminium alloys by laser atomic ionization spectrometry, in *Abstr. Ural Conf. Modern Methods of Analysis and Study of Chem. Composition of Metallurgy, Engineering Industry Materials and Environmental Objects*, Ustinov, U.S.S.R., 1985, 123.
111. **Marunkov, A. G., Reutova, T. V., and Chekalin, N. V.,** Determination of lead traces in natural waters by laser atomic-ionization spectrometry, *Zh. Anal. Khim.*, 41, 681, 1986.
112. **Turk, G. C., Havrilla, G. J., Webb, J. D., and Forster, A. R.,** Performance appraisal studies of laser-enhanced ionization in flames — the determination of nikel in petroleum products, in *Analytical Spectroscopy*, Lyon, W. S., Ed., Elsevier, Amsterdam, 1984, 63.
113. **Berglind, T., Nilsson, S., and Rubinsztein-Dunlop, H.,** Detection of metallic elements by laser enhanced ionization spectroscopy in flames on-line with high-pressure liquid chromatography, *Phys. Scr.*, 36, 246, 1987.
114. **Matveev, O. I., Zorov, N. B., and Kuzyakov, Yu. Ya.,** Detection of photons on resonance absorbance in atomic vapours, *Zh. Anal. Khim.*, 34, 846, 1979.
115. **Matveev, O. I.,** Resonance laser-enhanced detection of photons in atomic fluorescence spectroscopy, *Zh. Anal. Khim.*, 38, 736, 1983.
116. **Dorofeev, V. S. and Aidarov, T. K.,** Some possibilities for stepwise-2 resonance excitation and subsequent photoionization of atoms in atomic absorption spectral analysis, *Zh. Prikl. Spektrosk.*, 33, 973, 1980.
117. **Schenk, P. K. and Hastie, J. W.,** Optogalvanic spectroscopy — application to combustion systems, *Opt. Eng.*, 20, 522, 1981.
118. **Lin, K. C., Hunt, P. M., and Crouch, S. R.,** Flame temperature determination in dual laser ionization, *Chem. Phys. Lett.*, 90, 111, 1982.
119. **Mallard, W. G. and Smyth, K. C.,** Mobility measurements of atomic ions in flames using laser enhanced ionization, *Combust. Flame*, 44, 61, 1982.
120. **Salcedo Torres, L. E., Zorov, N. B., Kuzyakov, Yu. Ya., and Matveev, O. I.,** On the effect of the ion mobility in flame on the analytical signal of the selective laser ionization technique, *Vestn. Mosk. Univ. Khim.* 23, 474, 1982.
121. **Hall, J. E. and Green, R. B.,** Ion fraction determination by laser enhanced ionization spectrometry, *Anal. Chem.*, 57, 16, 1985.
122. **Hall, J. E.,** Evaluation of Flame Reservoirs for Laser-Enhanced Ionization Spectrometry, Ph.D. thesis, University of Arkansas, Fayetteville, 1984.
123. **Bradly, D. and Ibrahim, S. N. A.,** Determination of positive-ion mobilities and collision cross-section in flame gases using electrostatic probes, *J. Phys. D*, 7, 1377, 1974.
124. **Turk, G. C. and Omenetto, N.,** Optical detection of laser-induced ionization: a study of the time decay of strontium ions in the air-acetylene flame, *Appl. Spectrosc.*, 40, 1085, 1986.
125. **Turk, G. C., Axner, O., and Omenetto, N.,** Optical detection of laser-induced ionization in the inductively coupled plasma for the study of ion-electron recombination and ionization equilibrium, *Spectrochim. Acta*, 42B, 873, 1987.
126. **Hall, J. E. and Green, R. B.,** Sample desolvation for laser-enhanced ionization spectrometry, *Anal. Chem.*, 57, 431, 1985.
127. **Berglind, T. and Casparasson, L.,** Micro-wave detection of laser-enhanced ionization of metals in flames, *J. Phys. (Paris) Colloq.*, 44, C7-329, 1983.
128. **Suzuki, T., Fukasawa, T., Sekiguchi, H., and Kasuga, T.,** Detection of the optogalvanic effect in flames with a microwave resonant cavity, *Appl. Phys. B*, 39, 247, 1986.
129. **Letokhov, V. S.,** Photoionization of gases by the laser radiation, U.S.S.R. Patent 784,679, 1982 (appl. in 1970).

130. **Young, J. P., Hurst, G. S., Kramer, S. D., and Payne, M. G.,** Resonance ionization spectroscopy, *Anal. Chem.*, 51, 1050A, 1979.
131. **Kramer, S. D., Young, J. P., Hurst, G. S., and Payne, M. G.,** Resonance ionization spectroscopy of lithium, *Opt. Commun.*, 30, 47, 1979.
132. **Bjorklund, G. C., Ausschnitt, C. P., Freeman, R. R., and Storz, R. H.,** Detection of atomic hydrogen and deuterium by resonant three-photon ionization, *Appl. Phys. Lett.*, 33, 54, 1978.
133. **Marr, V. G.,** *Photoionization Process in Gases,* Academic Press, New York, 1967, 108.
134. **Ambartsumyan, R. V., Bekov, G. I., Letokhov, V. S., and Mishin, V. I.,** Excitation of high states of sodium atom by dye laser radiation and their autoionization in an electric field, *Pis'ma Zh. Eksp. Teor. Fiz.*, 21, 595, 1975.
135. **Ducas, T. W., Littman, M. G., Freeman, R. R., and Kleppner, D.,** Stark ionization of high-lying states of sodium, *Phys. Rev. Lett.*, 35, 366, 1975.
136. **Bekov, G. I., Letokhov, V. S., and Mishin, V. I.,** Laser photoionization detection of single-unit sodium atoms via Rydberg states, *Pis'ma Zh. Eksp. Teor. Fiz.*, 27, 52, 1978.
137. **Bekov, G. I. and Letokhov, V. S.,** Laser resonant photo-ionization spectroscopy for trace analysis, *Trends Anal. Chem.*, 2, 252, 1983.
138. **Bekov, G. I., Letokhov, V. S., and Radaev, V. N.,** Laser photoionization spectroscopy of ruthenium traces at the level of 1 part in 10^{12}, *J. Opt. Soc. Am.*, 2, 1554, 1985.
139. **Stebbings, R. F.,** High Rydberg atoms: newcomers to the atomic physics scene, *Science*, 193, 537, 1976.
140. **Bekov, G. I., Letokhov, V. S., Matveev, O. I., and Mishin, V. I.,** Detection of a long-lived autoionization state in the spectrum of a gadolinium atom, *Pis'ma Zh. Eksp. Teor. Fiz.*, 28, 308, 1978.
141. **Bekov, G. I., Egorov, A. S., and Mishin, V. I.,** Determination of ytterbium in solution using laser enhanced ionization, *Zh. Anal. Khim*, 38, 429, 1983.
142. **Atakhodzaev, A. A. and Fedoseev, V. N.,** Laser photoionization spectroscopy of autoionization states of the thulium atom, *Zh. Prikl. Spektrosk.*, 40, 386, 1986.
143. **Worden, E. F., Solarz, R. W., Paisner, J. A., and Conway, J. G.,** First ionization potentials of lanthanides by laser spectroscopy, *J. Opt. Soc. Am.*, 68, 52, 1978.
144. **Dobryshin, V. E., Karpov, N. A., Kotochigova, S. A., Krynetsky, B. B., Mishin, V. A., Stel'makh, O. M., and Shustrikov, V. M.,** Laser spectroscopy of atomic-samarium autoionization levels, *Opt. Spektrosk.*, 54, 415, 1983.
145. **Vidolova-Angelova, E., Bekov, G. I., Ivanov, L. N., Fedoseev, V. N., and Atakhodzhaev, A. A.,** Laser spectroscopy investigation of highly excited states of the thulium atom, *J. Phys. B*, 17, 953, 1984.
146. **Zherikhin, A. N., Kompanets, O. N., Letokhov, V. S., Mishin, V. I., Fedoseev, V. N., Alkhazov, G. D., Barzakh, A. E., Berlovich, E. E., Denisov, V. P., Dernyatin, A. G., and Ivanov, V. S.,** High-resolution laser photoionization spectroscopy of radioactive europium isotopes, *Zh. Eksp. Teor. Fiz.*, 86, 1249, 1984.
147. **Bekov, G. I., Vidolova-Angelova, E. P., Ivanov, L. M., Letokhov, V. S., and Mishin, V. I.,** Laser spectroscopy of narrow doubly excited autoionization states of ytterbium atom, *Zh. Eksp. Teor. Fiz.*, 80, 866, 1981.
148. **Bekov, G. I. and Vidolova-Angelova, E. P.,** Optimal system of stepwise photoionization of a lutetium atom by laser radiation, *Kvantovaya Elektron (Moscow)*, 8, 227, 1981.
149. **Bekov, G. I., Vidolova-Angelova, E. P., Letokhov, V. S., and Mishin, V. I.,** Multistage laser spectroscopy of higher triplet states of an ytterbium atom, *Opt. Spektrosk.*, 48, 435, 1980.
150. **Miller, C. M. and Nogar, N. S.,** Autoionizing and high-lying Rydberg states of lutetium atoms, in *Proc. AIP Conf., N90,* American Institute of Physics, New York, 1982, 90.
151. **Hurst, G. S., Payne, M. G., and Wagner, E. B.,** Resonance ionization for analytical spectroscopy, U.S. Patent 3,987,302, 1976.
152. **Letokhov, V. S.,** Future applications of selective laser photophysics and photochemistry, in *Tunable Lasers and Applications,* Mooradian, A., Jaeser, T., and Stokseth, P., Eds., Springer-Verlag, Berlin, 1976, 122.
153. **Letokhov, V. S.,** Problems of laser spectroscopy, *Usp. Fiz. Nauk*, 118, 199, 1976.
154. **Veksler, V. I., Groshev, L. V., and Isaev, B. M.,** *Ionization Methods of Investigation of Radiation,* Gostekhizdat, Moscow, 1950.
155. **Segre, E., Ed.,** *Experimental Nuclear Physics,* Vol. 1, New York, 1953.
156. **Hurst, G. S., Payne, M. G., Nayfeh, M. H., Judish, J. P., and Wagner, E. B.,** Saturated two-photon resonance ionization of helium, *Phys. Rev. Lett.*, 35, 82, 1975.
157. **Hurst, G. S., Nayfeh, M. H., and Young, J. P.,** One atom detection using resonance ionization spectroscopy, *Phys. Rev. A*, 15, 2283, 1977.
158. **Bekov, G. I., Letokhov, V. S., Matveev, O. I., and Mishin, V. I.,** Single-atom detection of ytterbium by selective laser excitation and field ionization from Rydberg states, *Opt. Lett.*, 3, 159, 1978.
159. **Letokhov, V. S. and Mishin, V. I.,** Highly selective multistep ionization of atoms by laser radiation, *Opt. Commun.*, 29, 168, 1979.

160. **Kudriavtzev, Yu. A. and Letokhov, V. S.,** Laser method of highly selective detection of rare radioactive isotopes through multistep photoionization of accelerated atoms, *Appl. Phys. B*, 29, 219, 1982.
161. **Matveev, O. I., Zorov, N. B., and Kuzyakov, Yu. Ya.,** Comparison of laser spectroscopy methods of individual atom detection, *Vestn. Mosk. Univ. Khim.*, 19, 537, 1978.
162. **Karlov, N. V., Krynetskii, B. B., Mishin, V. A., and Prokhorov, A. M.,** Selective photoionization of atoms and its use for isotope separation and spectroscopy, *Usp. Fiz. Nauk*, 127, 593, 1979.
163. **Letokhov, V. S.,** Laser selective detection of ultralow concentrations of atoms, *Comments At. Mol. Phys.*, 7, 93, 1977.
164. **Robinson, A.,** Analytical chemistry: using lasers to detect less and less, *Science*, 199, 1191, 1978.
165. **Letokhov, V. S.,** Laser spectroscopy. VI. Selective detection of ultra-low concentrations of atoms and molecules, *Opt. Laser Technol.*, 10, 175, 1978.
166. **Nayfeh, M. H.,** Laser detection of single atoms, *Am. Sci.*, 67, 204, 1979.
167. **Grey Morgan, C.,** Laser spectroscopy of ultra-trace quantities, *Chem. Soc. Rev.*, 8, 367, 1979.
168. **Hurst, G. S., Payne, M. G., Kramer, S. D., and Young, J. P.,** Resonance ionization spectroscopy and one-atom detection, *Rev. Mod. Phys.*, 51, 767, 1979.
169. **Balykin, V. I., Bekov, G. I., Letokhov, V. S., and Mishin, V. I.,** Laser detection of single atoms, *Usp. Fiz. Nauk*, 132, 293, 1980.
170. **Hurst, G. S.,** Counting the atoms: some applications in chemistry, *J. Chem. Educ.*, 59, 895, 1982.
171. **Payne, M. G. and Hurst, G. S.,** One-atom detection and statistical studies with resonance ionization spectroscopy, in *Analytical Laser Spectroscopy*, Martollucci, S. and Chester, A. N., Eds., Plenum Press, New York, 1985, 189.
172. **Letokhov, V. S.,** Laser selective single-atom detection, in *Chemical and Biochemical Application of Lasers*, Vol. 5, Moore, C. B., Ed., Academic Press, New York, 1980, 3.
173. **Letokhov, V. S.,** Laser photoionization spectroscopy of single atoms and molecules, *Opt. Acta*, 32, 1191, 1985.
174. **Hurst, G. S., Payne, M. G., Kramer, S. D., and Young, J. P.,** Resonance ionization spectroscopy with amplification, *Chem. Phys. Lett.*, 63, 1, 1979.
175. **Kramer, S. D., Bemis, C. E., Jr., Young, J. P., and Hurst, G. S.,** One-atom detection in individual ionization tracks, *Opt. Lett.*, 3, 16, 1978.
176. **Cerny, J. and Postkauzer, A. M.,** Exotic light nuclei, *Sci. Am.*, 238, 60, 1978.
177. **Bekov, G. I., Letokhov, V. S., and Mishin, V. I.,** Laser photoionization detection of impurities in solids and studies of hyperfine and isotope structures of radioactive atoms, in *Proc. AIP Conf., N90*, American Institute of Physics, New York, 1982, 101.
178. **Andreev, S. V., Letokhov, V. S., and Mishin, V. I.,** Laser resonance photoionization detection of trace of the radioactive isotope francium-221 in a sample, *Pis'ma Zh. Eksp. Teor. Fiz.*, 43, 570, 1986.
179. **Letokhov, V. S.,** Laser ultrasensitive high-resolution spectroscopy of short-lived radioactive atoms, *Comments At. Mol. Phys.*, 18, 209, 1986.
180. **Bahcall, J. N.,** Solar neutrino experiments, *Rev. Mod. Phys.*, 50, 881, 1978.
181. **Hurst, G. S., Payne, M. G., Kramer, S. D., and Chen, C. H.,** Counting the atoms, *Phys. Today*, 33, 24, 1980.
182. **Cleveland, B., Davis, R., Jr., and Ronley, J. K.,** The chlorine and bromine solar neutrino experiments, *Inst. Phys. Conf. Ser.*, N71, 241, 1984.
183. **Hurst, G. S.,** Feasibility of a $^{81}Br(\nu,e^-)^{81}Kr$ solar neutrino experiment, *Inst. Phys. Conf. Ser.*, N84, 283, 1986.
184. **Chen, C. H., Hurst, G. S., and Payne, M. G.,** Resonance ionization spectroscopy: inert atom detection, in *Progress in Atomic Sepctroscopy, Part C*, New York, 1984, 115.
185. **Lehmann, B. E. and Loosli, H. H.,** Use of noble gas radioisotopes for environmental research, *Inst. Phys. Conf. Ser.*, N71, 219, 1984.
186. **Kramer, S. D., Chen, C. H., Allman, S. L., Hurst, G. S., and Lehmann, B. E.,** Krypton-81 detection using resonance ionization spectroscopy, in *Proc. AIP Conf., N119*, American Institute of Physics, New York, 1984, 246.
187. **Lehmann, B. E., Oescher, H., Loosli, H. H., Hurst, G. S., Allman, S. L., Chen, C. H., Kramer, S. D., Payne, M. G., Phillips, R. C. et al.,** Counting krypton-81 atoms for analysis of groundwater, *J. Geophys. Res. B*, 90, 11547, 1985.
188. **Lehmann, B. E.,** Resonance ionization spectroscopy: application in isotope geophysics, *NATO ASI Ser., Ser. B*, N119, 203, 1985.
189. **Matveev, O. I., Zorov, N. B., and Kuzyakov, Yu. Ya.,** Yield of ions in pulse laser photoionization of atoms, *Vestn. Mosk. Univ. Khim.*, 20, 155, 1979.
190. **Bekov, G. I., Vidolova-Angelova, E. P., Letokhov, V. S., and Mishin, V. I.,** Selective detection of single atoms by multistep excitation and ionization through Rydberg states, in *Laser Spectroscopy IV*, Walther, H. and Rothe, K. W., Eds., Proc. 4th Int. Conf. Rottach-Egern, Springer-Verlag, New York, 1979, 283.

191. **Bekov, G. I., Egorov, A. S., Letokhov, V. S., and Radaev, V. N.,** Laser stepwise photoionization of atoms — a direct method of aluminium concentration determination in natural waters, *Okeanologiya*, 23, 171, 1983.
192. **Bekov, G. I., Yegorov, A. S., Letokhov, V. S., and Radaev, V. N.,** Direct determination of aluminium in natural waters by laser stepwise photoionization, *Nature*, 301, 410, 1983.
193. **Beterov, I. M., Kurochkin, V. L., Fateev, N. V., and Yudelevitch, I. G.,** Stepwise photoionization determination of trace elements, *Izv. Sib. Otd. Akad. Nauk S.S.S.R., Ser. Khim. Nauk*, N3, 67, 1983.
194. **Beterov, I. M., Ishchenko, V. V., Kochubei, S. A., and Kurochkin, V. L.,** Effective formation of alumunium photons under the radiation from a tunable xenon monochlodide laser, *Opt. Commun.*, 54, 100, 1985.
195. **Bekov, G. I. and Letokhov, V. S.,** Laser atomic photoionization spectral analysis of element traces, *Appl. Phys. B*, 30, 161, 1983.
196. **Bekov, G. I. and Letokhov, V. S.,** Laser atomic-photoionization spectral analysis, in *Laser Analytical Spectroscopy*, Letokhov, V. S., Ed., Nauka, Moscow, 1986, chap. 3.
197. **Matveev, O. I., Pribytkov, V. A., and Dibrova, A. K.,** Atomization of substances in a vacuum, U.S.S.R. Patent 1,223,094, 1986.
198. **Andreev, S. V., Mishin, V. I., and Sekatskii, S. K.,** Enhancement of the efficiency of atomic ionization by repetitively pulsed lasers, *Kvantovaya Elektron. (Moscow)*, 12, 611, 1985.
199. **Andreev, S. V., Mishin, V. I., and Letokhov, V. S.,** High efficiency laser resonance photoionization of strontium atoms in a hot cavity, *Opt. Commun*, 57, 317, 1986.
200. **Bekov, G. I., Maksimov, G. A., Nikogosyan, D. N., and Radaev, V. N.,** Enhancement of selectivity of laser photoionization analysis during two-pulse action of the electric field on Rydberg atoms, *Kvantovaya Elektron. (Moscow)*, 11, 1262, 1984.
201. **Bekov, G. I., Letokhov, V. S., and Mishin, V. I.,** Ionization of highly excited sodium atoms by a pulsed electric field, *Zh. Eksp. Teor. Fiz.*, 73, 157, 1977.
202. **Bekov, G. I., Letokhov, V. S., and Radaev, V. N.,** Direct determination of aluminium concentration in human blood through laser photoionization spectroscopy, *Laser Chem.*, 5, 11, 1984.
203. **Bekov, G. I., Kurskii, A. N., Letokhov, V. S., and Radaev, V. N.,** Determination of ruthenium traces in geological samples by laser photoionization spectroscopy, *Zh. Anal. Khim.*, 40, 2208, 1985.
204. **Akilov, R. and Bekov, G. I.,** Determination of sodium trace impurities in cadmium sulphide crystals by laser multistep photoionization of atoms, *Pis'ma Zh. Tekhn. Fiz.*, 8, 517, 1982.
205. **Akilov, R., Bekov, G. I., Devyatykh, G. G., Letokhov, V. S., Maksimov, G. A., Radaev, V. N., Shishov, V. N., and Shcheplyagin, E. M.,** Determination of aluminium and sodium as impurities in high-purity germanium by laser-enhanced stepwise atom photoionization, *Zh. Anal. Khim.*, 39, 31, 1984.
206. **Bekov, G. I. and Radaev, V. N.,** Laser photoionization determination of elements traces, *Izv. Akad. Nauk S.S.S.R., Ser. Fiz.*, 48, 771, 1984.
207. **Akilov, R., Bekov, G. I., Letokhov, V. S., Maksimov, G. A., Mishin, V. I., Radaev, V. N., and Shishov, V. N.,** Determination of aluminium content in high-purity germanium by the method of laser stepwise photoionization of atoms, *Kvantovaya Elektron. (Moscow)*, 9, 1859, 1982.
208. **Likonen, J., Auterinen, I., Bekov, G., Radaev, V., Lakomaa, E. L., Ojanpera, J., and Zilliacus, R.,** Resonance ionization spectrometric determination of gallium by use of electrothermal graphite atomizer, *Inst. Phys. Conf. Ser.*, N84, 343, 1986.
209. **Bekov, G., Radaev, V., Likonen, J., Zilliakus, R., Auterinen, I., and Lakomaa, E. L.,** Resonance ionization spectrometric determination of gallium using an electrothermal graphite atomizer, *Anal. Chem.*, 59, 2472, 1987.
210. **Beterov, I. M., Kurochkin, V. L., and Yudelevich, I. G.,** Determination of trace indium concentration in high purity materials by laser stepwise photoionization from the metastabile $5p^2P_{3/2}$ state, *Zh. Prikl. Spektrosk.*, 42, 17, 1985.
211. **Bekov, G. I., Radaev, V. N., Kurskii, A. N., Zdorova, E. P., and Makarov, Yu. B.,** Laser photoionization determination of platinum-group metals with fire-assay preconcentration, *Zavod. Lab.*, 51, 31, 1985.
212. **Bekov, G. I., Letokhov, V. S., Radaev, V. N., Baturin, S. N., Egorov, A. S., Kurskii, A. N., and Narseyev, V. A.,** Ruthenium in the ocean, *Nature*, 322, 748, 1985.
213. **Zilliacus, R., Lakomaa, E. L., Auterinen, I., and Likonen, J.,** Avoidance of contamination in trace element analysis by RIS, *Inst. Phys. Conf. Ser.*, N84, 341, 1986.
214. **Travis, J. C., Epstein, M., Schenk, P. K., Turk, G. C., Sweger, D. M., and DeVoe, J. R.,** Galvanic detection of optical absorptions in analytical reservoirs, in *Proc. 20th Coll. Spectrosc. Int. and 7th Int. Conf. At. Spectrosc.*, Prague, 1977, 118.
215. **Gonchakov, A. S., Zorov, N. B., Kuzyakov, Yu. Ya., and Matveev, O. I.,** Detection of submicrogram amount of sodium by laser stepwise photoionization technique and laser atomic fluorescence spectrometry with electrothermal atomization, *Zh. Anal. Khim.*, 34, 2312, 1979.
216. **Salsedo Torres, L. E.,** Application of Selective Laser Ionization for Determination of Indium in Semiconductor Alloys and Pure Substances, Ph.D. thesis, Moscow State University, Moscow, U.S.S.R., 1981.

217. **L'vov, B. V.,** 25 Years of analytical atomic absorption spectrometry, *Zh. Anal. Khim.* 35, 1575, 1980.
218. **Magnusson, I., Axner, O., Lindgren, I., and Rubinsztein-Dunlop, H.,** Laser-enhanced ionization detection of trace elements in a graphite furnace, *Appl. Spectrosc.*, 40, 968, 1986.
219. **Magnusson, I., Sjoestoem, S., Lejon, M., and Rubinsztein-Dunlop, H.,** Trace element analysis by two colour laser enhanced ionization spectroscopy in a graphite furnace, *Spectrochim. Acta,* 42B, 713, 1987.
220. **Minova, T., Katsuragawa, H., Kawamura, A., and Shimazu, M.,** Highly sensitive detection of thallium atoms using resonance ionization, *Opt. Commun.*, 60, 37, 1986.
221. **Mayo, S., Lucatorto, T. B., and Luther, G. G.,** Laser ablation and resonance ionization spectrometry for trace analysis of solids, *Anal. Chem.*, 54, 533, 1982.
222. **Parks, J. E., Schmitt, H. W., Hurst, G. S., and Fairbank, W. M., Jr.,** Ultrasensitive elemental analysis of solids by sputter-initiated resonance ionization spectroscopy, in *Proc. SPIE-Int. Soc. Opt. Eng.*, N426, 32, 1983.
223. **Parks, J. E., Schmitt, H. W., Hurst, G. S., and Fairbank, W. M., Jr.,** Sputter-initiated resonance ionization spectroscopy for trace element analysis, *Anal. Chem. Symp. Ser.*, N19, 149, 1984.
224. **Parks, J. E., Schmitt, H. W., Hurst, G. S., and Fairbank, W. M., Jr.,** Sputter initiated RIS (SIRIS) for analysis of semiconductor impurities, *Inst. Phys. Conf. Ser.*, N71, 167, 1984.
225. **Parks, J. E., Beekman, D. W., Schmitt, H. W., and Taylor, E. H.,** Materials analysis using sputter initiated resonance ionization spectroscopy, *Nucl. Instrum. Methods Phys. Res. B*, B10-11, 280, 1985.
226. **Parks, J. E., Beekman, D. W., Schmitt, H. W., and Spaar, M. T.,** Ultrasensitive elemental analysis of materials using sputter initiated resonance ionization spectroscopy, in *Mater. Res. Soc. Symp. Proc.*, N48, 309, 1985.
227. **Parks, J. E.,** Bioassays using resonance ionization spectroscopy, Report 1983, NURE G/CR-3454, Order No. DE84900713, p. 29; *Chem. Abstr.*, 101, 68495, 1984.
228. **Fairbank, W. M., Jr., Hurst, G. S., Parks, J. E., and Paice, C.,** Searches for fractional charges and superheavy atoms, *Inst. Phys. Conf. Ser.*, N71, 287, 1984.
229. **Fairbank, W. M., Jr., Petger, W. F., Riis, E., Hurst, G. S., and Parks, J. E.,** Optical searches for fractional charges and superheavy atoms, *Springer Ser. Opt. Sci.*, N49, 53, 1985.
230. **Fairbank, W. M., Jr., Riis, E., LaBelle, R. D., Parks, J. E., Spaar, M. T., and Hurst, G. S.,** A search for new elementary particles using suptter-initiated resonance ionization spectroscopy, *Inst. Phys. Conf. Ser.*, N84, 275, 1986.
231. **Parks, J. E., Beekman, D. W., Moore, L. J., Schmitt, H. W., Spaar, M. T., Taylor, E. H., Hutchinson, J. M. R., and Fairbank, W. M., Jr.,** Progress in analysis by sputter-initiated resonance ionisation spectroscopy, *Inst. Phys. Conf. Ser.*, N84, 157, 1986.
232. **Schmitt, H. W.,** Resonance ionization spectroscopy and a new venture in analysis, *Nucl. Sci. Eng.*, 90, 442, 1985.
233. **Gorbunov, S. V., Zakurdaev, I. V., Muchnik, M. L., Suslov, A. I., Sheroziya G. A., and Shishlakov, V. A.,** Selective laser ionization of atoms sputtered by an ion beam, *Pis'ma Zh. Tekh. Fiz.*, 12, 681, 1986.
234. **Keller, R. A. and Zalevski, E. E.,** Noise considerations, signal magnitudes, and detection limits in a hollow cathode discharge by optogalvanic spectroscopy, *Appl. Opt.*, 19, 3301, 1980.
235. **Keller, R. A., Engelman, R., and Zalevski, E. F.,** Optogalvanic spectroscopy in an uranium hollow cathode discharge, *J. Opt. Soc. Am.*, 69, 738, 1979.
236. **Miron, E., Smilanski, I., Liran, J., Lavi, S., and Erez, G.,** Dynamic optogalvanic effect in rare gases and uranium, *IEEE J. Quantum Electron.*, QE-15, 194, 1979.
237. **Donohue, D. L., Young, J. P., and Smith, D. H.,** Determination of rare earth isotope ratios by resonance ionization mass spectrometry, *Int. J. Mass Spectrom. Ion Phys.*, 43, 293, 1982.
238. **Young, J. P., Donohue, D. L., and Smith, D. H.,** Alternate ionization pathways for resonance ionization mass spectrometry *Int. J. Mass Spectrom. Ion Phys.*, 56, 307, 1984.
239. **Donohue, D. L., Smith, D. H., Young, J. P., McKown, H. S., and Pritchard, C. A.,** Isotopic analysis of uranium and plutonium mixtures by resonance ionization mass spectrometry, *Anal. Chem.*, 56, 379, 1984.
240. **Donohue, D. L., Young, J. P., and Smith, D. H.,** Spectral studies of actinide elements by resonance ionization mass spectrometry, *Appl. Spectrosc.*, 39, 93, 1985.
241. **Downey, S. W., Nogar, N. S., and Miller, C. M.,** Resonance ionization mass spectrometry of technetium, *Int. J. Mass Spectrom. Ion Phys.*, 61, 337, 1984.
242. **Downey, S. W., Nogar, N. S., and Miller, C. M.,** Resonance ionization mass spectrometry of uranium with intracavity laser ionization, *Anal. Chem.*, 56, 827, 1984.
243. **Fassett, J. D., Travis, J. C., Moore, L. J., and Lytle, F. E.,** Atomic ion formation and measurement with resonance ionization mass spectrometry, *Anal. Chem.*, 55, 765, 1983.
244. **Fassett, J. D., Moore, L. J., Travis, J. C., and Lytle, F. E.,** The characterization of thermally-produced metastable excited-state atomic species using resonance ionization mass spectrometry, *Int. J. Mass Spectrom. Ion. Phys.*, 54, 201, 1983.

245. **Fassett, J. D., Moore, L. J., Shideler, R. W., and Travis, J. C.,** Pulsed thermal atom source for resonance ionization mass spectrometry, *Anal. Chem.*, 56, 203, 1984.
246. **Fassett, J. D., Powell, L. J., and Moore, L. J.,** Determination of iron in serum and water by resonance ionization isotope dilution mass spectrometry, *Anal. Chem.*, 56, 2228, 1984.
247. **Moore, L. J., Fassett, J. D., and Travis, J. C.,** Systematics of multielement determination with resonance ionization mass spectrometry and thermal atomization, *Anal. Chem.*, 56, 2770, 1984.
248. **Miller, C. M. and Nogar, N. S.,** Continuous wave lasers for resonance ionization mass spectrometry, *Anal. Chem.*, 55, 1606, 1983.
249. **Miller, C. M., Nogar, N. S., Gancarz, A. J., and Shields, W. R.,** Selective laser photoionization for mass spectrometry, *Anal. Chem.*, 54, 2377, 1982.
250. **Nogar, N. S., Downey, S. W., and Miller, C. M.,** Multiple photon processes in tantalum resonance ionization mass spectrometry, *Anal. Chem.*, 57, 1144, 1985.
251. **Young, J. P. and Donohue, D. L.,** Ionization spectra of neodymium and samarium by resonance ionization mass spectrometry, *Anal. Chem.*, 55, 88, 1983.
252. **Fassett, J. D., Moore, L. J., Travis, J. C., and DeVoe, J. R.,** Laser resonance ionization mass spectrometry, *Science*, 23, 262, 1985.
253. **Beekman, D. W. and Callcott, T. A.,** Laser ablation studies using RIS, in *Resonance Ionization Spectroscopy 1984*, Hurst, G. S. and Payne, M. G., Eds., Institute of Physics, Bristol, England, 1984, 143.
254. **Moore, L. J., Heald, E. F., and Filliben, J. J.,** An isotopic fractionation model for the multiple filament ion source, *Adv. Mass Spectrom.*, 7A, 448, 1978.
255. **Moore, L. J. and Machlan, L. A.,** High accuracy determination of calcium in blood serum by isotope dilution mass spectrometry, *Anal. Chem.*, 44, 2291, 1972.
256. **Krönert, U., Bonn, J., Kluge, H.-J., Ruster, W., Wallmeroth, K., Peuser, P., and Trautman, N.,** Laser resonant ionization of plutonium, *Appl. Phys. B*, 38, 65, 1985.
257. **Kimock, F. M., Baxter, J. P., Pappas, D. L., Kobrin, P. H., and Winograd, N.,** Solid analysis using energetic ion bombardment and multiphoton resonance ionization with time-of-flight detection, *Anal. Chem.*, 56, 2782, 1984.
258. **Donohue, D. L., Christie, W. H., Goeringer, D. E., and McKown, H. S.,** Ion microprobe mass spectrometry using sputtering atomization and resonance ionization, *Anal. Chem.*, 57, 1193, 1985.
259. **Kimock, F. M., Baxter, J. P., and Winograd, N.,** Ion and neutral yields from ion-bombarded metal surfaces during chemisorption using low-dose SIMS and multiphoton resonance ionization, *Surf. Sci.*, 124, L41, 1983.
260. **Parks, J. E., Schmitt, H. W., Hurst, G. S., and Fairbank, W. M., Jr.,** Sputter-initiated resonance ionization spectroscopy, *Thin Solid Films*, 108, 69, 1983.
261. **Winograd, N., Baxter, J. P., and Kimock, F. M.,** Multiphoton resonance ionization of sputtered neutrals: a novel approach to materials characterization, *Chem. Phys. Lett.*, 88, 581, 1982.
262. **Miller, C. M. and Nogar, N. S.,** Calculation of ion yields in atomic multiphoton ionization spectroscopy, *Anal. Chem.*, 55, 481, 1983.
263. **Fassett, J. D., Travis, J. C., and Moore, L. J.,** Thermal atomization sources and resonance ionization mass spectrometry (RIMS), *Proc. Soc. Photo-Opt. Instrum. Eng.*, N482, 36, 1984.
264. **Nogar, N. S., Estler, R. C., and Miller, C. M.,** Pulsed laser desorption for resonance ionization mass spectrometry, *Anal. Chem.*, 57, 2441, 1985.
265. **Dittrich, K. and Wennrich, R.,** Laser vaporization in atomic spectroscopy, *Prog. Anal. At. Spectrosc.*, 7, 139, 1984.
266. **Moore, L. J., Fassett, J. D., Travis, J. C., Lucatorto, T. B., and Clark, C. W.,** Resonance-ionization mass spectrometry of carbon, *J. Opt. Soc. Am. B*, 2, 1561, 1985.
267. **Apel, E. C., Nogar, N. S., Miller, C. M., and Estler, R. C.,** RIMS diagnostics for laser desorption/laser ablation, *Inst. Phys. Conf. Ser.*, N64, 179, 1986.
268. **Becker, C. H. and Gillen, K. T.,** Surface analysis by nonresonant multiphoton ionization of desorbed sputtered species, *Anal. Chem.*, 56, 1671, 1984.
269. **Harrison, W. W., Savickas, P. J., Marcus, P. K., and Hess, K. R.,** Laser enhanced ionization in glow discharge mass spectrometry, in *Analytical Spectroscopy*, Lyon, W. S., Ed., Elsevier, Amsterdam 1984, 173.
270. **Hess, K. R. and Harrison, W. W.,** Laser resonance ionization in a glow discharge, *Anal. Chem.*, 58, 1696, 1986.
271. **Fassett, J. D., Moore, L. J., and Travis, J. C.,** Laser resonance ionization mass spectrometry of iron, in *Analytical Spectroscopy*, Lyon, W. S., Ed., Elsevier, Amsterdam, 1984, 137.
272. **Peuser, P., Herrmann, G., Rimke, H., Sattelberger, P., Trautmann, N., Ruster, W., Ames, F., Bonn, J., Kluge, H., Krönert, U., and Otten, E. W.,** Trace detection of plutonium by three-step photoionization with a laser system pumped by a copper vapor laser, *Appl. Phys. B*, 38, 249, 1985.

273. **Nogar, N. S., Downey, S. W., Keller, R. A., and Miller, C. M.,** Resonance ionization mass spectrometry at Los Alamos National Laboratory, in *Analytical Spectroscopy,* Lyon, W. S., Ed., Elsevier, Amsterdam, 1984, 155.
274. **Donohue, D. L. and Young, J. P.,** Detection of plutonium by resonance ionization mass spectrometry, *Anal. Chem.*, 55, 378, 1983.
275. **Apel, E. C., Anderson, J. E., Estler, R. C., Nogar, N. S., and Miller, C. M.,** Use of two-photon excitation in resonance ionization mass spectrometry, *Appl. Opt.*, 26, 1045, 1987.
276. **Savicas, P. J., Hess, N. R., and Harrison, W. W.,** Glow discharge atomization source for resonance ionization mass spectrometry, *Anal. Chem.*, 56, 817, 1984.
277. **Chen, C. H. and Hurst, G. S.,** Noble gas detection using resonance ionization spectroscopy and quadrupole mass spectrometer, *Proc. SPIE-Int. Soc. Opt. Eng.*, N426, 2, 1983.
278. **Frey, F., Weiss, G., Kaminski, H., and Schlap, E. W.,** A high-resolution time-of-flight mass spectrometer using laser resonance ionization, *Z. Naturforsch. Teil A,* 40A, 1349, 1985.
279. **Bekov, G. I., Kudryavtsev, Yu. A., Auterinene, I., and Likonen, J.** The laser ionization spectrometer, *Inst. Phys. Conf. Ser.*, N84, 97, 1986.
280. **Ambartsumyan, R. V. and Letokhov, V. S.,** Selective two-step (STS) photoionization of atoms and photodissociation of molecules by laser radiation, *Appl. Opt.*, 11, 354, 1972.
281. **Kramer, S. D., Hurst, G. S., Young, J. P., Payne, M. G., Kopp, M. K., Calcott, T. A., Arakawa, E. T., and Beekman, D. W.,** Report 1979 CONF-790882-1, p. 11; *Chem. Abstr.*, 92, 154857, 1980.
282. **Beekman, D. W., Calcott, T. A., Kramer, S. D., Arakawa, E. G., Hurst, G. S., and Nussbann, E.,** Resonance ionization source for mass spectrometry, *Int. J. Mass Spectrom. Ion Phys.*, 34, 89, 1980.
283. **Lucatorto, T. B., Clark, C. W., and Moore, L. J.,** Possibilities for ultrasensitive mass spectrometry based on two-photon, sub-Doppler resonance ionization, *Opt. Commun.*, 48, 406, 1984.
284. **Cannon, B. D., Bushaw, B. A., and Whitaker, T. J.,** Continuous-wave double-resonance ionization mass-spectrometry of barium, *J. Opt. Soc. Am. B,* 2, 1542, 1985.
285. **Fassett, J. D., Moore, L. J., and Travis, J. C.,** Resonance ionization mass spectrometry of iron — quantitative aspects, *Anal. Chem. Symp. Ser.*, N19, 137, 1984.
286. **Clark, C. W.,** Isotope shifts of carbon (C-I) spectral lines and their application to radioactive dating by laser-assisted mass spectrometry, *Opt. Lett.*, 8, 572, 1983.
287. **Donohue, D. L. and Young, J. P.,** Removal of isobaric interferences by resonance ionization mass spectrometry, *Proc. SPIE-Int. Soc. Opt. Eng.*, N426, 13, 1983.
288. **Nogar, N. S., Downey, S. W., and Miller, C. M.,** Analytical capabilities of RIMS: absolute sensitivity and isotopic analysis, in *Resonance Ionization Spectroscopy 1984,* Hurst, G. S. and Payne, M. G., Eds., Institute of Physics, Bristol, England, 1984, 91.
289. **Miller, C. M., Engleman, R., Jr., and Keller, R. A.,** Resonance-ionization mass spectrometry for high resolution mass-resolved spectra of rare isotopes, *J. Opt. Soc. Am. B,* 2, 1503, 1985.
290. **Donohue, D. L., Young, J. P., and Smith, D. H.,** Isotopic measurements of uranium and plutonium by resonance ionization mass spectrometry, *Anal. Chem. Symp. Ser.*, N19, 143, 1984.
291. **Nogar, N. S., Sander, P. K., Downey, S. W., and Miller, C. M.,** Resonant multiphoton ionization for the detection of technetium, *Proc. Soc. Photo-Opt. Instrum. Eng.*, N380, 291, 1983.
292. **Rimke, H., Peuser, P., Sattelleerger, P., Trautman, N., Herrman, G., Ruster, W., Ames, F., Kluge, H.-J., and Otten, E. W.,** Determination of trace amounts of actinides and technetium by resonance ionization mass spectrometry, *Inst. Phys. Conf. Ser.*, N84, 118, 1986.
293. **Walker, R. J. and Fassett, J. D.,** Isotopic measurement of subnanogram quantities of rhenium and osmium by resonance ionization mass spectrometry, *Anal. Chem.*, 58, 2923, 1986.
294. **Franks, L. A., Borella, H. M., Gates, M. R., Hurst, G. S., and Payne, M. G.,** Detection of trace amounts of transuranics by resonance ionization spectroscopy of noble gases, *Nucl. Instrum. Methods,* 173, 317, 1980.
295. **Nogar, N. S. and Keller, R. A.,** Effect of very weak laser sidebands on optical spectra involving easily saturable intermediate states, *Anal. Chem.*, 57, 2992, 1985.
296. **Turk, G. C. and Watters, R. L., Jr.,** Resonant laser-induced ionization of atoms in an inductively coupled plasma, *Anal. Chem.*, 57, 1979, 1985.
297. **Churchwell, M. E., Beeler, T., Messman, J. D., and Green, R. B.,** Laser-induced ionization in an atmospheric-pressure microarc-induced plasma, *Spectrosc. Lett.*, 18, 679, 1985.
298. **Bushaw, B. A.,** Double resonance multiphoton ionization determination of mercury vapor, *Anal. Chem.*, 57, 2397, 1985.
299. **Dyer, P., Baldwin, G. C., Sabbas, A. M., Kittrele, C., Schweitzer, E. L., Abramson, E., and Imre, D. G.,** Isomerically selective photoionization of mercury-197, *J. Appl. Phys.*, 58, 2431, 1985.
300. **Green, R. B.,** Laser-enhanced ionization spectrometry, in *Topics in Current Chemistry,* Anal. Chem. Prog. N126, Springer-Verlag, Berlin, 1984, 1.
301. **Travis, J. C.,** Analytical optogalvanic spectroscopy in flames, in *NATO ASI Ser., Ser. B, Analytical Laser Spectroscopy,* Vol. 119, Martellucci, S. and Chester, A. N., Eds., Plenum Press, New York, 1985, 213.

302. **Camus, P.,** Optogalvanic spectroscopy application to trace analysis, in *Euroanalysis 5,* Hulanicki, A., Ed., Akad. Kiado, Budapest, 1986, 107.
303. **Letokhov, V. S.,** Laser-induced processes in spectroscopy, isotopes separation and photochemistry, *Usp. Fiz. Nauk,* 148, 123, 1986.
304. **Ochkin, V. N., Preobrazhenskii, N. G., Sobolev, N. N., and Shaparev, N. Ya.,** Optogalvanic effect in plasma and gas, *Usp. Fiz. Nauk,* 148, 473, 1986.
305. **Green, R. B.,** Laser-enhanced ionization in flames, in *Analytical Application of Lasers,* Piepmier, E. H., Ed., John Wiley & Sons, New York, 1986, 75.
306. **Toelg, G.,** Extreme trace analysis of the elements — the state of the art today and tomorrow, *Analyst,* 112, 365, 1987.
307. **Antonov, V. S., Letokhov, V. S., and Shibanov, A. I.,** Laser photoionisation selective determination of molecules, *Usp. Fiz. Nauk,* 142, 177, 1984.